The effect of fuel additives on diesel fuel delivery system and combustion performance

by:

Baptiste Duboc

Submitted for the degree of

Doctorate of Philosophy (PhD)

in

Mechanical Engineering

Supervisors:

Prof. Nicos Ladommatos

Dr. Ramanarayanan Balachandran

Declaration of authorship

I, Baptiste Duboc confirm that the work presented in this thesis is my own. Where information has been derived from other sources, I confirm that this has been indicated in the thesis.

_____

Abstract

The thesis presents an investigation of several aspects of fuel additive performance, including the effects of additives on the pump torque required to deliver high pressure fuel to engine injectors, the fuel droplet size distribution at sub-zero diesel fuel temperature, when wax formation occurs, and the ignition delay of diesel fuel combustion in an engine as well as constant volume combustion vessel. Exhaust emissions due to fuel additives were also investigated in an engine.

A pump torque rig was designed and commissioned to investigate fuel additive performance at various pump speeds, fuel delivery (common rail) pressures and fuel temperatures, including sub-zero temperatures at which fuel waxing occurs. An existing constant volume combustion vessel was adapted to allow observations of fuel spray with additives and it was used for spray and combustion investigations. Various components of the combustion vessel were modified to support the fuel spray instrumentation. Also, a sub-zero fuel temperature system was developed to allow fuel to be cooled down for investigations; finally, a fuel pressure intensifier was designed which allowed ease of dismantling and thorough cleaning so as to eliminate additive cross-contamination between successive tests with additives.

Results have shown that in general, additives have very small effects on many aspects of the fuel delivery system performance when the primary purpose of the additive is not related to the fuel delivery system. That is, there are virtually no side effects on pumping system performance from additives not intended to affect this system. This is mainly due to the small quantity in which the fuel additives are added, which is too small to affect any of the overall fuel properties. Additionally, it was proven that a constant volume combustion vessel is unsuitable to carry out combustion performance tests on fuel with additives, due to the high error in test repeatability. In contrast, the engine tests were able to reveal the effects of several combustion modifying additives on engine combustion performance and exhaust emissions. The fuel spray analysis at sub-zero temperatures revealed that wax formation was not the likely cause of an increase in droplet size but, instead, the likely cause is an increase in fuel viscosity.

Acknowledgements

First and foremost, I would like to thank Prof. Nicos Ladommatos for his help, patience and council over the past four years. Along with Dr. Rama Balachandran, you have taught me much over the years, providing invaluable expertise and encouragement, during the good and the bad times. Thank you.

Thank you to Innospec for sponsoring this thesis. Specifically, I would like to thank Trevor Russell, Anthony Cooney and Paul Richards for their great ideas, and for providing invaluable expertise in fuel additives.

I am also incredibly grateful to the UCL mechanical engineering staff and students, for their assistance and constant encouragement.

Mart. Thank you for your help, your support, the impeccably clean lab and for everything else! We did it!

Elina, Aaron, Midhat, Taaha, Aadil. Thank you for the ULU lunches, the coffee breaks, the long chats, but mostly thank you for your continuous help and valuable expertise in and out of the lab throughout the years. You have made working in the sub-basement a pleasure!

Thank you to all members of London Ju-Jitsu for helping with all the distractions and frustrations that are part of a PhD thesis for the past three years, and also to my new colleagues for their understanding and support in the last few months. I would like to specifically thank Alizé, Tawna, Alex B., Alex J., Gregoire and Lawrence for their great help.

The support from my mother, father and brothers has unquestionably allowed me to get where I am today. Thank you for your constant encouragement and unfailing optimism, even from afar.

Lastly, and above all, I would like to thank my partner Anne-Charlotte for her incredible day to day support and patience. She has been the best help anyone could hope for, and I am incredibly grateful for it.

To you all,

MERCI!

Table of contents

List of Figures

Table of Tables

Nomenclature

Abbreviations

AS	Anti-static additive
BDC	Bottom dead centre
CAD	Crank angle degrees Computer aided design
CF	Cold flow additives
CFPP	Cold filter plugging point
CI	Combustion Modifier additive
CN	Cetane number
CO	Carbon monoxide
CO_2	Carbon dioxide
CVCV	Constant volume control vessel
D_{32}	See SMD
DAQ	Data acquisition
DCA	Deposit control additives
DG	Diffraction granulometry
DPF	Diesel particulate filter
EGR	Exhaust gas recirculation
FEA	Finite element analysis
FM	Friction modifier
HCCI	Homogeneous charge compression ignition
HFRR	High frequency reciprocating rig
HMN	Heptamethylnonane
IMEP	Indicated mean effective pressure
LTFT	Low temperature flow test
MDFI	Middle distillate flow improvers
NO_x	Nitrous oxides
O_2	Oxygen
PDPA	Phase Doppler particle analysis
PID	Proportional integral and derivative
ppm	Parts per million
PRV	Pressure relief valve
RPM	Revolutions per minute
SMD	Sauter mean diameter
TDC	Top dead centre
THC	Unburnt hydrocarbons
TTL	Transistor-transistor logic
WASA	Wax anti-settling additives

Greek Symbols

γ	c_p/ c_v [no units]
ΔP	Pressure difference [bar]
ΔT	Temperature difference [°C or K]
μ	Viscosity [Pa.s]
ν	Kinematic viscosity [m^2/s]
ρ	Density [kg/m^3]
σ	Surface tension [N/m]
τ	Shear stress [N/m^2]
ω	Rotational speed [rad/s]

Roman Symbols

$\dot{Q}$	Net heat transfer [W] Net energy flow [W]
$\dot{V}$, $\dot{v}$	Volume flow rate [m^3/s]
$\dot{W}$	Net work transfer [W]
$\dot{m}$	Mass flow rate [kg/s]
C_1	Rate of change of torque with pressure [Nm/bar]
C_2	Zero-pressure equivalent torque (y-intercept of pressure vs. torque curve) [bar]
c_p	Specific heat at constant pressure [J/kg.K]
c_v	Specific heat at constant volume {J/kg.K]
e	Specific internal energy [J/kg]
F	Power [W] Friction losses [N]
h	Specific enthalpy [J/kg]
p	Specific pressure [bar/kg]
P	Power [W] Pressure [bar]
Q_n	Energy release from the fuel [J]
T	Torque [Nm] Temperature [°C or K]
V	Volume [m^3]
v	Specific volume [m^3/kg]

Chapter 1

Introduction

The need for diesel fuel has been increasing exponentially since the 1940s, as diesel engines are the main type of engine used for transportation of goods (container ships, Lorries). The quality of diesel engines, since the invention of this type of engine in the 1800s, has been gradually improving: with, for example, diesel engines in 2000 providing almost twice as much power as those of the 1960s, with about half the fuel consumption. Engine maintenance costs have been reduced, and engines produce less smoke and other exhaust emissions due to catalytic particulate filters and electronically controlled engine units (ATC, 2004).

Fuel additives have played a major role in improving fuel performance for many decades. Additives are chemical compounds added in very small quantities (in the order of mg of additives per kg of fuel) to diesel base fuel to modify or create certain fuel properties. Some examples include combustion improvers, detergents, cold flow additives and lubricity additives. The diesel fuel additive industry has existed since the 1920s. At that time, it mostly consisted of cetane number improvers to improve fuel ignition, and thus shorten ignition delay. Since the 1920s, the need for additives has grown, for economic as well as legislative reasons (ACEA, et al., 2006).

For economic reasons, in the refining process, increasingly more usable fuel oil is extracted from each barrel of crude oil. This results in fuels which are of lesser quality. Modern diesel fuels contain more olefins and aromatics, which can cause poorer and less stable combustion. Additives are added as a means of stabilising and improving these fuels, bringing them to the required regulated standards.

Legislation in the past few years has been a major influence on the additives market. For example, lubricity improvers are now a necessity in all diesel fuels, as the sulphur content of diesel fuels has been drastically reduced by law (ATC, 2007) (ACEA, et al., 2006). Similarly,

the government requirements to limit emissions of carbon monoxide (CO), nitrous oxides (NO_x) or particulates encourage the use of additives in diesel fuel.

Additives companies are very secretive with their products, especially the so called "vehicle fuel system additives" (ATC, 2004) that provide benefits in the engine inlet system and combustion chamber. These additives are usually added at the fuel loading terminal immediately before the fuel is shipped to the retailers, usually as a package of additives specific to the company selling the fuel.

"Distribution system additives" tend to be less secretive. They are additives put in the fuel in the refinery to help the handling and distribution of the fuel by suppliers and retailers. These include flow improvers, antioxidants, stabilisers, pipeline drag reducers, demulsifiers, antifoam additives, dyes and markers.

1.1. Types of additives

Additives are classified based on their desired effect. Most additive molecules can be described as having a polar head and a tail. The polar head is attracted to a variety of materials (e.g. rust, metal, deposits, wax crystal nuclei) and the tail has a specific function (e.g. decrease the boundary layer effect, being hydrophobic, disabling agglomeration).

In this introduction to additives, combustion improvers, deposit control additives, flow improvers, lubricity improvers, drag reduction additives and anti-static additives are described and their basic chemistry is discussed. These groups may contain several types of additives acting on different aspects of the fuel, with the same goal. The standard industrial measurement method to assess the effect of these additives is also described.

1.1.1. **Combustion improvers**

Diesel fuel in a compression-ignition engine auto-ignites under high temperature and pressure conditions. It is possible to obtain a measure of the ignition delay (time between fuel injection and start of combustion) of a diesel fuel using its cetane number, a fuel quality either determined experimentally or calculated from knowledge of the fuel composition (see section 2.2.2.1.). A high cetane number is desirable in diesel fuel, so as to reduce the time necessary for the fuel to ignite, and hence prevent violent and noisy combustion (Heywood, 1988). The cetane number of a fuel relates closely to its composition (i.e. its constituent compounds). High cetane number can be achieved by converting aromatics in the raw fuel to saturated and unsaturated alkanes through high pressure hydro-treatment, a very expensive post-refining process (ATC, 2004). Section 2.2.1.2. describes in detail how the chemistry of fuel may affect the different characteristics of combustion.

Combustion improvers (CIs), added to the fuel typically in 250 mg/kg, work by raising the cetane number of a base fuel, without the need for further post-refining processing. Cetane improvers have been in use for over 70 years. They work by the additive breaking down during combustion to form free radicals. These free radicals accelerate decomposition of the parent fuel by creating a greater frequency of intermediate reactions. In this way, the improver quickens the pre-combustion process, and reduces the ignition delay.

The most commonly used cetane improver is 2-ethyl-hexyl nitrate (2-EHN), which is one member of a family of alkyl nitrate improvers (ATC, 2004). Alkyl nitrates are chain hydrocarbons (n- or iso-paraffins) bonded to the NO_3^- ion. It is assumed that very quickly after injection the nitrate ion helps the breaking down of the fuel molecules to provide further free radicals. This allows for some preliminary reactions, which would otherwise be needed when no additive is used, to be skipped and for branching to occur sooner. As a result, the ignition delay is shortened. Cetane improvers have also been shown to improve cold starting significantly and to reduce several emissions (particulates, NO_x and hydrocarbons) (Ickes, et al., 2009). Some results however show that 2-EHN can have a negative effect on NO_x emissions (Ickes, et al., 2009), and this is assumed to be caused by the nitrate ion present in all CI additives becoming part of the NO_x emissions from the engine. This negative effect on NO_x is however very small compared to the benefit on NO_x of reducing the ignition delay and the duration of high temperature pre-mixed combustion.

1.1.2. **Deposit control additives**

Deposits are a common problem in diesel injector nozzles, as they are able to diminish the fuel delivery and the torque output of an engine significantly, when every other parameter remains constant (Birgel, et al., 2008). Deposit control additives (DCAs) include various sub-types of additives. Detergents, demulsifiers and stabilisers are the major ones, and are commonly used together to control deposit formation.

Detergents are used to prevent the formation of deposits by providing a film on the metal surface of the injector and fuel supply pipe, preventing the accumulation of deposits. Detergents also act by forming a protective coating around the developing deposit precursors, to prevent deposits from even forming. In the case of diesel fuels, detergents are predominantly succinimide and other ashless polymeric products. The polar head in detergents is derived from oxygen or nitrogen moieties, but is not composed of metals, making them ‘ashless’, an ideal attribute for diesel combustion where the combustion of metals forms unwanted ash particles. Deposit precursors such as soot or sludge are attracted to this polar head, and are trapped within multiple additive molecules in micelles. The tail of the detergent molecule is a long hydrocarbon chain molecule, which is highly oleophilic (ATC, 2007). This formulation allows the deposit precursors to be burned, thus avoiding deposition.

Demulsifiers are almost always used in combination with detergents. Detergents can cause the formation of fuel-water emulsions. These effects are countered by demulsifiers. The demulsifier molecule is attracted to the water molecule. It modifies the water emulsion's surface tension to induce coalescence of the water and the fuel. This prevents emulsions of water in fuel, which is unwanted as it is a strong catalyst to corrosion (through oxidation). Typical chemistries include alkoxylated polyglycols and aryl sulfonates (ATC, 2004).

Stabilisers are used intensively in the military industry where fuel may require storage for prolonged periods. Stabilisers ensure that a fuel can be used after long-time storage, using antioxidants to prevent sediment formation, dispersants to make sure the sediments that do form stay suspended and do not accumulate, and metal deactivators to deactivate the catalytic effect of some metals that could produce unstable reactions. Stabilisers are very similar in structure to detergents, where the polar head is a polymeric compound with a variable base or charge depending on what it needs to be attracted to. The tail is an oleophilic hydrocarbon chain (ATC, 2007). Antioxidants are overbased detergents (the head has a very high base number) that provide the large amount of base required to neutralise acidic components such as mineral and organic acids. It also reduces corrosive wear of the surfaces of metals. Dispersants are detergents that neutralise the charge of specific particles by forming a stabilising layer around the particle. This prevents agglomeration of other particles, which would otherwise create localised high density sediments that would fall to the bottom of the tank. Metal deactivators are additives with a polar head that is attracted to metal surfaces, forming a protecting film around the metal. This prevents corrosion, nullifies the catalytic effect of the metal, and in some cases prevents oxidation of the metal.

Engine tests are used by industry to measure the effects of DCAs. The Peugeot XUD-9A/L is the standard European test engine for deposit measurement (ACEA, et al., 2006). Flow rate through a clean nozzle and a nozzle with deposits are compared in a flow bench, after a nozzle has spent 10 hours in a running engine (Caprotti, et al., 2007).

1.1.3. **Flow improvers**

Diesel fuel is used under various weather conditions. When diesel becomes cold (around 10ºC or colder), the long n-paraffins chains (around 15 Carbon atoms or more (Kasza & Hancsok, 2011)) present in the fuel begin to solidify. The solidified groups of atoms of paraffins agglomerate to form what are called wax crystals. These wax crystals form a rigid matrix which can cause blockage of filters or fuel lines (ATC, 2004). Although it is possible to refine the fuel to remove such n-paraffins, and thus prevent wax formation, it is generally undesirable to do so as the n-paraffins have good combustion characteristics, and produce low emissions. Thus doing so would be costly and wasteful of the crude oil (ATC, 2004).

During the solidification process, the n-paraffins first form nuclei, on which other n-paraffin molecules accumulate to form crystals. When crystals are large enough, they start to adhere to each other to form even larger crystals.

Middle Distillate Flow Improvers (MDFI) are the most commonly used wax modifier. They are ashless low molecular weight co-polymers. They co-crystallise with the n-paraffins, which slows down crystal growth (by altering the shape of the crystal, and also reducing the crystal's adhesion). This forces new nuclei to start forming. As a result, multiple small crystals form that have difficulty agglomerating, instead of large agglomerating crystals. The effect, macroscopically, manifests itself as better flow conditions of the fuel, and retarded wax formation (ATC, 2004). Ethylene vinyl acetate co-polymers were used at first, but now a wider range of other compounds are used as MDFIs.

When the outside ambient temperature is low for a long time, the wax crystals treated with MDFIs will settle at the bottom of the diesel fuel tank in cars due to their increased density. Once settled, the wax crystals bond together over time, forming crystals large enough to be able to block filters. Thus, although the cold filter plugging point (CFPP) of fuel is lowered substantially with MDFIs, their use is limited on their own to a net improvement of about 10°C (Cestoil Chemical Inc., 2012) because of the uneven properties of the fuel in the tank. If winter conditions lower the fuel temperature below this limit, wax anti-settling additives (WASA) can be used as a co-additive to MDFIs, ensuring that the wax crystals are smaller. WASAs make the reactions faster which ensures the n-paraffin nuclei and MDFI bond together before agglomeration preventing further growth by completely preventing agglomeration of particles. The use of WASAs produces much smaller wax crystals which keep a similar density to that of the un-waxed fuel. Similarly to stabiliser additives, the nuclei coated with WASAs stay suspended within the fuel rather than agglomerating at the bottom of the tank (ATC, 2004) (Cestoil Chemical Inc., 2012).

To measure the effectiveness of a cold flow additive, a widely used method known as the cold filter plugging point (CFPP) is employed. This method involves letting fuel fall under gravity through a filter. The procedure is repeated, successively cooling the fuel further in 1°C steps. If the time required to fall through the filter is more than 60 seconds, the fuel has reached the CFPP temperature (European Standard, 1997).

There are other widely varying methods used to determine the waxing point of fuels. For example, in some instances the freezing point is used, although it is hard to determine precisely. A more commonly used alternative method is the cloud point temperature, which is the temperature at which the wax starts becoming visible (ATC, 2004) (Zhang, et al., 2009) (Han, et al., 2010). These methods however have a higher error associated with them than the CFPP test, which is the standard method used to test flow improvers. The low temperature flow test

(LTFT) is used in the United States as an alternative to the CFPP where a vacuum rather than gravity is used to pass the fuel through a 17 micron filter, and separate fuel specimens are used rather than cooling the same fuel specimen in 1°C steps (ASTM, 2010).

1.1.4. **Lubricity improvers**

Lubricity improvers have been introduced very recently to the additives market as a result of the change in regulations on diesel fuels. Diesel fuel has natural lubricity properties such as sulphur and other impurities. However, to limit pollutant exhaust emissions, the EURO 4 directive on emissions, and other subsequent European emissions standards have drastically lowered the allowed sulphur content to less than 10 mg/kg of fuel. The hydro-treating process, which is used to reduce the sulphur content of the fuel, also removes as a by-product the oxygen-containing polar impurities, which are the naturally occurring lubricity compounds in diesel fuel (Stanislaus, et al., 2010) (Wei & Spikes, 1986).

Similarly, the fuel aromatic content has been reduced to limit particulate emissions (ACEA, et al., 2006). The decrease of poly-aromatics has severely influenced the natural lubricity of the fuel, as poly-aromatics were another important natural occurring lubricity improver in fuel (Wei & Spikes, 1986).

There are two regimes of lubrication: boundary and hydrodynamic lubrication. The former is a type of lubrication that relies on the protective layer that forms on the surfaces of the interacting components by additives or other molecules in the fuel. The latter relies on the properties of the lubricating fluid, notably viscosity and surface tension (see section 2.3.1.), to form a film separating the interacting surfaces. Lubricity improvers tend to focus on the boundary lubrication regime, as it is the one that is affected by the recent changes on diesel fuel described above. They can nevertheless be designed to improve the lubrication of either regime.

It is very difficult to alter the viscosity of a fuel without changing its other characteristics, essentially creating a new blend of fuel. The viscosity modifiers, more commonly used with lubricating oils rather than fuels, can be used in very high concentrations (between 5 and 50%) to alter the viscosity of fuel or oil. Viscosity modifiers are high molecular weight polymers whose viscosity is less sensitive to temperature than diesel fuel (ATC, 2007). The problem with viscosity modifiers is that a large quantity of the additive is required to induce a significant change in viscosity. Furthermore, this change is usually only noticeable at high (over 80°C) or low (under 10°C) temperatures (ATC, 2007).

Due to the very large quantity of additive required to induce a change in viscosity, viscosity modifiers are rarely used in everyday diesel fuels. Instead, crude oil is refined into component streams and the streams are then blended in order to fit within the viscosity requirements of the

World Wide Fuel Charter (ACEA, et al., 2006). For diesel fuel, this is between 2.0 and 4.5 mm^2/s at 40°C.

Although hydrodynamic as well as boundary lubrication occur in several components of the fuel delivery system, the lubrication regime that is affected most by the removal of the sulphur and aromatics in diesel fuel is the boundary lubrication regime. Friction modifiers (FMs) are added to the fuel to act on the metal surfaces. FMs have a polar head which is attracted to the metal surfaces, either by adsorption, or by chemically reacting with the metal surface to form oxides. The tail is a long molecular chain, normal to the surface of the metal. The additives coat the metal surface, forming a layer. When the metal surfaces come in contact with one another, the tail molecules slide on one another, reducing metallic contact. Sulphur and metal impurities as well as aromatic molecules present in the fuel are attracted to metallic surfaces, and act similarly to natural FMs (Williams, 1994).

Other additives also have an effect towards lubricity improvement (Mitusova, et al., 2002). In sub-zero conditions, for example, wax anti-settling additives will decrease the viscosity of the fuel, making it less prone to hydrodynamic friction losses. DCAs also have an effect in keeping the lubrication properties uniform throughout the fuel. If they weren't present, the settling of particles would eventually create a dense phase of fuel with high viscosity at the bottom of the tank. (ATC, 2007).

The high frequency reciprocating rig (HFRR) was devised to measure the lubricity of a fuel, and is in use in Europe and around the world as the prime lubricity measurement tool. It involves an oscillating ball against a flat piece of metal immersed in fuel. The depth of wear on the metal flat over a large number of reciprocations is a measure of the lubricity figure (ATC, 2004) (ATC, 2007) (Mitusova, et al., 2002). This depth needs to be lower than 400 microns with the fuel at 60°C.

1.1.5. **Drag reduction additives**

Drag in fuel systems is often measured by means of the reduction in flow rate or the rise in pressure drop in turbulent pipe flow (Berman, 1978). In pipelines, where fuel is required to flow in pipes for very long distances, the energy required to pump the fuel through the pipes is heavily affected by the drag of the fuel. Drag losses are caused by surface and bulk frictional forces created by turbulent flow in the pipes. Velocity fluctuations normal to the pipe wall and Reynolds shear stresses start forming at small scale imperfections, and evolve into larger scale turbulent structures (Warholic, et al., 1999). In order to counteract this effect, drag reduction additives (also called drag reducing agents, DRA) are added to the fuel.

DRAs are typically very high molecular weight polymers (over 10^5) randomly coiled in diesel, forming tangled balls filled with fuel. They are added in low concentration in order to reduce

friction losses in pipes (Berman, 1978). The mechanism by which DRAs work is not fully understood, but it is believed that the turbulent structures responsible for drag interact with the tangled polymers. The interaction untangles the polymer, dissipating the energy of the small vortex. This ensures that it does not grow into larger vortices (Warholic, et al., 1999).

DRAs untangle during fluid flow, and thus lose their effectiveness (Warholic, et al., 1999). It has also been seen that these large molecules get broken down (destroyed) very easily in pumps and filters. DRAs are added regularly along a pipeline to replace the previous ones that were destroyed. The presence of filters, pumps and injectors makes DRAs ineffective in diesel fuel delivery systems (Russell, 2013).

There are no legal requirements for the maximum drag of a fuel, and thus no standardised method to measure the effectiveness of a DRA. DRAs are mainly used to transport fuel in pipelines over long distances. The cost of pumping is reduced by using DRAs, but too much may cause an unwanted increase in fuel viscosity. Furthermore, the heavy de-tangled molecules end up in the fuel after the DRA has been used, and these heavy molecules can contribute to deposit build-up in internal combustion engines (Al-Khodair, et al., 2009).

1.1.6. **Anti-static additives**

Static electricity in hydrocarbon fuels can discharge onto other surfaces, creating a spark powerful enough to ignite fuel vapour in air. This is due to the fact that modern low sulphur, raw diesel fuel, has a low conductivity (less than 1 pS/m) and a generally positive charge forms when it flows in pipes. Due to its higher volatility, the problem of static discharge in fuels is more significant for gasoline that diesel fuels, as a spark will only successfully ignite the less volatile diesel fuel in conditions of high temperature (ATC, 2004).

Static charge in fuel occurs due to ionic impurities present in the fuel. When the fuel is at rest, the impurities are adsorbed on the tank surfaces, essentially grounding the fuel. However, when the fuel flows at high velocity, the impurities are separated from the walls, creating a positive charge. The fuel requires a certain amount of time (between 1 and 100 seconds) to lose the charge created by grounding the charge to the walls. If the charge dissipation rate is too low, a high potential discharge to a grounded object could create a spark powerful enough to ignite a fuel vapour/air mixture (Leonard, 1981).

Multiple attempts have been made to prevent charge build-up in the fuel, mostly by improvements in storing and handling of the fuel, as well as creating vehicle system components that have a high discharge capacity (Belz & Koch, 1991). However, with the desulfurization of modern fuels, the natural conductivity of diesel has dropped greatly, requiring anti-static (AS) additives to restore that property.

The American Society for Testing and Materials (ASTM) requires the electrical conductivity of diesel fuel to be above 25 pS/m (ASTM, 2013). Anti-static additives include fuel-soluble chromium materials, polymeric sulphur and nitrogen compounds. They act by improving fuel conductivity (an increase of more than 50 pS/m for 1 ppm has been reported (Leonard, 1981) (Carney, et al., 2004)), and reduce the potential for static charge build-up (ATC, 2004).

The conductivity of diesel fuel is simply measured using a clean conductivity cell, which measures how conductive the liquid is, using a sensitive DC ammeter (ASTM, 2012). The effectiveness of anti-static additives is measured this way.

1.2. The additives market

Each additive is designed as a response to a particular problem. These problems may be due to legislative issues such as the EURO 5 directive. They may also arise due to economic factors such as drag-reduction additives (DRA) being a cheaper alternative to the power required by pipeline pumps. Because of this, additives are usually created in order to pass a certain test. For example, the effectiveness of a lubricity additive will only be assessed using the HFRR test, because it is the one that the industry uses to determine the lubricity quality of the fuel.

Test measurement methods are designed to be repeatable, to have strict conditions, and to bring out a single quantitative value to allow comparison between various fuel aspects. As fuel requirements become harder to meet, new and more complicated test methods arise.

Particular additives have two major limitations. The first is that the additive ends up being only as good as the limitations of the additive test method allow. In that sense, a very good lubricity additive is essentially only an additive which passes the HFRR test successfully. As test measurement methods change and improve to better represent real fuel system conditions, so do the additives, making them more effective in practical fuel systems.

Another significant limitation of additive testing is that each test is carried out to evaluate the effect of the additive on its own (i.e. not looking at the effect additives may have on each other). In addition, validation measurements of a particular additive are usually only carried out to determine the additive's own desired effect, using the additive's test method. Some additives could have negative effects on several other fuel aspects. These effects are usually only detected when several additives are combined in multifunctional packages. However, these additive packages often contain many additives and the unwanted effect is often never traced back to a specific combination. At this final stage, the additive industry concentrates mostly on making sure their additives are miscible amongst themselves, and with the base fuel. This means that the full effect of a fuel with a single additive is rarely investigated thoroughly (ATC, 2004).

1.3. Summary and objectives

The following thesis reports on the effect of some commercially competitive diesel fuel additives on certain aspects of the combustion process, using blends of these additives with a common diesel base fuel. The aim was to determine whether individual blends of additives had the potential to affect parts of the combustion system. Furthermore, the potential negative and positive effects, in terms of engine efficiency and performance, on other aspects of the combustion process in an automotive engine were investigated. As a result, a stronger understanding of the effects and limitations of diesel fuel additives on certain aspects of the combustion process (fuel delivery pump torque, spray quality and combustion quality) was acquired.

A rig was designed and assembled to investigate the effect of various diesel fuel additive blends on the torque of a standard high pressure fuel pump and common rail system for the medium duty automotive industry (large SUV car/small lorry). Many types of additives provided by Innospec were tested on the fuel pump torque rig to find out the friction effect from an additive in fuel, and of its concentration in fuel. Additionally, the fuel pump torque rig was used to investigate the effect of cold flow (CF) additives on the torque required to drive the pump when the fuel was at temperatures below its cold filter plugging point, of about -10ºC, which corresponds to the onset of waxing. The objective was to determine how diesel fuel additive blends affected the torque required to operate a diesel fuel pump, and if that effect was a significant percentage of the overall torque required to operate the pump.

The effect of spray behaviour on engine power output and efficiency is well known from the literature (see next section). Furthermore, it is known that the addition of diesel fuel additives in minute quantities in fuel are unlikely to affect spray formation and droplet size, as they are known to be affected by fuel's physical properties such as viscosity, density or surface tension, which are not altered significantly by most additives. The thesis objectives for the spray investigations were therefore to study the droplet size distribution of fuel sprays below the CFPP temperature of -10ºC for blends of diesel fuel with CF additives. The aim was to investigate whether waxing of the fuel in diesel injectors had any effects in modifying the droplet size distribution and whether CF additives mitigated any such effects.

Finally, the effects of CI additives on combustion delay were investigated in a constant volume combustion vessel as well as in an engine bed. This was to validate the use of a combustion vessel as an effective means to measure additive effects. As well as combustion delay, the exhaust-generated emissions products and the particulates in the combustion products were investigated for various blends of CI additives with diesel fuel.

This thesis consists of seven chapters. The first is the introduction. The second chapter is a literature review of work on effects of diesel additives on combustion, sprays and fuel pumping

power. The third chapter describes the experimental systems that were designed and used to carry out the experiments and data presented in this thesis. Chapters four, five and six are the chapters on experimental results for the pump power, spray, and combustion experiments, respectively. The seventh (final) chapter is the conclusion.

Chapter 2

Literature review

Due to the competitive nature of the additives market, information on the specific effects on different aspects of the combustion process of particular additives, or in some cases group of additives, is rarely available in the open literature. Some general knowledge of additive compositions is available through looking at patents of particular additive groups. Additionally, the general method of operation for groups of additives, such as combustion improvers, is often known, as all additive manufacturers use the same chemical mechanisms. Nevertheless, variations in specific compositions are kept confidential.

With that in mind, the literature review attempts to assess the effects of diesel fuel additives on the three aspects of the combustion process of interest in this thesis: the fuel spray, the combustion, and the fuel pumping power.

The various diesel fuel spray characteristics of interest are described in this literature review, as well as various methods to investigate sprays. The effects on sprays of fuel temperature were of particular interest, as cold spray tests with additives were carried out.

Previous research related to the effect of additives on diesel combustion is presented, focusing particularly on combustion in constant volume combustion vessels. The chemistry of combustion is briefly discussed so as to gather understanding of combustion improver (CI) additives and how they affect the chemistry of combustion. The effects of additives on heat release, ignition delay, and exhaust emissions are reviewed.

Finally, the effects of varying fuel properties on pump power are discussed. The lubricity inside a diesel fuel pump was of particular interest, as it is substantially dependent on fuel properties. The effects of various additives on the lubricity in a pump are also reviewed.

2.1. Spray formation with diesel fuel additives

2.1.1. **Spray characteristics**

The air-fuel mixture formation in the combustion chamber of a diesel engine is affected by the characteristics of the fuel spray (Takeuchi, et al., 1983).

The fuel spray characteristics have therefore been studied extensively, as certain spray characteristics have been shown to facilitate the combustion process. Three main aspects of fuel spray characteristics are reviewed: Cone angle, spray length and droplet size distribution. Some studies also analysed the liquid length of the spray (Svrcek, et al., 2010).

Spray cone angle is how wide the spray is as it comes out of the injector nozzle hole and penetrates into the combustion chamber. As the spray comes out of the injector, it has a very high velocity (typically 100 m/s) and the droplet sizes are smaller by about an order of magnitude than the injector nozzle hole diameter (typically 150 μm). As the liquid jet leaves the nozzle, it becomes turbulent and spreads out, mixing with the air. The initial fuel jet velocity of about 100 m/s is slowed down as the spray moves away from the nozzle, due to the mass of entrained air within the spray. Because the spray spreads out and mixes with the air progressively, the spray diverges more, and velocity reduces, as the spray penetrates further into the combustion chamber. The result is a spray cone, which has very high concentration of fuel (and very little air) in the centre and low concentration of fuel (and mostly air) at the edges (Heywood, 1988). If the cone angle is narrow, the spray will be denser and more localised, and so will the combustion event when ignition occurs. The cone angle should therefore be wide in order to provide less localised, less dense air-fuel mixture and for the spray to be easier to break up and thus mix the fuel and air.

Spray length, or penetration length, is the distance required for the fuel to either have no velocity at the spray tip or for the fuel at the tip to become fully vaporized. The optimum penetration length varies from engine to engine. If the spray is too long, it could impinge on and wet the piston wall, leading to combustion instability, reduction of engine efficiency and increase of exhaust emissions, particularly unburnt hydrocarbons and particulates (Heywood, 1988). However, too short a spray would provide insufficient mixing between the injected fuel and the available air, which then causes an increase in the equivalence ratio in the combustion chamber (Park, et al., 2011). This has a detrimental impact on pollutant emissions and engine fuel efficiency.

The droplet size distribution of a fuel spray is usually measured as a histogram, relating the droplet size to the frequency of that particular size. The result can be a simple single-mode normal distribution (bell shaped histogram), or could be bi-modal, with two distinct droplet size distributions in the spray (Malvern Instruments Ltd., 1997). In the case of diesel fuel, the

literature agrees that the droplet size distribution has a single mode bell shape (Dumouchel, et al., 2009). However, the value of droplet size distribution in a fuel spray varies with time and location (Heywood, 1988). From a droplet size distribution histogram, researchers usually deduce an "average" droplet size for a given time and space called the Sauter mean diameter (SMD – see definition below).

A diesel fuel droplet is a three dimensional object, which can be distorted to any shape by mainly aerodynamic forces. However, in order to be able to analyse and compare data with different sprays, the multitude of droplets in a spray can be analysed and averaged into one number. This can only be done by assuming droplets to be spherical, which makes their diameter the only variable (Malvern Instruments LTD, n.d.). These diameters are calculated from a distribution which, in reality, includes a wide range of droplet diameters and shapes.

When averaging a droplet size, different types of average diameters can be taken. The simple arithmetic average adds all diameters and divides the result by the number of droplets. This is often not a useful average as it tends to be dominated by numerous small droplets with the fewer larger droplets not represented well in the average; nevertheless, those larger droplets are important as they hold much of the spray mass. Instead, other diameters such as the Sauter mean diameter (SMD) are used. SMD is the diameter of the droplet that has the same volume to surface area ratio as that of the total spray (Heywood, 1988), and is often the preferred mean value used in spray studies. It is a convenient mean diameter to use because in many spray systems the designer is interested in the total surface area of a spray for a given volume, as the surface area is an important parameter controlling evaporation of the spray. Therefore, in spray mixing the total surface area of a spray is a major influence on vapour/air mixing.

Although the SMD is useful for comparing results for different sprays, the full droplet size distribution curves or histograms carry additional information that the SMD does not. Usually, analysis is carried out using both SMD and size distribution, with the SMD acting as a single value summarising the distribution.

For a given fuel volume, having small spray droplets is advantageous because it provides more surface area from which to evaporate the fuel into the ambient air. For this reason, a small average droplet size is often sought from an injection system.

Spatially, the SMD will be largest at the axis of a spray, decreasing radially. It will also be highest closest to the nozzle, and decrease along the axis of the spray (Lu, et al., 2007). Temporally, droplets are initially very large, undergoing a rapid decrease in SMD as time progresses due to aerodynamic breakup and evaporation, after which the SMD stays fairly constant for the duration of the injection (Park, et al., 2011).

2.1.2. **Effects of gas conditions on spray characteristics**

Extensive research has been carried out to determine what controls diesel spray characteristics. These may depend on either the fuel properties or the environment into which the fuel spray is injected.

The shape of the nozzle, for example, has an effect on the spray angle, penetration length and SMD (Takeuchi, et al., 1983). Larger holes tend to increase the SMD and the penetration length. When keeping everything else the same, a nozzle length to diameter ratio of 4 results in, approximately, the minimum droplet size at low and intermediate injection pressures; it also achieves the minimum value of spray breakup length, and the maximum spray cone angle. The length of the nozzle is, in practice, often designed to be four times the nozzle diameter (Heywood, 1988).

A fuel temperature increase will decrease the spray penetration length, as evaporation is helped by the temperature rise. Similar trends occur for an ambient gas temperature increase (Heywood, 1988). With a gas temperature rise, droplets evaporate more quickly, losing momentum; thus sprays have a lower penetration length.

The effect of injection pressure has also been investigated (Wang, et al., 2010). Injection pressure, when already high (e.g. 1500 bar as in modern diesel injection systems), has negligible effect on spray angle or maximum spray penetration length. However, a higher injection pressure will decrease the time it takes for the spray to reach maximum spray penetration and a stable cone angle, as the fuel velocities are much higher. When the fuel leaves the injector at high velocities, the aerodynamic interaction between the liquid jet and the surrounding gas creates large shear stresses on the fuel jet. These stresses break up the liquid jet into many small droplets: a process called spray atomization. Thus, if the fuel velocity is higher (due to an increased difference in pressure or density between fuel and surrounding gas), better atomization occurs, which results in smaller average particle diameter (Heywood, 1988).

Ambient density (ambient pressure and temperature) has a pronounced effect on spray angle, penetration length and SMD. An increase in ambient density decreases the ratio of densities between the fuel and the ambient air and this affects the spray shape. Spray angle is increased when the fuel is injected in a denser environment, and as a result spray penetration is smaller (Wang, et al., 2010). The SMD is also affected by the air density: it will increase with an increase in air density, as shown in empirical correlations developed by (Hiroyasu & Kadota, 1974) and (Tabata, et al., 1990).

Injection nozzles are also designed to suit the combustion chamber size and shape. This is to prevent wall wetting, while promoting maximum diffusion of the fuel into the whole combustion chamber. This maximises the use of the available air for mixture formation. Droplet

size distribution is also affected by fuel-related parameters such as viscosity and surface tension (Heywood, 1988) (Elkotb, 1982). Fuel additives can be designed to modify those parameters, thus affecting the droplet size distribution without affecting the other spray characteristics.

2.1.3. **Methods of measuring droplet size in sprays**

There are three main methods in use to measure droplet size in sprays, and especially diesel sprays: Phase Doppler Particle Analysis (PDPA), diffraction Granulometry (DG), and imaging.

PDPA uses two laser beams to resolve the droplet size at the point at which the beams cross. In PDPA, the two laser beams are passed through a series of optics so that when the beams meet there is optical interference, resulting in a series of light and dark fringes or bands. When a droplet passes through the fringes, it interacts with the fringe pattern, causing a scattered light signal (scatter during passage through a light fringe and lack of scatter through a dark fringe). This scattering will have a frequency which is dependent on the droplet velocity. A photomultiplier tube monitors the scattered light to determine this velocity from the known distance between the fringes. Additionally, the temporal shift between one laser beam and the other can be measured if two (usually three) photomultipliers are used and arranged at different angles to the laser beams. This is used to measure the droplet size (TSI, 2006). The main issue with PDPA is that in order to get overall spray behaviour, many spray locations have to be probed and characterised. Recording enough positions to fully characterise a spray may prove to be difficult, and time consuming. Although with PDPA it is possible to measure the droplet behaviour inside a spray, when the spray is dense, as in the case for diesel sprays, the precision of the measurement is down to 50% due to a very scattered and diffracted laser beam (Yule, et al., 1998).

DG uses a single laser beam pointing to a receiver. As the droplets pass through the laser beam, the light is refracted depending on the size of the droplets. The refracted rays are caught by photo-sensor arranged in a ring-like structure around the axis of the unaltered beam. The refraction angle depends on the droplet size (small droplets will have a larger refraction angle). By measuring the intensity of the light on a particular photo-detector ring, it is possible to determine how many particles of a particular size are present. This method is, once again, limited in terms of spatial coverage, as it can only measure droplet size along a line of sight. So, to characterise the full spray behaviour, many lines of sight have to be measured. However, all the spray sizes in the line of sight of the DG are measured by the system, and global image behaviour of the spray is possible, in less time than with the PDPA system which analyses the spray at a particular spot. The DG only works if the laser light is not excessively absorbed and scattered by the spray. With DG, if the spray is too dense then the light transmission will be too low and most of the droplets in the spray will not have been counted, resulting in wrong results.

The Malvern Spraytec system is a diffraction granulometry system widely used for spray analysis of fuel (Priol, et al., 2006).

Spray imaging can be carried out in various different ways, but the same principles apply in most cases. Snapshots of the spray are taken as images, which are analysed (using software) for droplet size and number, giving a distribution. Droplet sizing with imaging can be spatially quite productive. The camera could be capturing the whole spray at a time, depending on its resolution. Alternatively, the camera could precisely capture a small area, if it has a microscopic lens. Because the droplets are very small, large magnifications are needed which reduce the depth of field. A high speed camera can be used to resolve multiple images in short time steps, but such cameras can be expensive, or only allow for small images to be recorded, thus reducing the spatial precision of the image. Also, as the picture is taken, all droplets will be in the photograph, even the ones out of focus. Out of focus droplets are a big issue in measuring droplet size using imaging, and may result in the software over-estimating the droplet size distribution as a result (Blaisot & Yon, 2005) (Fdida, et al., 2010).

It is very difficult to compare the above three methods of droplet size distribution, as each method has different spatial and temporal resolution. The error of measurement of each method can be more than 20%. Although the three methods can give very different results in terms of the Sauter mean diameter, the droplet size distribution curve shapes are often similar for all three techniques (Fdida, et al., 2010). The method to be chosen depends on what information is required from the experiment. PDPA is best for spatially resolved droplet size analysis, but will take time to fully characterise a typical spray, as not only will one have to do repeats for one position, but many positions will be required. Furthermore, for dense sprays, the analysis of the inside of the spray lacks precision. Imaging will be very useful for an ensemble view of spray behaviour, but could lose precision due to out of focus particles. Imaging also often needs large magnifications to measure droplet sizes with precision, and this reduces depth of field, requiring multiple experiments to be conducted. DG seems to be the best ‘middle option’ where the droplet size distribution of a spray is averaged in a chosen line of sight.

As diesel sprays are generally conical, it is often assumed that the spray behaviour is axi-symmetric. By making this assumption, a considerable number of observations can be omitted when characterising a typical spray, and methods such as PDPA and DG become less time consuming.

2.1.4. **Droplet sizing in diesel fuels**

Additives in some cases may alter the physical characteristics of a fuel such as viscosity or surface tension. Very little literature mentions spray analysis using diesel fuel additives. However, experiments have been conducted on fuels with different physical properties,

particularly viscosity and surface tension, and droplet sizing analysis was carried out. Thus, it is possible to gain an indication of what the additive effect on the spray might be in the case of those additives that change the viscosity or surface tension.

2.1.4.1. The effect of injection pressure

Injection pressure has a major effect on droplet size. The effect of injection pressure on the SMD can be seen in Figure 2.1 and Figure 2.2. At low pressures (up to 600 bar, depending on fuel properties), an increase in pressure results in a very large decrease in SMD. This behaviour is assumed to be due to the increased shear forces exerted on the fuel as it comes out of the injector nozzle. The higher shear rate increases the break up and atomization of the fuel, resulting in smaller droplets. As pressure increases beyond about 600 bar, the effect of pressure on reducing SMD becomes less significant. However, injection pressure still has an effect on SMD, even above 1000 bar (Wang, et al., 2010). Generally, at injection pressures above 600 bar, parameters such as fuel density, fuel viscosity (Figure 2.1) and nozzle shape take-over as the parameters that significantly influence the droplet size.

Although fuel characteristics have an influence for all injection pressures, it has been found that at lower pressures, the effect of viscosity, surface tension and density will be more significant than at higher pressure (Heywood, 1988) (Svrcek, et al., 2010) (Elkotb, 1982) (Hiroyasu, 1985)(see also Figure 2.1 and Figure 2.2). The contribution of the fuel properties towards the atomization process is generally less significant at higher injection pressures. This is especially true for surface tension (Figure 2.2).

2.1.4.2. The effect of viscosity and surface tension

The individual effects of viscosity and surface tension on a liquid spray have been known for quite some time.

Figure 2.1: The effect of viscosity on the SMD at a relatively low injection pressure (Hiroyasu, 1985)

The effect of viscosity on SMD depends on the injection pressure (see Figure 2.1). Above 800 bar, the SMD increases by 33% for an increase in kinematic viscosity from around 1 x 10^6 m^2/s to 25 x 10^6 m^2/s, and is doubled for an increase from 1 x 10^6 m^2/s to 61 x 10^6 m^2/s (Hiroyasu, 1985). Furthermore, as the viscosity is lowered, the sensitivity of SMD to pressure increases (Figure 2.1).

It is almost impossible to alter the surface tension of a fuel without altering its viscosity (Heywood, 1988). So, rather than using one fuel and changing its surface tension, different fuels are used which have the same viscosity but different surface tension values, as shown in Figure 2.2. Similar to the viscosity effect, SMD stabilises at higher pressures. The higher the surface tension, the higher the injection pressure required to stabilise SMD. At higher pressures the SMD stabilises to a quasi-similar value for all surface tensions. The value of SMD for high pressure injection will therefore be mostly governed by the viscosity rather than the surface tension (Hiroyasu, 1985), and is likely to be almost independent of surface tension and further increases in pressure.

Figure 2.2: The effect of surface tension on the SMD (Hiroyasu, 1985)

In order to determine the effects of viscosity and surface tension on SMD, liquids of different viscosities and surface tension were individually tested by various researchers, but diesel fuel presents some difficulties. Viscosity and surface tension in diesel fuel, along with density, tend to be affected together when fuel composition is altered. This is because for most hydrocarbon compounds all three variables are controlled by their molecular structure. Changing the molecular structure by selecting a different blending compound in the fuel tends to affect all three properties together and significantly. Introducing bio-diesel to a fossil diesel fuel changes the physical properties and thereby the spray characteristics. All papers agree that the observed effects on the spray, such as droplet size, are explicable by the changes in surface tension and viscosity. In general, the cohesion between fuel molecules decreases when the surface tension and viscosity of a fuel decrease. This decreases the droplet diameter as a result (Lu, et al., 2007).

These results however only become apparent for significant changes of fuel composition (25-75%).

From such experiments, equations have been derived to link surface tension, injection pressure, viscosity and fuel density with spray parameters such as droplet sizes and cone angle (Elkotb, 1982) (Hiroyasu, 1985). These equations also show dependencies on injector geometry.

The equation derived by Elkotb (1982) was designed to work for a particular range of fuel viscosity, surface tension, density and pressure difference.

$$\boldsymbol{D_{32} = 6556\nu^{0.385}\sigma^{0.737}\rho_f^{0.737}\rho_a^{0.06}\Delta P^{-0.54}} \quad \textbf{(1)}$$

Where:

- D_{32} is the Sauter mean diameter of the particles in μm
- ν is the kinematic viscosity of the fuel in m^2/s and $0.81 \cdot 10^{-6} \leq \nu \leq 8.6 \cdot 10^{-6} m^2/s$,
- σ is the surface tension of the fuel in N/m and $20.4 \leq \sigma \leq 27.5\ mN/m$,
- ρ_f is the density of the fluid in kg/m^3 and $732 \leq \rho_f \leq 847\ kg/m^3$,
- ρ_a is the density of the ambient air in kg/m^3 and $1.20 \leq \rho_a \leq 8.20 kg/m^3$,
- ΔP is the pressure difference between the injection pressure and the ambient pressure in bar and $78\ bar \leq \Delta P \leq 200\ bar$

It has been found that this particular equation can also be used to describe the behaviour of some bio diesels whose properties fall within the fuel properties and pressure ranges described above (Ejim, et al., 2007).

2.1.4.3. Droplet sizing with additives

Additives added to a fuel in very small quantities may not have a noticeable effect on SMD, as the fuel properties may stay unaltered. In fact, the added quantity of additives is so small that the effect on viscosity, surface tension, or any physical property of the fuel at a given set of conditions may be negligible.

Most experiments on diesel additive sprays have been carried out with ignition improving additives and show no change in the SMD or other spray characteristics (Higgins, et al., 1998). CI additives are not expected to alter the physical properties of the fuel and, in that sense, the fact that no effect on SMD was noticed is to be expected.

Certain lubricity additives like viscosity modifiers can be added to the base fuel in quantities from 5% to 50% to reduce the effect of temperature on viscosity. It should be noted that these additives, if added in these quantities, can be expected to alter other fuel properties such as surface tension and fuel density as well.

Deposit control additives (DCAs) have been shown to prevent and remove coking in injector nozzles (ATC, 2004). In addition to a reduction in fuel flow rate through the nozzle holes, it is conceivable that coking may change the nozzle hole geometry and affect fuel spray characteristics such as cone angle, liquid length and SMD (through a reduction of spray velocity).

Although no information is readily available as to the effect of cold flow (CF) additives and wax formation on sprays, some information can be found regarding spray development in extreme cold conditions (Payri, et al., 2008). When fuel is taken from room temperature to extreme cold conditions (circa -15°C), the density and viscosity of diesel are increased (more than double for viscosity, and about 1.5% increase for density). Payri's results show the effects of density and viscosity changes on spray characteristics, but they do not show the effects of wax formation. This is because Payri et al (2008) used winter diesel, which uses CF additives to prevent wax formation and/or is refined to lower the overall CFPP of the fuel. The effectiveness of CF additives on spray, and particularly droplet size is unavailable, as no open literature could be found on spray tests done specifically on fuels in extreme cold conditions without CF additives.

2.2. Combustion with diesel fuel additives

There are many ways to study the diesel combustion process. Four main ways are vehicle field tests, engine bed tests, optical research engine tests and combustion vessel tests.

- Field tests are usually carried out by the manufacturers on every fuel or additive blend package product to see the behaviour of the vehicle in actual running conditions. Usually, this is a final process used to determine the effects that the final fuel or additive blend package product may have on the engine and vehicle performance when the vehicle is operating under realistic conditions.
- Engine bed tests are conducted with real engines, under a load provided by a dynamometer. Engine bed tests can be used to determine the effect that a certain fuels may have in real engine conditions, but in the case of additive evaluation such tests do not usually consider details of the combustion process. Engine bed tests usually measure power and emissions, sometimes cylinder gas pressure, but have no optical access.
- Optical research engines are specially designed or modified real engines so as to have windows that allow visualisation of the inside of the combustion chamber during running conditions. Optical engines allow the study of the combustion process inside an engine, but are restricted to certain running conditions because the optical access components are fragile.

- Combustion vessels are not engines. They are made to study a single combustion event under controlled ambient conditions. They can be very helpful for the understanding of the combustion process, as many more parameters such as vessel pressure, temperature and gas composition can be controlled independently in a combustion vessel. Similar control parameters would be difficult to achieve in an engine. Combustion vessels also allow extensive optical access that is not usually possible in an engine. Although combustion vessels are used to characterise combustion, they never fully match engine tests, as those are more complex in nature.

Due to the secrecy by manufacturers of their additive testing schedules and results, very little literature was found on additive combustion experiments. Most experiments on additives are conducted in engine bed tests. This is mostly due to the fact that when additives are tested, the effect that is investigated is either the one that the additive was made for, such as the Peugeot XUD-9A/L test on DCAs (ATC, 2004), or on exhaust emissions (McCreath, 1971) (Labeckas & Slavinskas, 2005) (Keskin, et al., 2011). Engine tests are useful to assess the effect of a particular additive on engine running performance, but they are less helpful in studying and understanding the way the additive works.

2.2.1. **Combustion with additives in constant volume combustion vessels**

2.2.1.1. Why use a combustion vessel

Constant volume combustion vessels (CVCV) are usually made of steel and allow pressure and temperature to be controlled, either independently or together. They also allow changes in gas composition and enable extensive optical access. The gas volume is constant, and fuel can either be premixed with air or it can be injected in this volume into a preheated gas, resulting in spontaneous combustion in the case of diesel. The CVCV generally includes windows to allow optical analysis of the process, and the results of combustion can also be analysed from the gaseous combustion products.

The major drawback of the CVCV is that it cannot represent accurately the turbulence present in an engine generated by the injection process and the piston motion. Similarly, in an engine, the gas pressure and temperature vary throughout the combustion. Finally, the CVCV is a one-off measurement method. Each injection and combustion event is monitored separately, with at least a period of 10 minutes between each event, with possible window-cleaning required between events. The effect of one combustion event on the next one is therefore not possible to be studied in a CVCV (Baert, et al., 2009).

Nevertheless, CVCVs are very popular for the study of spray and combustion characteristics, because of the precision with which individual parameters can be controlled and the relative ease of optical access. When looking at different fuel properties, and the effect of additives, a

full range of combustion events can be studied in a CVCV, with independent variations of temperature, pressure, and the gaseous composition in which diesel fuel self-combusts. Combustion products can be analysed easily, and the optical access to the spray and combustion event can help interpret the various data collected.

2.2.1.2. Chemistry of combustion

In diesel combustion, the fuel reacts with the oxygen in the air that is present in the combustion chamber. Air is often assumed to be composed of 21% oxygen, and 79% inert gases (by volume), taken as nitrogen. The fuels used in internal combustion engines, whether diesel fuel or gasoline, are blends of many different hydrocarbon compounds which are mostly obtained by refining crude oil. They are typically composed of about 86% carbon and 14% hydrogen atoms by weight (Heywood, 1988).

There are many molecular structures in which hydrocarbons can be found in nature and most of these can be found in commercial gasoline and diesel fuels. They include:

- Paraffins or alkanes which are single bonded open chain saturated hydrocarbon molecules. They can either be straight-chain molecules (e.g. methane, ethane, propane), which are called normal (n-), or, for bigger molecules, they can also be branched-chained, called isomers (iso- compounds). For example, octane can be n-octane, a single chain of 8 carbon atoms, or iso-octanes, which can be any combinations of 8 atoms of carbon, with branching.
- Cycloparaffins (also called naphthenes or cyclanes) are single bonded ring hydrocarbons. They are single-bonded so the ring can be easily broken. Examples include cyclopropane, cyclobutane, and cyclopentane.
- Olefins or alkenes are unsaturated open chain hydrocarbons containing a double bond between two carbon atoms. Both straight and branch-chain structures can exist. Olefins include one, two, or more double bonds. Ethene, propene, butene are olefins (also called ethylene, propylene, butylene)
- Acetylenes or alkynes are unsaturated open-chain hydrocarbons containing one triple bond of carbon-carbon.
- Aromatics are very stable ring structure hydrocarbons containing six carbon atoms and three single and three double bonds. The simplest of the aromatics is benzene (C_6H_6), which can accommodate additional CH_2^-groups in side chains. Examples include toluene, xylene. Several benzene rings can be bonded together to make poly-aromatics with two, three and more rings.
- Alcohols are organic compounds where a hydroxyl group (-OH) replaces a hydrogen atom. Methanol and ethanol are common examples of alcohols, the first having one carbon atom and the second two.

- Fatty acids esters are present in modern fuels as they are used in the making of bio-diesels refined from vegetable oil or animal fat. They are composed of a long saturated or unsaturated open chain bonded with a carboxyl group (-COOH) or a carboxylic ester (-COOR), where R can be a methyl, ethyl or propyl group. They are not found in crude oil, but can be added in various quantities (up to 100%) to crude oil. Linoleic acid methyl ester is one of the many examples of fatty acid esters used in bio-diesel.

Diesel fuel is composed of about 25% aromatics and 75% saturated hydrocarbons (primarily paraffins, including cycloparaffins). Unsaturated hydrocarbons are found in very low concentrations in both diesel and gasoline fuels. Diesel fuel also contains sulphur, although modern diesel fuels for road vehicle applications use diesel fuels with sulphur contents of ~10 mg/kg of fuel. Modern diesel fuels have a reduced aromatic content that can be as low as 15%, to reduce the content of poly-aromatics which are carcinogenic (World Health Organisation, 2014).

Gasoline fuels are refined to mostly straight and branched alkanes (there is a small portion of cyclanes and aromatics too, but no alkenes or alkynes). Gasoline fuels contain alkanes which are much shorter (fewer carbon atoms) than diesel (Taylor, 1985). The shorter paraffins make gasoline a much more volatile fuel than diesel, which does not vaporize at room temperature. They also make gasoline more difficult to auto-ignite.

Diesel fuel, contrary to gasoline, is not sufficiently volatile to form sufficient combustible vapour under atmospheric pressure and temperature. In an engine, a high pressure and temperature environment causes diesel fuel to auto-ignite. The diesel fuel reaction with air is therefore spontaneous, and cannot occur unless the conditions of pressure and temperature are correct (in an engine, that is around 15 bar pressure, 400°C). However, diesel fuel will auto-ignite under atmospheric conditions as long as the fuel temperature is elevated enough (circa 400°C). The high pressure is simply a consequence of the way air temperature is raised in a compression-ignition engine, but is not a requirement for spontaneous combustion.

The combustion reactions are complicated. The various hydrocarbons break down first to form radicals, which are needed for further reactions. Chain reactions then occur using the newly formed radicals, until a process known as branching occurs (for every one radical consumed at least two are generated), leading to a large release in chemical energy known as combustion. The time between injection and start of combustion is known as the ignition delay, and varies depending on how quickly the fuel breakdown reactions occur and branching reactions are reached.

It is impossible to determine all the chemical reactions that occur during a combustion process. Not all diesel fuels are the same, and the temperature and pressure conditions are such that

certain reactions may occur more quickly than others. The auto-ignition process has been studied in detail as a function of the type of hydrocarbon, because the auto-ignition capabilities of fuels are important for both diesel fuel (where it is sought) and gasoline (where it is unwanted) (Heywood, 1988).

Alkane length has an effect on compression-ignition. As alkane length increases, the ignition is easier and ignition delay shortens. Long chains are sought, so branching is unwanted. Double bonds and aromatic molecules are difficult to auto-ignite, so their maximum proportion in diesel fuel is controlled.

Long olefins with two or three double bonds are generally unwanted, but olefins with a single bond have a fairly small effect on fuel ignitability.

Naphthenes, being single bonded, are better in auto-ignition than the corresponding ring-size aromatics. Increasing the side chain of both naphthenes and aromatics improves auto-ignition of diesel fuel (Lovell, et al., 1948).

2.2.1.3. Pre-combustion in a constant volume combustion vessel

Unlike gasoline combustion, diesel combustion is a compression-ignition process, which requires a certain set of pressure-temperature conditions to auto-ignite. In a CVCV, these conditions are very difficult and time consuming to achieve using conventional means (i.e. heaters, and pressurised air). Furthermore, the energy losses to the walls through heat transfer and leakages of such vessels make them increasingly difficult to control so as to obtain the perfect conditions rapidly. CVCVs can also be very heavy due to the thick walls required to contain high pressures at continuously high temperatures, where the tensile strength of metals reduces substantially.

A safer and easier method than maintaining a CVCV continuously at high temperature is to use a pre-combustion event (Baert, et al., 2009). The principle is to introduce a controlled quantity of mixed gases in a previously evacuated CVCV. These gases are then ignited using conventional means (spark plug). After ignition and combustion, the resulting combustion products still have sufficient air for a second combustion event. Pressure and temperature conditions after combustion can be similar to those in a traditional diesel engine. Diesel fuel is then injected in this hot pressurised products mixture and auto-ignites, similarly to the ignition process in a diesel engine (Baert, et al., 2009).

2.2.2. **Heat release rate and ignition delay**

2.2.2.1. Definition and methods of measurement

When conducting combustion experiments, information on the rate of combustion can be obtained by means of heat release rate analysis. This is the rate of release of the fuel's chemical

energy, or rate of fuel burning with respect to time (in the case of a CVCV), or crank angle (in the case of an engine). For most diesel fuel analysis, the gas is considered to be ideal and the apparent net heat release can be calculated knowing the rate of change in volume, and the rate of change in pressure, as well as the ratio of specific heats $\gamma = c_p/c_v$ such that (Heywood, 1988):

$$\frac{dQ_n}{dt} = \frac{\gamma}{\gamma-1} p \frac{dV}{dt} + \frac{\gamma}{\gamma-1} V \frac{dp}{dt} \quad (2)$$

In a constant volume combustion vessel, the equation simplifies with the volume rate set to zero and the rate of heat release can be approximated using only the pressure gradient.

The above expression has its origins in the First Law of thermodynamics. The left hand side of the equation represents the net rate of energy release from the fuel, which is the net rate of energy release after energy from endothermic reactions and heat losses from the system have been subtracted from the energy released due to exothermic reactions. The right hand side represents the way the net energy release is used within the system, that is for work (represented by rate of change of volume) and internal energy changes (represented by dp/dt because it is easier to measure than dT/dt). The heat release rate can be useful in showing when the combustion has started and how it is progressing within the engine combustion chamber or CVCV.

As explained in section 2.2.1.2. , as soon as the diesel fuel comes in contact with the high temperature air, primary chemical reactions occur to form radicals. These radicals then induce further chain reactions, until there are enough radicals to induce a phenomenon known as branching. When branching occurs, the chemical reactions multiply exponentially and energy is released very rapidly. On a macroscopic level this is seen as an outburst of energy including light: that is, combustion.

Another quantity which can be deduced from the heat release rate is the ignition delay. The ignition delay is the time between injection of the fuel and the start of combustion. The timing of fuel injection can be determined in various ways. Fast image acquisition can determine when fuel is actually injected into the combustion chamber. Alternatively, a sensor can be placed to find out when the injector needle lifts. The start of combustion is more difficult to determine. It can be determined from changes in the pressure or heat release rate. In some cases, the change in slope of the in-cylinder pressure data (or in-vessel) may be difficult to discern. Sometimes, a luminosity sensor can be used to find out when the flame occurs, although this method has been found to be uncertain, and occurring late compared to the actual chemical energy release (Heywood, 1988) that causes a detectable rise in the gas pressure.

During the ignition delay, the fuel must undergo some physical changes: atomization, vaporization, mixing with air, and then pre-combustion reactions need to occur in order to lead

to auto-ignition. It is known, from the previous section on sprays, that the atomization, vaporisation and mixing depend greatly on the spray characteristics, the injection pressure and the physical properties of the fuel (notably viscosity). The chemical processes occurring after vaporisation and mixing of the fuel and air mainly depend on the fuel composition, but also cylinder temperature and pressure.

As cylinder/vessel gas pressure increases, ignition delay decreases. This relationship is linear as long as there is no effect from the fuel spray interacting with the walls (Heywood, 1988). Gas temperature has a similar effect. As it rises in the combustion chamber, the ignition delay is decreased.

In order to define the ignition quality of a diesel fuel, the cetane number (CN) is used. The CN scale is defined by blends of two pure hydrocarbon references. The first, n-cetane (hexadecane, $C_{16}H_{34}$), is a hydrocarbon with very high ignition quality (ignites easily) and represents the top of the scale, 100. The other, heptamethylnonane (HMN), a greatly branched iso-cetane, has a very low ignition quality and represents the bottom of the scale with a CN of 15. Thus, CN is given by:

$$CN = \%\left(\text{n-cetane}\right) + 0.15\ \%(HMN) \quad (3)$$

In a cetane test of a new fuel, it is tested in a specially designed diesel engine. Mixtures of n-cetane and HMN of different proportions are then tested until a proportion is found which has the same ignition characteristics (ignition delay) as the new fuel. The CN of the real fuel is finally calculated from the CN equation above.

The Cetane number test is standardised, but very expensive to realise (ACEA, et al., 2006) (Heywood, 1988). Often, a calculated Cetane index is used instead to estimate ignition quality of diesel fuels. It is based on fuel properties, notably API gravity and mid boiling point. However, this index is not accurate when the fuel contains oxygen, as in the case of bio-fuels.

Cetane number is known to have a very strong correlation with ignition delay for a particular fuel blend. If the CN of a fuel is too small, the ignition delay will be large. This will mean that the fuel will be almost entirely injected in the combustion chamber before it is ignited, which will increase the rate of heat release in the premixed combustion phase of the diesel combustion. This results in a very violent, noisy, and highly exothermic reaction (high combustion temperature) which can be damaging to the engine. Since NO_x emissions occur at high temperatures (see section 2.2.3.), a low cetane number will also increase the NO_x emissions of the engine. Furthermore, because the fuel is burned later, more fuel has time to wet the walls of the combustion chamber, resulting in more soot and unburned hydrocarbons in the exhaust of the engine. An extremely low CN (e.g. CN = 30) could result in an overly delayed combustion,

which is quenched too fast by the piston movement, resulting in poor fuel conversion efficiency. A high CN (~50) is always sought.

2.2.2.2. Additive effect on ignition delay

The addition of combustion improver additives (CI) in diesel fuel has become a very common and effective way of lowering ignition delay. Addition of CI will increase the CN by up to about 10, even with a small quantity of additive of 250 to 2500 ppm. As discussed in the previous sections, the addition of Cetane improver can also help reduce emissions. Some reactions cannot occur straight away as they require the radicals provided by earlier reactions. CN additives provide free radicals early in the breaking down chemical reactions of the diesel fuel, thus accelerating the chain reaction process that occurs during pre-ignition (ATC, 2004).

The effect of other additives (other than ignition improvers) on ignition delay is not available in the literature as very few additives are tested for effects, such as ignition delay, that they have not been specifically developed for. It is however possible that other additives, which are composed of hydrocarbon chains, provide free radicals too when the breaking down of fuel occurs, or conversely, increase ignition delay by absorbing radicals (e.g. anti-knock additives).

2.2.3. **Emissions**

Emissions constitute the products of the combustion reaction in an engine exhaust. These products are released to the atmosphere after the combustion reaction has taken place. In a car, that takes place through the exhaust.

Intensive research is being carried out on diesel emissions so as to limit the damage they might have to human health and environment. Nitrous oxides (NO_x), carbon monoxide (CO) as well as particulates and unburnt hydrocarbon emissions are all regulated exhaust emissions.

NO_x formation occurs when the Nitrogen present in the air, or, in some instances, in the fuel, reacts with the oxygen in the air. This reaction cannot occur unless the temperature is very high (>1500 K). Thus, temperature of the flame is known to have a large effect on NO_x emissions in diesel combustion. The temperature of the flames can be reduced by using exhaust gas recirculation (EGR), which involves diverting part of the exhaust gases back to the combustion chamber, reducing the oxygen concentration and peak combustion temperature.

Carbon monoxide (CO) emissions are highly dependent on the local air to fuel ratio of the combustion. Diesel combustion is, overall, lean and CO emissions are small and of less concern than CO emissions from gasoline engines.

Hydrocarbon emissions occur in diesel engines for three main reasons:

- Overleaning: In diesel sprays, the outer layer of the spray can become too lean to self-combust, leaving unburnt hydrocarbons. The thickness of the overlean and non-combustible layer increases with longer ignition delay, as more spray has time to vaporise and over-mix with the surrounding air. The overleaning process can be reduced by shortening the ignition delay, resulting in a decrease in hydrocarbon emissions.
- Undermixing occurs when fuel leaves the injection nozzle at very low velocity (end of the injection process). Undermixing leads to a rich localised equivalence ratio, with not enough velocity to mix with the surrounding air, and not enough air for complete combustion. This produces unburnt, or partly burnt, hydrocarbons which are then released to the atmosphere.
- Fuel remaining trapped in the injector nozzle holes vaporizes late in the combustion process when gas temperatures are reduced and thus fails to burn completely.

In addition to the principal reasons listed above, when the reactions are quenched or misfire occurs, the hydrocarbon content in the exhaust also increases, due to some unburnt fuel (Heywood, 1988).

Particulates start off as soot spherules (almost pure carbon particles) on which some organic compounds and condensed water vapour are absorbed. They are solid particles, which can be seen as smoke or deposits in the combustion chamber and exhaust. The spherules combine into larger clusters of hundreds of spherules to become the particulates. Some particulates accumulate in the combustion chamber, valve seats (gasoline) and injector to form deposits.

Finally, spray characteristics and emissions are closely related. For example, reduction of droplet size provides an easier burnout of fuel. This means that there will be fewer residual hydrocarbons, and thus improved emissions (Jones, 1977).

2.2.3.1. Methods of measuring emissions

Emissions are usually measured using standalone systems such as the Horiba MEXA 9100 HEGR used for this research project. These systems employ various methods of analysis to measure the different components in the exhaust gases.

For NOx emissions, chemiluminescence is used. This method is based on the principle that when NO reacts with ozone (O_3) it forms NO_2, but also releases a photon in the process. A photomultiplier can be used to find out the amount of photons emitted, and thus define the concentration of NO present in the exhaust through calibration. A chemiluminescence analyser can measure, in addition to NO concentration, the concentration of NO_2 in the exhaust. By using

a heated catalyst, the NO_2 gases present in the exhaust can be converted to NO and passed through the analyser which gives the concentration of NO_2 after calibration. By measuring the exhaust gas sample with and without the catalyst, the concentration of NO and NO_2 can both be found (Ferguson, 1986).

To measure CO and CO_2 content, a non-dispersive infrared analyser is used. This method can be used for many gases. Infrared energy is used to excite the gases. At certain wavelengths, the gas absorbs radiation. By using an infrared detector to measure the amount of radiation absorbed, the amount of gas, here CO or CO_2, can be found through calibration. The source of infra-red radiation is usually broadband and separate narrowband filters are used to select which specific gas is being absorbed and detected (Ferguson, 1986).

Hydrocarbon content can be measured using the flame ionisation method. This involves passing the exhaust gases through a hydrogen flame. The flame's high temperature breaks the carbon-carbon bonds in the unburnt hydrocarbons producing charged ions, which are counted using electrodes which measure total ion charge. The limitation with this method is that it can only count the number of carbon atoms, as these are the atoms that ionise. Thus, the molecular structure of the unburnt hydrocarbon cannot be determined, only the total number of carbon-carbon bonds. Furthermore, the ionising response of the sample depends on how the molecule is structured. Alkenes and alkynes will not respond in the same way as alkanes to the instrument, producing different total charge for the same number of carbon-carbon bonds. For all these reasons, the flame ionisation method reports measurements in ppmC rather than using a specific gas or molecular structure. The calibration hydrocarbon gas (e.g. propane or methane) is often stated. For more precise analysis of hydrocarbon content, such as molecular structure, gas chromatography and/or mass spectrometry should be used (Ferguson, 1986).

Paramagnetic analysis is used to determine oxygen concentration. This method is based on the fact that oxygen is a polar molecule and is attracted to a strong magnetic field, which most other gases are not. The sensor usually consists of a cylindrical shaped container inside of which is placed a small glass dumbbell full of nitrogen. The dumbbell is suspended on a platinum wire with a non-uniform magnetic field. When a sample gas flows through the system, the oxygen will be attracted to the stronger of the two magnetic fields, resulting in a rotation of the dumbbell. This rotation is then measured using optics, or by measuring the current required to force the dumbbell back into its initial position.

2.2.3.2. Additive effects on emissions

Additives are chemical compounds added in very small quantities (parts per million) to a fuel. For this reason, it is expected that all additives, as they break down during combustion, will have some effect on emissions. This effect is, however, insignificant for most additives (ATC,

2004) compared to the effect of combustion and fuel properties. The additives may have an effect on a particular aspect of combustion, which in turn, may have a positive or negative effect on emissions. This is the case for CIs, which reduce ignition delay, and thus improve NO_x and other emissions.

2.3. Research in pump power for diesel fuels

2.3.1. **Theory on lubrication**

Lubrication is a process widely used to prevent fretting or other wear damage to two metal surfaces moving relatively to each other. Depending on the thickness of the lubricating film, different regimes of lubrication exist. These regimes define the way the lubrication process occurs. Different engineering applications may require different lubrication regimes (Pirro & Wessol, 2001).

There are two main regimes of lubrication: boundary and hydrodynamic (or fluid film) lubrication. There is also a range of mixed lubrication conditions between boundary and fluid-film lubrication (Khonsari & Booser, 2001).

In the hydrodynamic or fluid film lubrication regime, the moving surfaces are completely separated by a film of liquid or gaseous lubricant. In this regime, a load-supporting pressure is generated by squeezing the film trapped between the moving surfaces. The squeezing is generated as a result of the relative motions, or in other cases film supporting pressure can be generated by external pressurisation of the gap between the surfaces. Because of this, the viscosity of the lubricating fluid and the geometry of the sliding surfaces are important in hydrodynamic lubrication. Because viscosity of a fluid changes with temperature, the relationship between viscosity and temperature of the lubricant is also important. In hydrodynamic lubrication, viscosity, temperature, and shape of the components are important in order to determine what the friction coefficient is. Various approximations exist to calculate this coefficient, depending on the type of application (Khonsari & Booser, 2001).

Boundary lubrication occurs when the fluid cannot maintain separation of the two surfaces. This may happen because the pressure of the fluid films is insufficient to carry the load. The only lubrication that remains is from the adsorbed or bonded surface layer of the lubricant onto the metal surface. This layer is a molecular film that coats the relatively rough sliding surfaces. It is very small, of the order of 0.0025 microns, which is less than 1% of the typical roughness of the surface of machined parts. The molecules, typically long polar chains, are adsorbed or bonded to the metallic surfaces, with the polar head attached to the metal surface, and the molecular chain perpendicular to the surface. The molecules may even bond to each other. When the metal surfaces come in contact with one another, the molecules slide on one another, reducing true metallic contact (Williams, 1994).

For this reason, when boundary lubrication occurs, such as between the engine piston and liner, the transport properties of the lubricant are not important, but the molecular structure of the adsorbed molecules on the metal surface is what governs the coefficient of friction. Generally speaking, a longer molecular chain will reduce the coefficient of friction further. Also, fatty acids have been shown to be more efficient than hydrocarbons, of equal molecular weight (Williams, 1994). In diesel automotive engines, these adsorbed molecules are present in both the lubricating oil and the diesel fuel. They can occur naturally in both diesel fuel and lubricating oil, or be added later as friction modifier (FM) additives if necessary, such as in low sulphur diesel fuels (see section 1.1.4.)

Another significant aspect in boundary lubrication is the strength of the bond between the active end of the protecting molecule and the metal surface to which it adheres. Two types of bonds exist,

- Physical bonds, where electrostatic or dipole forces link the molecules to the surface. This is a weaker bond, but allows the lubricant to be detached from the metal surface while leaving it unchanged.
- Some molecules on the other hand chemically react with the metal surface making irreversible chemical reactions that permanently modify the state of the surface. This type of reaction forms a surface called a metallic soap. It is very efficient at reducing the friction coefficient, and usually forms a compound which has a high melting point and is thus efficient for a wider range of operating temperatures (Williams, 1994).

In the case of FMs, the additives act during boundary lubrication. They need to be added in sufficient quantity to coat the full surface of the metal. However, too much of the additive may adversely affect the bulk properties of the carrier lubricant, or in the case of fuel additives, the fuel. It is also important to note that the viscosity of a fuel has no effect on the action of the friction additive; also, the FMs that act by surface coating will not be effective during hydrodynamic lubrication (ATC, 2007) (Williams, 1994).

Finally, it should be noted that temperature has a strong effect on boundary lubrication, but not because of the change in viscosity. When molecules are adsorbed on the metal surface, the increase in temperature tends to make the molecules more mobile and will render those molecules more soluble in the bulk lubricant; the number of bonded layers (and the thickness of the molecular layer) will decrease as a result. On the other hand, if the bond is a chemical one, the increase in temperature will tend to speed up the rate of reaction, and improve the friction coefficient. However, after reaching a certain temperature, the metallic soaps will start to undergo thermal decomposition, and the rate of decomposition will increase exponentially, rendering them ineffective and causing scuffing (permanent damage caused by the surfaces rubbing together).

In order to create boundary lubrication at extreme temperatures, other types of additives exist which react with the hot metal surface. They include small quantities of organic compounds containing sulphur, chlorine or phosphorous. Those compounds are inert at low temperatures, but react with high temperature metal to form protective films of solid metal chloride, sulphide or phosphide. A mix of these additives with other lubricant additives in fuel could provide a low frictional behaviour on high temperature surfaces (Williams, 1994).

2.3.2. **Pumping power**

2.3.2.1. Lubricity inside a pump

In the light/medium duty high pressure pump of a diesel engine (Figure 2.3), an eccentric cam (2), driven by the driveshaft (1) activates usually three or sometimes more pumping elements, or plungers (3). The fuel is supplied to the inlet (6), and goes to the high pressure pump's lubrication and cooling circuit, as well as above the piston through an inlet valve during the suction stroke. The inlet valve (4) closes when the pump piston passes through Bottom Dead Centre (BDC), and the fuel is then compressed beyond the delivery pressure. The increasing pressure opens the outlet valve (5) as soon as the pressure above the piston reaches rail pressure, and the compressed fuel enters the high-pressure circuit. The fuel is delivered as the plunger rises to Top Dead Centre (TDC), where the outlet valve closes. The fuel left in the chamber relaxes, and the cycle starts again.

Figure 2.3: High-pressure diesel pump (schematic, cross section) (Robert Bosch GmBH, 1999)

Since three or more delivery strokes take place every revolution, the pump is hydraulically balanced and the radial stress on the pump shaft remains uniform during operation. The power required to drive the pump climbs in proportion to the pump delivery pressure which is determined by the pressure in the rail, and the pump's speed (delivery quantity) (Robert Bosch GmBH, 1999).

A typical diesel high pressure common rail pump is not in synchronisation with the engine and runs at half the engine speed (through the use of a belt). This can approximately be anything between 500 to 3000 revolutions per minute (RPM), or 8.3 to 50 Hz. The maximum common rail pressure in a diesel engine has been increasing steadily over the years, and nowadays pressures higher than 1500 bar are used in some light and medium duty diesel engines. This means that common rail pumps now require a significant amount of energy to run, up to 7 kW in some cases (Richards, 2010).

The pump is required to provide high pressure at various engine speeds. Furthermore, the high pressure diesel pump is a positive displacement machine, meaning that all fuel that goes into the pump has to come out at the same rate; no slipping of the pump parts is possible. This implies that excess high pressure fuel is delivered at engine idle and part load operation. This excess fuel is returned to the tank via a pressure control valve located on the pump itself. This valve can be electronic, and thus control the delivery pressure accurately, or it can be mechanical, acting as a safety valve, or a spill valve. When an electronic pressure relief valve is present on the common rail, a spill on the pump itself can be redundant. However, since common rails and pumps are usually built to accommodate multiple systems, all high pressure diesel pumps are fitted with a safety spill valve to ensure the pump is not damaged. The safety valve of high pressure pumps is designed to be able to spill the full amount of fuel being pumped; this ensures the pump still rotates, even if there is a blockage in the common rail (Robert Bosch GmBH, 1999).

The fuel itself is the lubricant for all moving parts of most medium duty pumps. It flows through the whole pump and lubricates the cam, the piston, and the rest of the pump. As the fuel gets pressurised, fresh fuel enters the pump and becomes the lubricant, while the fuel inside the pump is expelled by the piston. This ensures that the fuel is renewed, but also that the pump is cooled by the fuel so that it does not get too hot.

Pumps operate in both boundary and hydrodynamic lubrication regimes, depending on which moving part of the pump is being considered. FMs act during boundary lubrication as replacements for natural boundary lubricants which are nowadays removed, to an extent, due to the removal of sulphur and aromatic molecules from the fuel. Hydrodynamic lubrication is generally preserved by ensuring the fuel properties such as viscosity stay within specifications (Kajdas & Majzner, 2001) (ACEA, et al., 2006).

Cold flow (CF) additives are known to improve the flow properties of the fuel at cold temperatures by preventing wax formation. As wax in fuel is essentially fuel that is starting to freeze solid, the viscosity of the waxed and partly-waxed fuel is increased by wax formation. Therefore, although the addition of CF additive is not expected to have any effect at room

temperature, it is expected that CF additives will improve the hydrodynamic lubrication regime of untreated raw fuel by simply not allowing the fuel to form large wax crystals.

2.3.2.2. Experiments on different fuels in pumps

Although some literature can be found on the design of pumps, and how they work with certain fuels, very little literature mentions the effect of various fuels on common rail diesel pump operation.

It has been found that wear on the various components of a pump is not a major operational issue (Armas, et al., 2011). Wear in a pump rarely occurs under normal conditions, as the lubricating properties of the fuel and its additives prevent scuffing from occurring by providing protection during boundary lubrication.

2.3.3. **Lubricity of additives measurements**

Using the HFRR test, common FMs (fatty acids) have been shown to be effective in avoiding surface scuffing with low sulphur diesels (Kajdas & Majzner, 2001). Generally, it was observed that the wear scar diameter is reduced on any fuel when a small concentration of fatty acid is added to the fuel (Kajdas & Majzner, 2001). This is due to the boundary lubrication improvement as described in section 2.3.1. It was also found that the concentration of the fatty acid used does not influence the wear scar diameter significantly. This can probably be explained by the fact that as long as the ball and disc are both coated by at least one molecular thickness layer any extra molecules are not necessary. This shows that a very low concentration of additive is enough to reduce wear.

It has also been found that adding the same fatty acid to different diesels can result in different wear ratios, suggesting that some kind of molecular interaction exists between the fatty acid and the base fuel. Therefore, some FMs are more effective on certain fuels than on others (Kajdas & Majzner, 2001).

An experiment is reported in the literature where one base fuel was refined progressively to greater levels, so as to give progressively lower sulphur content. All the resulting fuels were tested, and it was found that the wear increased with lower sulphur content (although, as mentioned in section 1.1.4. , the hydro-treating process to remove the sulphur is the cause of lubricity loss). However, the fuels also had different viscosities since viscosity of the fuel decreases with the refining process. The decrease in viscosity caused by hydro-treating of the fuel may have had the effect of increasing the wear scar as well. Whether the effect on the scar is due to viscosity reduction or sulphur removal is impossible to tell from these results. However, when an additive was added to these fuels, the wear scar diameter dropped to a consistently lower wear scar diameter, proving that the additive acted regardless of viscosity or sulphur content, as it simply coated the surfaces (Kajdas & Majzner, 2001).

These results and any HFRR results always measure a wear scar diameter. It has been shown that there is a strong correlation between friction and wear, although the relationship is complex. Aspects such as metal corrosion or material relocating on the edges of the wear cavity without breaking off, a phenomenon known as ploughing, are effects of wear that contribute differently to friction. Corrosion on a metal surface will have a negative effect on friction, but will not be induced by wear. Ploughing creates increased surface roughness, which is seen as an increase in friction, but not as an increase in wear scar diameter. In some specific systems, where corrosion and ploughing are negligible, a relationship can be established (Kajdas & Majzner, 2001).

2.4. Conclusions from literature review

This literature review has assessed the effects of some environmental properties as well as fuel properties on three specific aspects of the combustion process: spray formation, combustion and pump torque.

Cone angle, spray length and droplet size distribution were discussed, along with the various methods used to measure those spray characteristics. It was determined that cone angle and spray length were mostly affected by set conditions of pressure, density, temperature, or nozzle geometry rather than through an effect of fuel properties. Therefore, the literature survey focused on the droplet size distribution analysis of sprays, as viscosity and surface tension, which are both fuel dependant properties, are known to affect them. As additives are known not to affect fuel properties, it was concluded that additives were not expected under normal conditions to have any effect on droplet sizing. However, no literature could be found to prove this theory. Furthermore, little is known of the spray behaviour when fuel waxes, as fuel filters usually catch all of the wax before injection.

The principles of diesel combustion are briefly discussed in this chapter, including the chemistry of combustion, the advantages and limitations of a combustion vessel, heat release rate analysis and measurements, and emissions analysis and measurements. This section concluded that little was known about the effects of particular additives on combustion properties, such as ignition delay or emissions measurements, as the additives were not designed to affect these parameters. Combustion improvers are the exception, where they are known to affect the cetane number (CN) of a fuel.

Research on lubrication and lubrication theory showed that the additives play a crucial role in the boundary lubrication regime of moving parts in a fuel delivery system. The lubrication of pump parts was found to affect torque significantly, and yet no data was found to link the effect of pump torque to the concentration of lubricity additives in a fuel delivery system.

A series of three separate experiments were devised to bridge some of the gaps found in the literature survey regarding the effects of additives. To link the pumping power to fuel

lubrication, different additives were tested in a fuel pump and the torque was recorded. It was decided to investigate the effect of waxing fuel on droplet size distribution, with and without the help of CF additives. To determine the effect of CI additives on combustion delay and emissions, tests were carried out on an engine bed and in a combustion vessel. The effects of some groups of additives on these three aspects of the combustion cycle were understood further as a result.

Chapter 3

Experimental systems

3.1. Fuel pump torque characterisation rig

3.1.1. **Initial design and build**

In diesel engine fuel delivery systems, the power required to drive the high pressure diesel fuel pump at full load can be up to 10% (more than 7 kW) of an automotive engine's power output. Furthermore, common rail fuel pressure requirements in car diesel engines have been increasing steadily over the years in order to improve the air-fuel mixing, and thus increase the engine power output and efficiency, and reduce pollutant exhaust emissions. The increase in common rail pressure has made the diesel fuel high pressure pump a much more important part of the fuel delivery system. In particular, careful consideration has gone into the design and performance, including friction losses and durability.

The diesel fuel pump is usually not a component of the diesel automotive engine and is not lubricated by the engine oil, like many engine parts. However, diesel fuel pumps have pistons and moving parts undergoing extreme stresses in order for the fuel to reach pressures above 1500 bar. The constant flow of diesel fuel is what lubricates the high pressure pump. The fuel, acting as a lubricant, reduces damage to the pump internal surfaces and friction torque.

Lubricity additives are used to enhance the operation of the pump by reducing damage in pump regions operating under boundary lubrication, and also reduce frictional torque. Lubricity improvers act by improving the boundary lubrication regime of diesel fuels, and prevent the premature wear and failure of pumps (see section 1.1.4.). A maximum wear scar diameter of 400 micron on the HFRR test is considered adequate to control the fuel lubricity in modern diesel fuels in current automotive engines (ACEA, et al., 2006).

The power required to drive the pump is only partly dependant on fuel lubricity. Common rail pressure and fuel pump rotational speed (which is governed by the engine rotational speed) together have by far the largest effects on the overall power required to drive the pump. In turn, fuel lubricity is influenced by the fuel chemical composition and the fuel temperature, which affect the fuel physical properties (such as viscosity, density and surface tension). There is however limited knowledge as to how important the fuel properties and additives, such as lubricity improvers, affect the power required to drive a pump. Finally, there is limited knowledge as to whether fuel additives which are not lubricity improvers may affect some of the physical properties of certain fuels, to an extent where the power required to operate a high pressure diesel fuel pump is altered.

With these requirements in mind, a rig was designed that would measure power required to drive a commercial automotive high pressure diesel pump at various conditions found in an automotive engine's delivery system. The pump rotational speed, common rail pressure, fuel temperature and the type of fuel would all be varied independently of each other over the ranges corresponding to modern diesel engine delivery systems. It was therefore possible to measure the effect of various fuel additives on pump power.

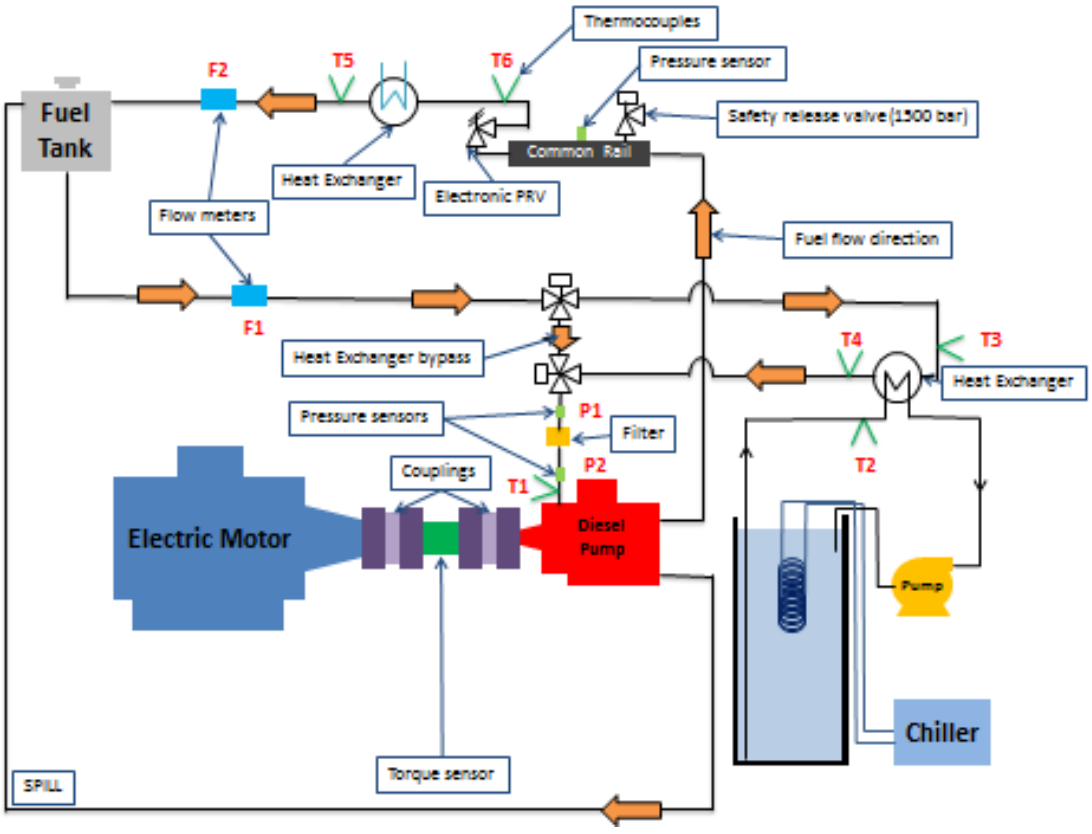

Figure 3.1: Schematic of the fuel pump torque characterisation rig including chiller and instrumentation (T = thermocouple, F = Flow meter, P = Pressure sensor)

The system consists of an automotive high pressure fuel pump driven by an electric motor at various speeds to simulate vehicle engine rotational speeds. An axial torque sensor was used to

determine the torque provided by the electric motor in order to drive the diesel pump, as seen in Figure 3.1. Knowing the rotational speed and the torque, the power required to drive the pump could be determined via the equation $P = T\omega$ where P is power in W, T is torque in Nm and ω is rotational speed in rad/s.

An automotive engine commercial common rail and associated electronic pressure relief valve (PRV) and pressure sensor were used in order to regulate the fuel pressure in the common rail. The common rail system stores fuel for a short duration at a constant high pressure. From the common rail, fuel is supplied to all the injectors. The common rail was used to simulate conditions found in car engines, with the exception that fuel was not injected from the common rail into an engine combustion chamber. Instead, pressurised diesel fuel was released by the rail's PRV back to the fuel tank, in a closed loop system.

Two heat exchangers were used to control the fuel temperature before the pump fuel inlet. The heating of the diesel fuel in this closed loop system as a result of fluid friction losses, especially high pressure throttling from the common rail, was sufficient to raise the fuel to high temperatures. The first heat exchanger (cooler) used cooling water from the mains and was located after the common rail PRV. This heat exchanger allowed cooling of the fuel down to room temperature before it reached the fuel tank (see Figure 3.1). The second heat exchanger (chiller) was located right before the diesel pump and was only used (it could be bypassed) when temperatures below room temperatures needed to be reached. This heat exchanger was supplied with refrigerated ethylene glycol from a chiller system at temperatures down to -20°C to cool the fuel down in order to simulate temperatures found in cold climates.

The system was a closed loop one, where about 4 litres of fuel were recirculated at the desired conditions of common rail pressure, pump speed and fuel temperature. A valve at the system's lowest point allowed for complete draining of the fuel, and pressurised air was used to blow out the fuel left in the pipes between experiments with different fuels. The fuel filter could also be changed between tests involving different fuel blends with additives.

Finally, the rig was designed to allow temperature, pressure, and flow rate to be measured at various points in the system. A particular configuration of the measuring sensors is shown in Figure 3.1; however the instrumentation could be readily relocated around the system to suit experimental needs. A high speed data acquisition card linked to a PC running Labview software was used to control the fuel temperature and pressure in the system, as well as record the necessary data.

3.1.2. **Pressure control**

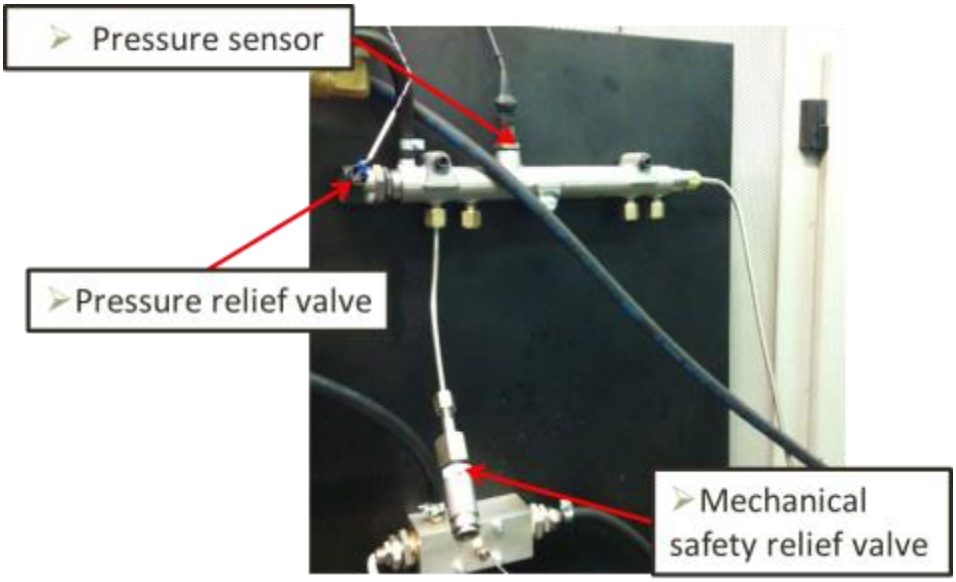

Figure 3.2: The common rail system

A Bosch diesel common rail was chosen to control fuel pressure. This commercial vehicle common rail was chosen in order to design the system to be representative of the conditions found in a typical commercial automotive engine. The common rail chosen is used on modern cars at up to 1500 bar fuel pressures. An electronic pressure relief valve (PRV) and a pressure sensor were used to regulate the pressure in the rail using software. For safety reasons, a mechanical pressure relief valve was also added to the system to ensure the common rail was not inadvertently pressurised beyond its design pressure (Figure 3.2) should the electronic valve fail with the pump still in operation.

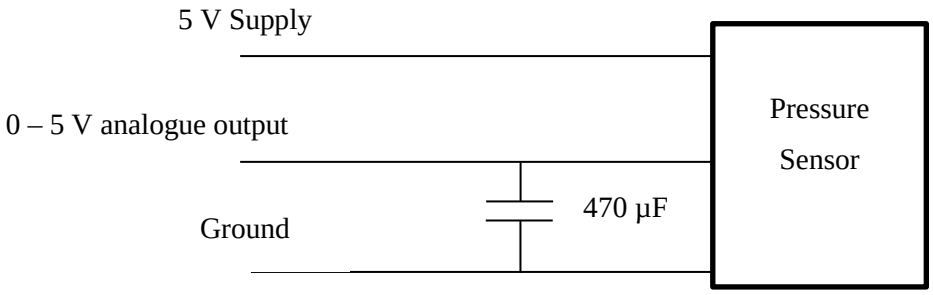

Figure 3.3: Circuit diagram of pressure sensor

The measurement and control of the common rail pressure was carried out using a DAQ USB6210 National Instruments (NI) card, running custom built Labview software developed by the author. The software received the 0-5V analogue signal from the common rail pressure sensor, and used a conversion factor to determine the common rail pressure in bar. The electronic noise was filtered using a 470 µF electronic capacitor. A circuit diagram for the pressure sensor can be seen in Figure 3.3.

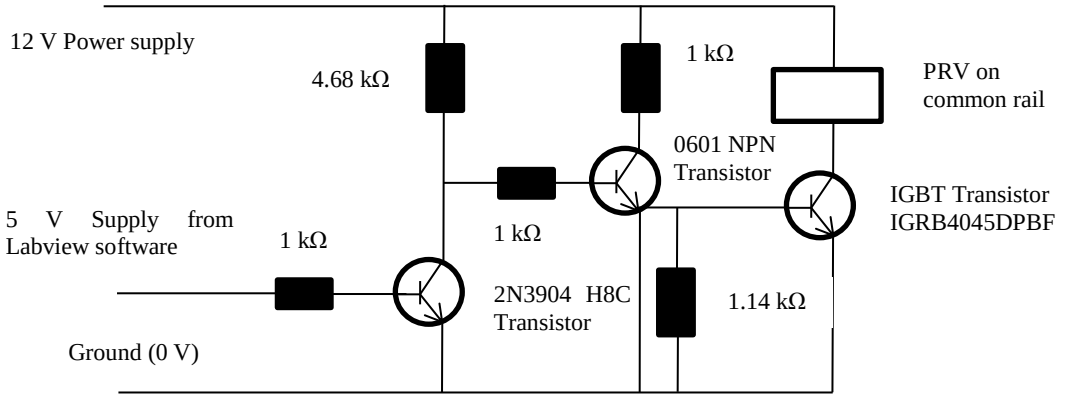

Figure 3.4: Circuit diagram of Pressure relief valve

The software used a proportional, integral and derivative (PID) software controller relying on pulse-width modulation (PWM). The Labview software generated a 5V PWM signal at 1 kHz frequency and this was applied to the electronic PRV. Depending on the desired pressure, the software computed how long the PRV needed to be open in order to release a sufficient amount of fuel to keep the pressure in the rail constant. A high voltage pulse supplied to the PRV closed the valve, while a low signal opened it. The 5V signal from the NI card did not have sufficient voltage and current to drive the PRV, so it was amplified after the card and supplied to the PRV at the correct level of 4A, 12V. This was done using a high speed amplifier which used a set of transistors as shown in Figure 3.4 constructed by the author. The IGBT transistor can take high current (18A) while maintaining the very short response time (93 ns turn off time), required for this particular system.

The constant fuel pressure in the common rail could be controlled from a lowest level of about 100 bar, depending on the motor speed, up to a maximum level of 1500 bar. When a pressure set point was changed, it took a short time for the new pressure to be reached (less than 30 s). The Labview software controller could maintain constant pressure to about 2% of the desired value. This range and accuracy are similar to those found in the common rail of commercial vehicles.

3.1.3. **Temperature control above room temperature**

The temperature was recorded by the data acquisition card using various thermocouples positioned in the system. These thermocouples were connected to amplifiers to raise the very low voltage thermocouple signal to an analogue 0-5V readable by the DAQ (see Figure 3.5).

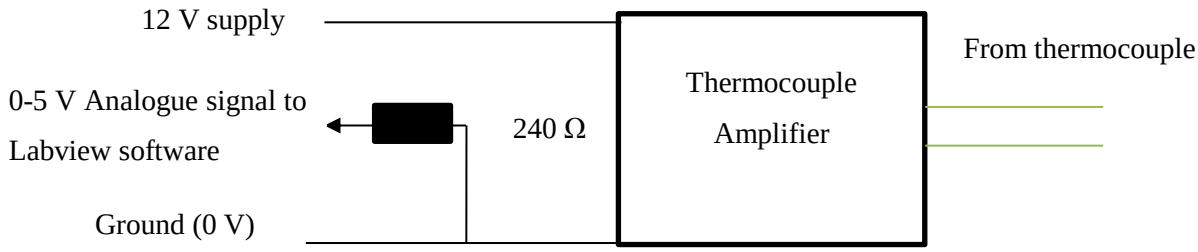

Figure 3.5: Circuit diagram for thermocouple amplifiers

The fuel rapidly heated up due to throttling from the high pressure common rail. Since the system had a limited amount of fuel (about 4 litres), and was in closed loop configuration, the fuel could quickly reach temperatures up to 70°C or greater. The temperature of the fuel was controlled using software via a heat exchanger using cooling water around 8°C from the mains as its cooling fluid.

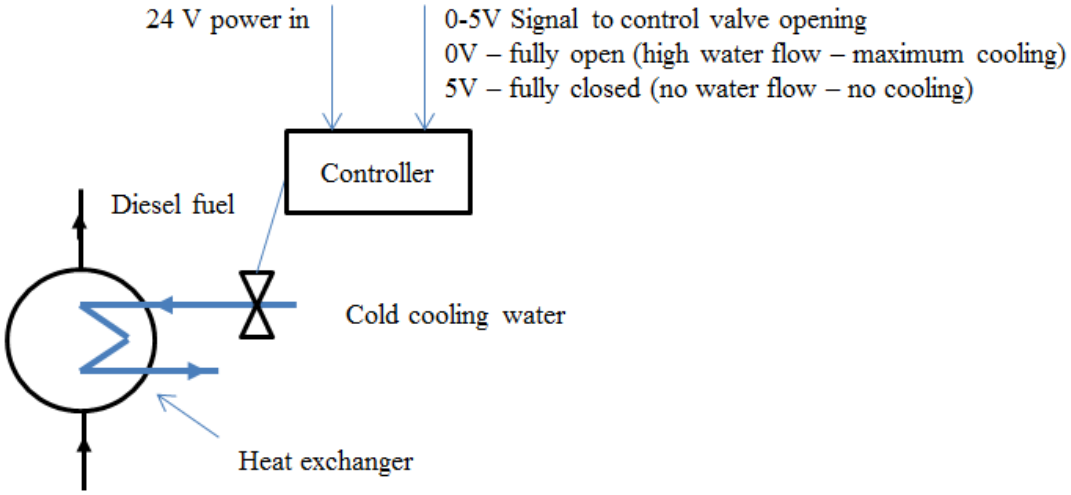

Figure 3.6: Circuit diagram for cooling water heat exchanger control

The heat exchanger cooler (see Figure 3.1) was controlled in a similar manner to the common rail pressure, using a software PID controller. The Labview software monitored fuel temperature as it entered the high pressure fuel pump, and adjusted the opening of a water valve to let more or less water through the heat exchanger, depending on the desired fuel temperature. As it was a closed loop system, the heat exchanger cooler controlled the overall temperature of the fuel in the system. The electronic valve diagram is shown in Figure 3.6. When the valve opened, the efficiency of the heat exchanger was increased due to a higher water flow rate. This cooled the fuel down more rapidly. When the valve was completely closed, the heat exchanger did not provide any cooling to the fuel. On its own, the heat exchanger could lower the temperature of the fuel to about 30°C for the full range of motor speed and pressure. This lowest temperature of 30°C was measured during the commissioning stage.

3.1.4. **Torque signal**

The torque required to drive the pump was measured by a torque sensor which was installed between the shaft of the pump and the shaft of the electric motor driving the pump (see Figure 3.1). The torque sensor was a Kistler 4502A with a range of -50 Nm to 50 Nm. It used a strain gauge to measure torque. It was powered by a 12 V power supply, and provided a -5 to 5V analogue output directly to the data acquisition system depending on the torque value. The sensor was calibrated so that a 0.1 V increment was equivalent to 1 Nm.

The torque sensor was chosen to have a range slightly larger than that of the maximum torque required to drive the pump at the maximum pressure of 1500 bar. Details on the calculations of the sensor range can be found in appendix A.

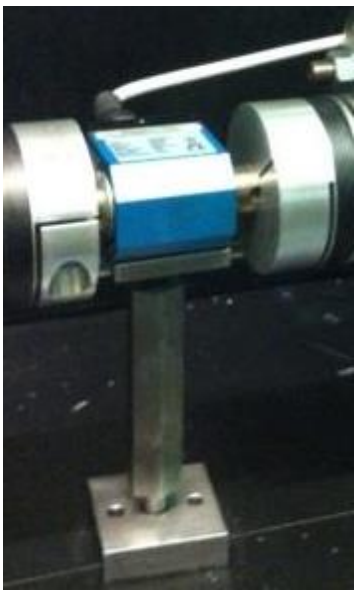

Figure 3.7: The torque sensor

3.1.5. **Speed control**

An AC 11kW, 3000 RPM Marell electric motor was chosen to drive the high pressure fuel pump via the torque sensor. It was controlled by a Lenze inverter which was located under the motor. The motor speed was controlled remotely using a keypad.

The motor was chosen to provide sufficient torque output to drive the fuel pump even at very low speeds. It could provide sufficient torque (see appendix A) at speeds even as low as 480 RPM, which is equivalent to 960 engine RPM; in most medium duty engine applications, the diesel pump runs at half the engine speed (Robert Bosch GmBH, 1999).

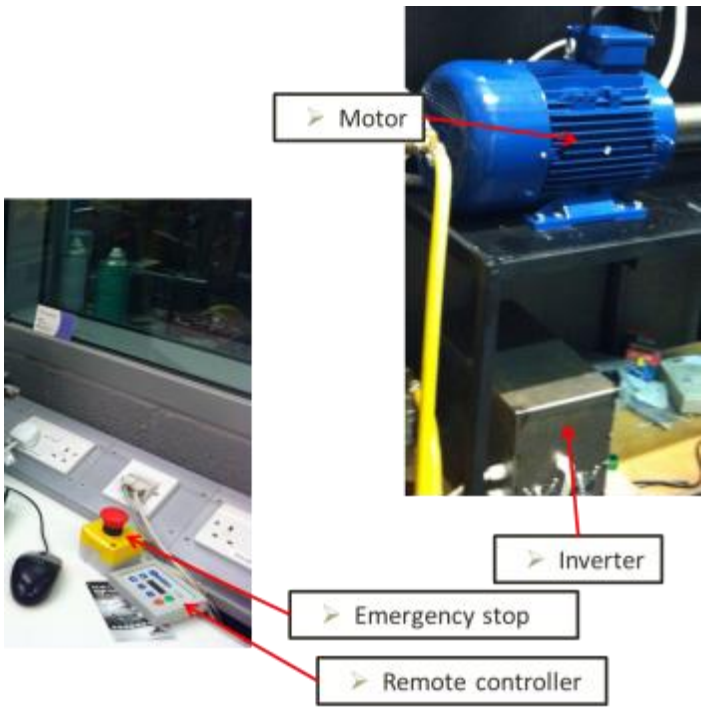

Figure 3.8: The speed control system

The motor was controlled manually by setting the speed and start/stop on the remote keypad. Additionally, an emergency safety switch was in place to instantly cut power to the motor.

3.1.6. **End user interface**

The pump test system used bespoke Labview software written by the author. The Labview software simultaneously controlled the pressure and the temperature of the system, and could adjust them while the system was running. The torque and other variables could be recorded simultaneously for any duration of time, at rates up to 20 kS/s. The software graphical interface can be seen in Figure 3.9.

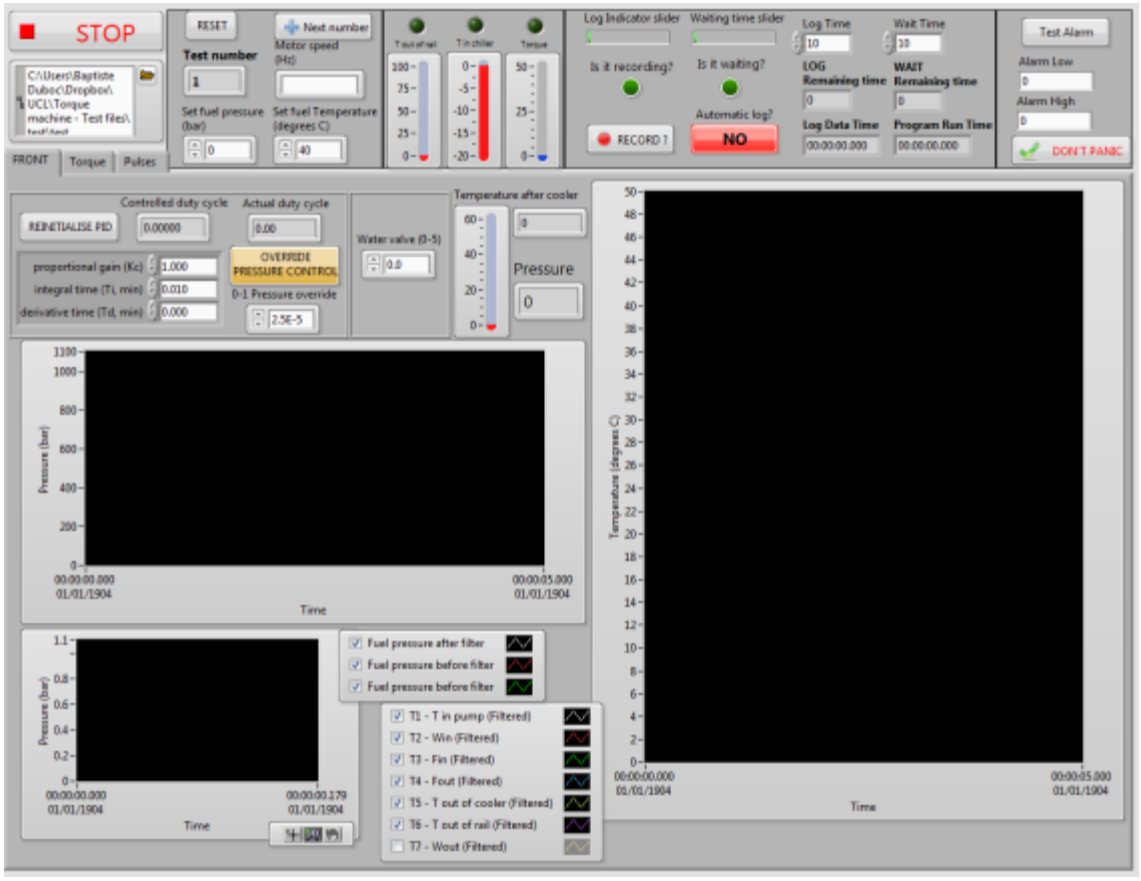

Figure 3.9: The Labview customised software graphical interface

3.1.7. **Fuel and additives cross-contamination considerations**

Because the tests carried out in the fuel pump torque characterisation rig were mainly aimed at investigating the effects of diesel fuel with different blends of additives on pump torque, it was crucial to design a way to limit the contamination of the system from one blend of additive with base fuel to the next. Cross contamination was a real possibility, as additives were added at the ppm level. The main method used to prevent cross contamination was ensuring the whole system was well drained of fuel between each test. To ensure this, the piping of the system was designed so that the closed loop could be broken at the fuel filter, and compressed air could be blown into the tubes to force all the fuel into a spill tank, thus emptying the pipes, spill pipe and all other components of the system. Additionally, the fuel filter was changed after each new additive was blended with base fuel to prevent contamination from filter deposits.

A test protocol was designed to limit the cross contamination further. For each set of tests, involving a single additive, a fuel additive blend was prepared usually at two concentrations (1x and 10x where x is the additive concentration in ppm). Also, before the 1x and 10x blends of fuel with additive were tested, a baseline test using fuel with no additives (base fuel) was carried out to bracket the tests with additives. Each test with additives was carried out from lowest to highest additive concentration. Thus, each test for an additive blend consisted of, first, a base fuel test, then a 1x, and finally a 10x concentration test. Furthermore, base fuel was pumped through the system for 30 minutes to an hour between every set of additives tests to ensure the system was flushed thoroughly of the previous 10x concentration. More information on the protocol can be found later in this thesis in section 4.1.

3.1.8. **Chiller system**

When the temperature of diesel fuel falls below about -10°C, it can form wax crystals, which remain in suspension, as described in section 1.1.3.

The fuel pump rig had a chiller system designed and installed by the author in order to lower the diesel fuel temperature down to waxing temperatures (-10°C or lower). This allowed for simulation of engine start-up conditions in extremely cold climates, but also to investigate the effect of waxing fuels in a fuel delivery system, with and without the help of flow improver additives.

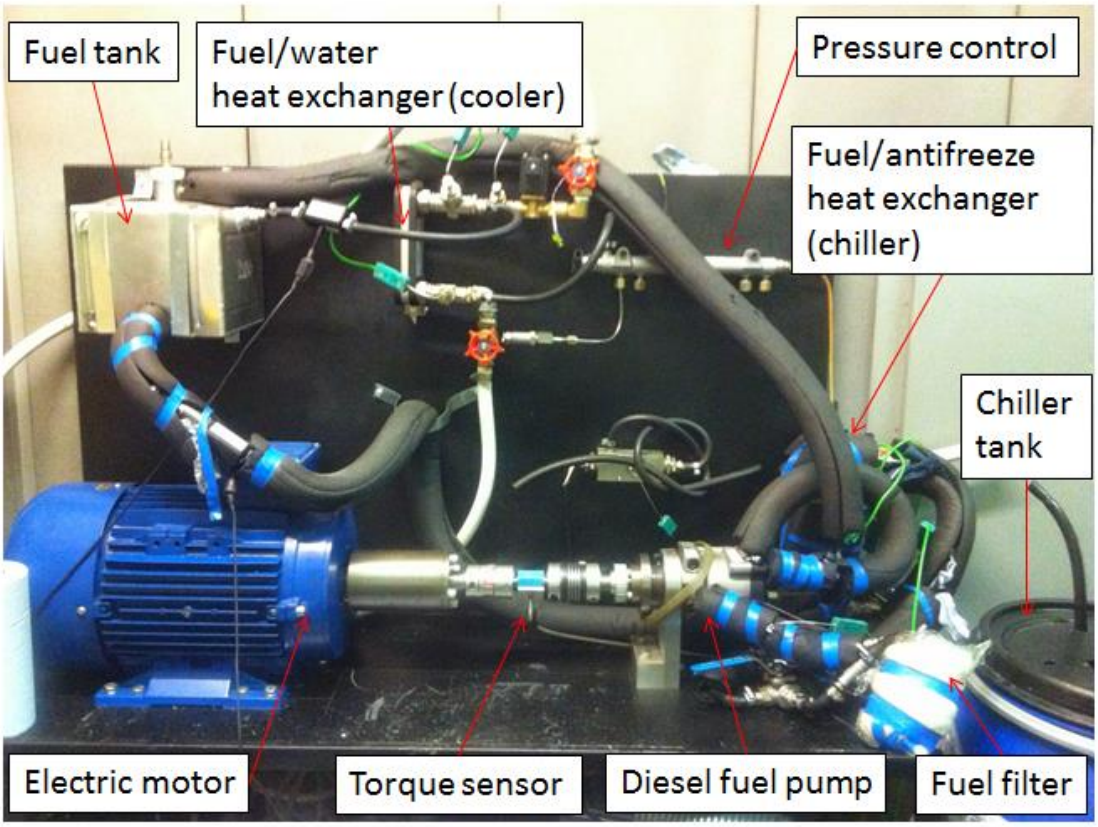

Figure 3.10: Fuel pump torque characterisation rig with chiller system

The system configuration is shown in Figure 3.1. The chiller system was composed of a 150 litre tank of a 60% ethylene glycol mixture with water (antifreeze) which was cooled down slowly (up to 12 hours) to -20°C or lower (depending on the room temperature), using a Cole Parmer refrigerated chiller unit. The chiller had an immersion coil with a cooling capacity of 265 W at -30°C and a minimum temperature capability of -45°C. However, the heat energy generated by the fuel pump/common rail is several times bigger than 265 W (up to 7 kW). Therefore, the working principle adopted was to chill the 150 litre tank overnight and then use the water antifreeze mixture in the tank to cool the fuel over the test period of about one hour, after which the fuel was too warm to be useful for further cold tests. One hour was sufficient time to acquire the necessary data. During this one hour period, the fuel temperature rose at a

rate of 1°C every 10 minutes, due to the addition of energy to the fuel mainly by the PRV throttling process.

Appendix A describes the calculations that were carried out to size the ethylene glycol tank and chiller unit.

Figure 3.10 shows the system used in combination with a chiller unit used to induce fuel waxing. The 150 litre tank containing the solution of 60% of ethylene glycol and water used a Davies Craig EWP150 electric water pump with a flow rate of 150 L/min to pump the cold solution through the fuel heat exchanger. The pump was left running constantly to ensure proper mixing of the solution, and a constant temperature throughout.

The ethylene glycol solution, which could reach -30°C on cold days, served to chill down the fuel passing through the fuel heat exchanger (see Figure 3.10). The heat exchanger used was a Buehler BWT B8x30 with a cooling performance of 10-25 kW. As shown on Figure 3.1, using two sets of 3-way valves, the fuel could be directed from the fuel tank to the filter and pump either though the heat exchanger, or directly through a bypass. This was to allow the chiller to cool down independently of the system, allowing the operator to use the pump torque rig at ambient conditions or higher while the ethylene glycol was cooling down.

The whole system including the tank, the pump, the pipes and the heat exchanger were insulated using fiberglass blankets and foam insulation. The temperatures of the circulating antifreeze mixture before and after the heat exchanger were monitored. Additionally, the temperature of the fuel before and after the heat exchanger could be monitored.

The flow rate of ethylene glycol (antifreeze mixture) through the heat exchanger was not regulated. The flow rate was purposely maximised at all times in an effort to minimise the fuel temperature, as for all tests involving the chiller, the coldest fuel temperature was sought so that the fuel temperature reduced below the fuel waxing point.

3.1.9. **Commissioning**

The raw fuel was provided by Innospec without any additives; the lubricity of the raw fuel was too low and could have resulted in damage to the rig (especially the high pressure fuel pump) due to the low natural lubricity of the raw fuel. For this reason, it was decided, following advice from Innospec, to add 50 ppm of additive FM-N, a commercial friction modifier (FM) to the raw fuel for all experiments involving the fuel pump torque characterisation rig.

FM-N, like all FM additives, acts by coating the surfaces that rub against each other inside the fuel pump (see section 1.1.4.), resulting in less damage to the pump and other components subject to contact, thus decreasing the wear rate. In the rest of this thesis, “raw fuel” denotes fuel with no additives at all and “base fuel” denotes raw fuel with 50 ppm of FM-N.

The base fuel subsequently had further additives added to it to create the various fuel blends used in the experiments. The exception was fuel tests involving FM additives, where the test fuel blend did not include the 50 ppm of FM-N to start with, but instead the FM additives were added to raw fuel at the desired concentration.

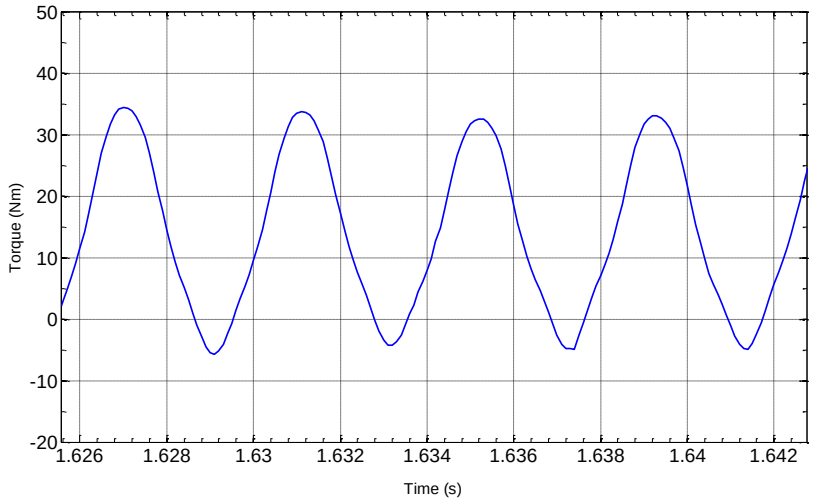

Figure 3.11: Example of the torque oscillation pattern (base fuel, 500 bar rail pressure, 50°C fuel temperature, 31 Hz pump rotational speed)

The preliminary commissioning tests carried out on the fuel pump torque rig showed some unexpected results. It was found that the torque recordings from the Kistler torque sensor were not constant, but oscillated in a pattern as shown in Figure 3.11. The oscillations changed in frequency and amplitude depending on motor speed. Some of these oscillations were so large in amplitude that they were outside the DAQ system recording range.

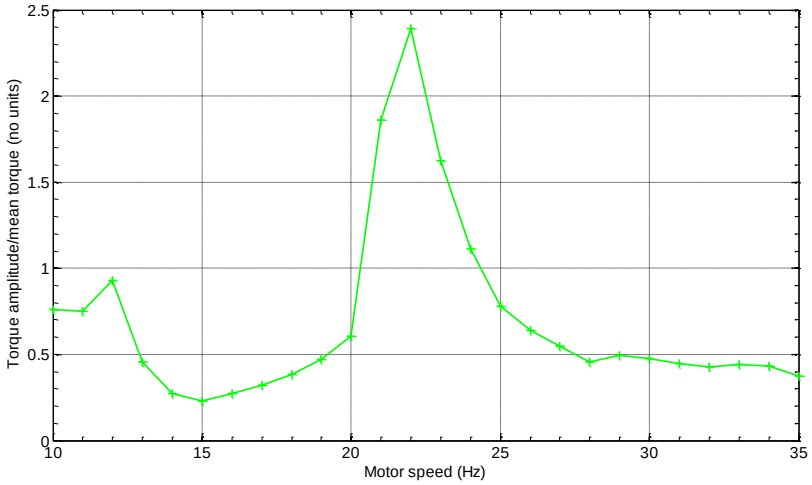

Figure 3.12: Oscillation amplitude vs. pump rotational speed at 700 bar fuel pressure, 50°C fuel temperature

Further investigations established that these large torque oscillations were due to torsional oscillations of the shaft between the electric motor and the diesel fuel pump. The dominant frequency of these oscillations was proportional to motor speed as seen on Figure 3.13. When the dominant oscillating frequency matched the natural torsional oscillation frequency of the

shaft and its coupling, the system entered into resonance, as shown in Figure 3.12 and Figure 3.13.

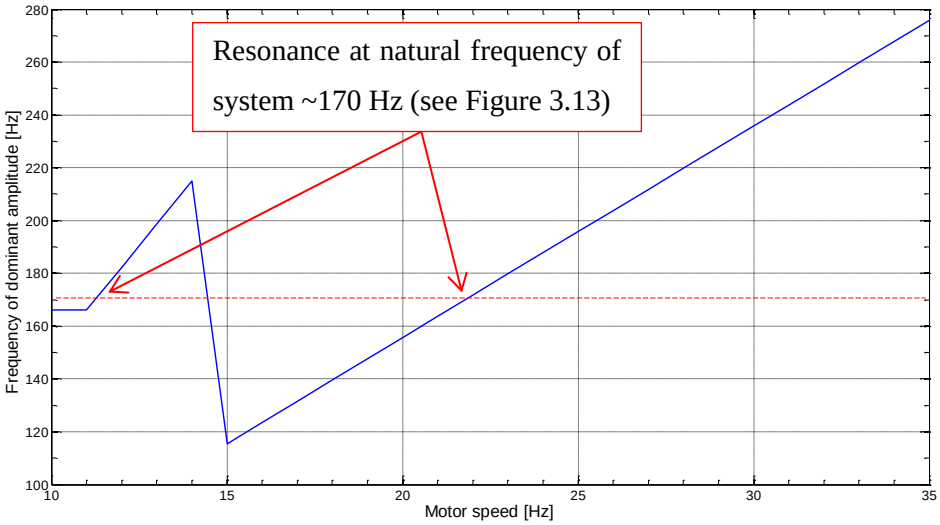

Figure 3.13: Frequency of dominant torque amplitude vs. pump rotational speed at 700 bar fuel pressure, 50°C fuel temperature

The problem was solved by changing the natural frequency of the shaft that joined the motor to the fuel pump using a different coupling between the electric motor and pump, which had greater damping. The resonant peaks of the new shaft coupling were determined experimentally, using the rig, and occurred when motor speed was 10.4 and 20.4 Hz. At these motor speeds, the dominant oscillating frequency of the torque signal was ~160 Hz, the natural frequency of the new system. For all subsequent tests, motor test speeds were therefore chosen away from those natural frequencies: 10, 17, 28 and 35 Hz (see Figure 3.14). The torque signal sampling rate was also changed from the initial 1000 to 10000 samples per second to prevent data aliasing from occurring.

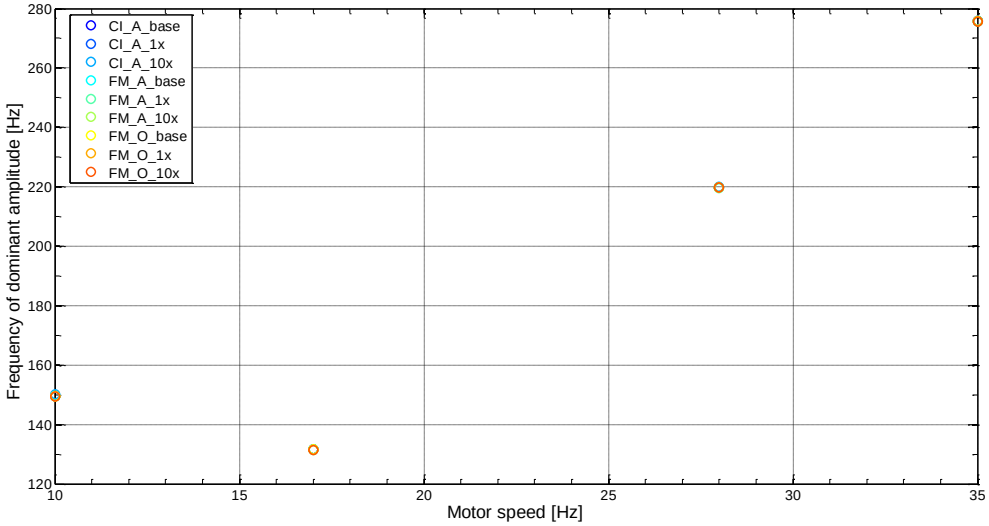

Figure 3.14: Frequency of dominant amplitude of raw torque signal at the tested motor speeds for various blends of additives

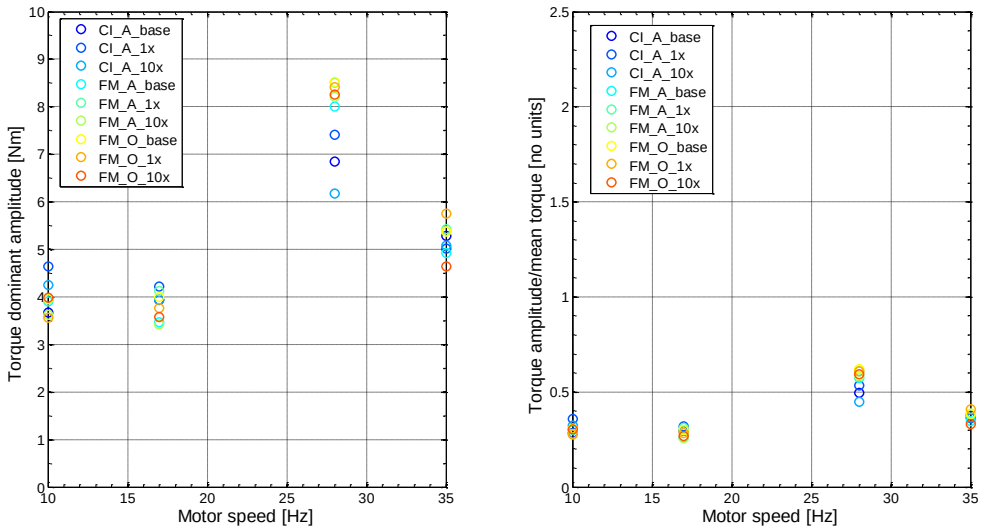

Figure 3.15: Dominant amplitude of raw torque signal at the tested motor speeds for various blends of additives (Left: Raw amplitude, right: amplitude normalised with mean torque)

While carrying out experiments in the fuel pump torque rig, the frequency and amplitude of the torque wave were monitored to ensure that the raw torque signal behaved similarly regardless of the fuel blend present in the system, or other factors. The frequency of the dominant amplitude was found to be very consistent across various blends of fuel with different additives for every motor speed tested, as seen on Figure 3.14. Figure 3.15 shows that the dominant amplitude of the raw torque signal was also found to be fairly consistent across various additive samples. Throughout the duration of the experiments, the torque amplitude to mean ratio varied as expected from the initial commissioning tests.

For all subsequent tests, the torque sensor output voltage was recorded by the DAQ card at 10kS/s for a period of 8 seconds and the average value of the torque over the period was calculated. It was found that 8 seconds was sufficient for the torque average to become constant and invariable with further increases in recording period beyond 8 seconds.

As mentioned previously, the common rail fuel pressure was controlled automatically using a Labview PID controller to stay within 2% of the desired set rail pressure. At rail pressures higher than 1000 bar, a steady state error of a few percent was corrected manually by changing the proportional and integral component of the PID controller. For all speeds and temperatures, the pressure could be accurately maintained as low as 300 bar or as high as 1500 bar. Lower pressures could only be achieved at low rotational speeds. This was because, even when the common rail PRV was fully open, the fuel friction losses and restriction of flow through the PRV in the system meant that a pump outlet pressure of about 300 bar was needed to circulate the fuel at low pump speeds and flow rates through the rig.

The pump speed inverter was capable of maintaining pump speed within 0.1 Hz and pump speed could be set at increments of as low as 6 RPM.

The temperature of the fuel before it entered the high pressure pump could be adjusted to the desired value using the water-cooled heat exchanger.

The ethylene glycol in the chiller tank took up to 24 hours to cool down from room temperature to about -20°C. Despite the insulation around the tank, this minimum temperature varied by about ±3°C depending on the room temperature which itself varied substantially with season and also depending on what other heat generating equipment were working in the room shared with other researchers.

After the coolant in the tank reached a low temperature overnight, it was then available to cool the fuel entering the high pressure diesel fuel pump. It took about 10-15 minutes to reach the coldest possible fuel temperature at the entry to the high pressure diesel fuel pump using a heat exchanger (chiller) as described previously. During a test, the fuel temperature at the inlet to the high pressure pump rose slowly because the chiller's ethylene glycol temperature also gradually rose. When the common rail fuel pressure and diesel high pressure pump speed were highest (900 bar, 35 Hz) energy dissipation to the fuel from throttling losses was at its greatest, and the chiller temperature rose much faster. Nevertheless, the rise in temperature was slow enough to allow about an hour of tests, which was sufficient time for torque to be recorded at various temperatures between -10°C and 30°C. Therefore, the gradual rise in the ethylene glycol temperature and the fuel temperature was not a significant disadvantage, as it allowed the pump torque to be measured over a wide range of fuel temperatures from -10°C to 30°C.

3.2. The constant volume combustion vessel

3.2.1. **Overview**

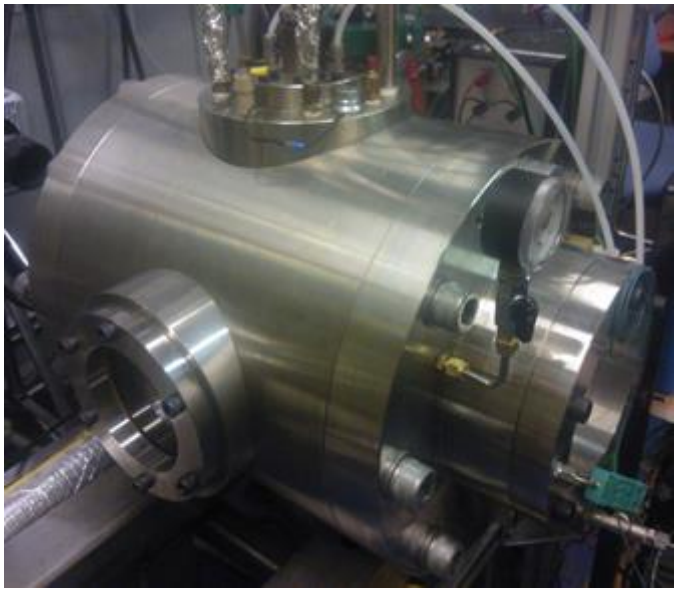

Figure 3.16: The constant volume combustion vessel

The constant volume combustion vessel (CVCV) used for the combustion and spray experiments can be seen in Figure 3.16. The vessel was about 23 litres in volume, making it much larger than most constant volume combustion vessels used in research today. It allowed for the study of combustion and spray events with very much reduced wall impingement effects (Patel, 2013). Furthermore, the vessel was designed to withstand a high combination of vessel pressure and temperature (100 bar at 500°C). To a certain extent, pressure and temperature of the gas within the vessel could be controlled independently by the use of a flow heater in line with the gas supply to the vessel. The gas supplied to the vessel was usually air but sometimes nitrogen when combustion was suppressed. The gas in the vessel could also be elevated in pressure and temperature with pre-combustion when diesel fuel experiments were being carried out. The vessel offered multiple attachment points to accommodate various instruments for pressure and temperature measurements. Four large quartz glass windows arranged orthogonally into two pairs gave extensive optical access to the vessel. One pair of the quartz glass windows had a diameter of 150 mm and the other pair 120 mm.

In order to use the CVCV for diesel sprays as well as diesel combustion, the vessel was designed with an exhaust system to remove the combustion gases into the laboratory exhaust system. A cooling jacket around the diesel or gasoline injector allowed a constant fuel injection temperature.

3.2.2. **Fuel high pressure system**

For experiments with different blends of additives, careful consideration had to be given to cross contamination between successive fuel-additive blends. Additives were added in minute quantities (as low as 2 mg of additives per kg of untreated diesel fuel). To assess the effects of individual additive blends, one had to ensure that successive experiments were free of any contamination from previous additive blends.

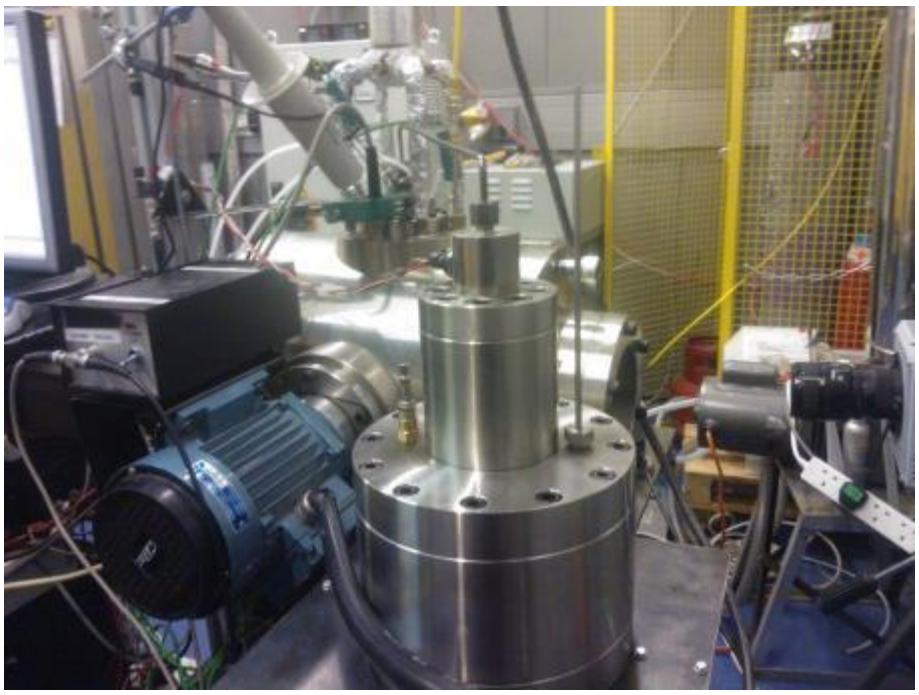

Figure 3.17: Fuel pressure intensifier and constant volume combustion vessel

A fuel intensifier was designed and built to bring the test fuel to the required pressure of 700 bar upstream of the fuel injector and yet be able to be taken apart and cleaned easily between each experiments with fuel additives. The pressure intensifier can be seen in Figure 3.17. This fuel system replaced a common rail fuel system and a conventional high pressure pump which were more wasteful of fuel, and gave rise to a higher risk of cross contamination between tests on fuels due to the presence of a pump, pipes and a common rail which could not be taken apart and cleaned after each fuel blend was tested.

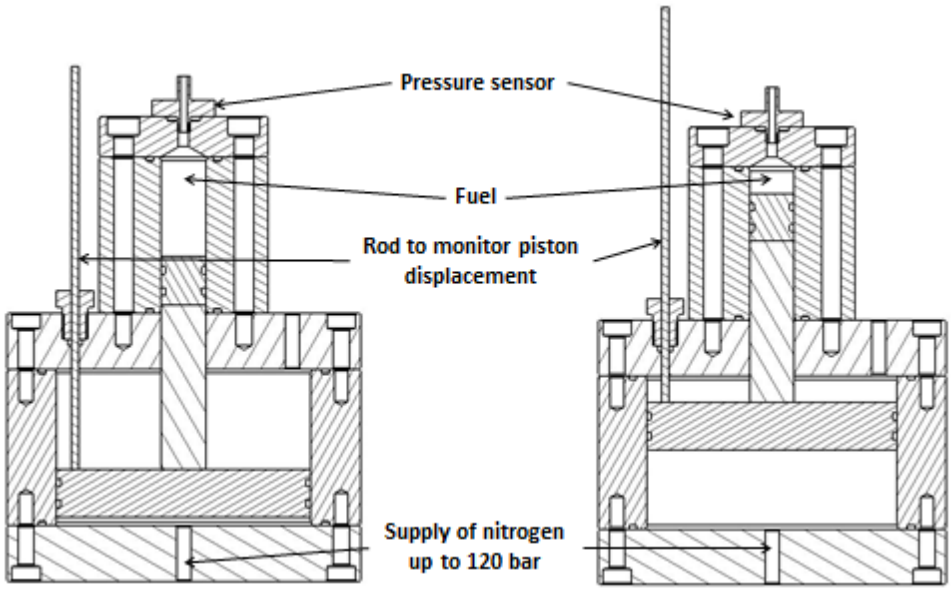

Figure 3.18: Cross section of the fuel pressure intensifier

The system was a pressure intensifier and it composed of two pistons of different surface areas as shown in Figure 3.18. The large piston (158 mm diameter) could be pressurised up to 120 bar with nitrogen from a bottle. As this piston moved, it displaced the small piston (28 mm diameter) which then pressurised the liquid fuel located above it up to a maximum of 700 bar pressure.

The supply pressure of the nitrogen could be adjusted using a pressure regulator, and in this way the fuel pressure could reach any desired value up to 700 bar. The fuel pressure in the pipe supply to the injector was monitored by a pressure sensor.

The wall thicknesses were calculated using finite element analysis to ensure that the pressure amplifier could withstand the maximum pressure of the fuel and nitrogen. The fuel tank was capable of holding a small quantity of fuel (about 50 mL), which allowed for more than 500 spray events from either a gasoline or a diesel injector. This was deemed to be sufficient for a CVCV, as spray and combustion events are often investigated individually, rather than as part of an ensemble average.

O-rings and bolts were chosen to withstand the pressure force, with a safety factor of two on the material yield strength. The casing was designed using finite element analysis with the same factor of two on the material yield strength.

Figure 3.19: Dismantled fuel tank from pressure amplifier

The top of the pressure intensifier (including the upper fuel cylinder, the fuel small piston, the cap and the pressure sensor mount before the tube to the injector) was designed to be easily removable so as to be cleaned in the ultrasonic bath between each fuel blend test (see Figure 3.19). The cleaning process took about an hour. Only the injector and the fuel line to the injector were not cleaned in the bath. This was because the injector could have been damaged by the ultrasonic bath, and the line was too long to fit in the bath. Instead, the fuel line was dismantled

between each test, and the remaining fuel was blown out using pressurised air. It was assumed that the small quantity of fuel still present in the fuel line and the injector (generally less than 5mL) would be 'pushed out' by the new fuel after a few injections.

3.2.3. **Malvern Spraytec spray sizer**

A Malvern Spraytec system was used to measure droplet size distribution of the injected fuel spray. It was decided to mount the Malvern Spraytec system around the CVCV in order to be able to conduct droplet size distribution analysis on diesel injected sprays in the vessel.

The Malvern Spraytec system is a diffraction granulometer. The system consists of a laser and receiver, which are aligned facing each other. The receiver consists of a set of 32 photoreceptors arranged in concentric rings which measure light intensity. When a spray crosses the laser beam, the light from the beam is diffracted to these rings. The intensity measured by each ring determines the average spray size through the manufacturer's calibration. More information on diffraction ganulometry can be found in section 2.1.3.

It was found that the original mounting bracket provided by the manufacturer to mount the laser and receiver of the Malvern Spraytec system did not fit around the combustion vessel. The laser and receiver could not be aligned independently without a single piece bracket, as the system was found to be very sensitive to angular alignment.

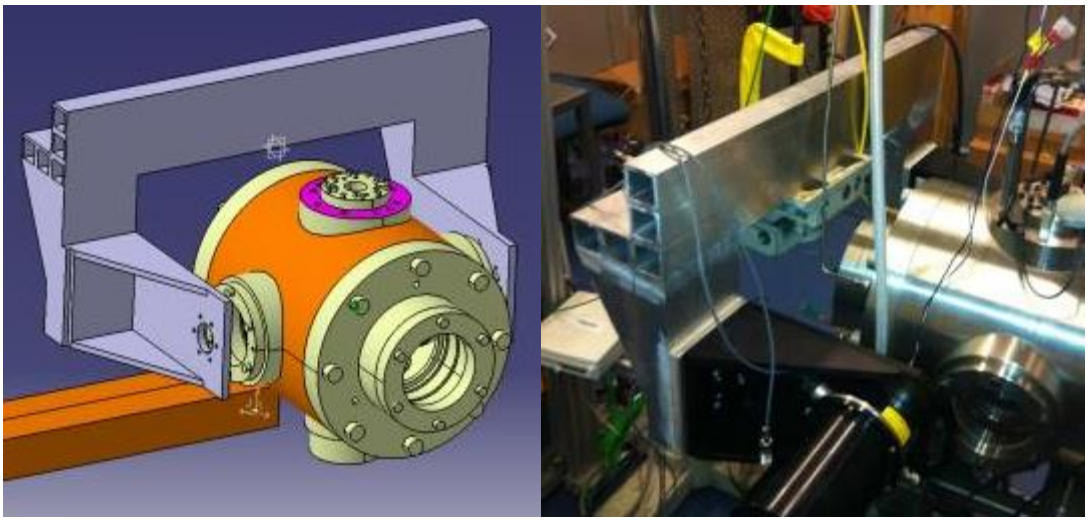

Figure 3.20: New Malvern laser bracket design (left) and built around the combustion vessel (right)

A new bracket was designed to go around the CVCV. The original bracket was reproduced using CAD, and finite element analysis was conducted to determine how the weight of the laser and receiver affected the displacement of the original bracket. The angular displacement of the original bracket on the virtual axis that represented the laser beam was estimated as 0.0145° (0.0364 mm of vertical displacement over the 575 mm laser length) using finite element

analysis. The new bracket was made stiff and strong enough to provide similar maximum angular displacement.

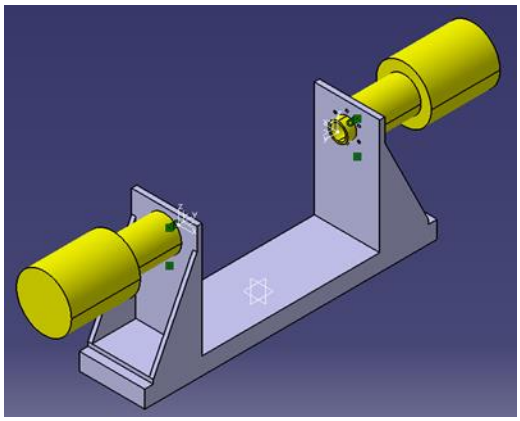

Figure 3.21: Original bracket with line of sight

The new bracket involved the laser being hung on its side rather than upright as in the original design (see Figure 3.20 and Figure 3.21). Parts of the original bracket were kept, but the platform was redesigned in aluminium to accommodate the shorter side of the combustion vessel and reinforced with stiffeners to minimise angular deflection. It was bonded together with a very strong bonding adhesive to ensure that there would be no permanent thermal distortion resulting from the metal being welded. The final design can be seen in Figure 3.20.

The bracket was held by an adjustable stand around the CVCV, allowing for movement of the whole Malvern Spraytec system upwards and horizontally. In this way, the 10 mm diameter line of sight laser beam between the laser transmitter and receiver could be moved vertically and horizontally so as to sample the spray at different axial or radial positions.

The Malvern Spraytec could measure the droplet size distribution and average droplet size in a line of sight inside the combustion vessel. Due to refraction of the laser beam from the thick CVCV windows, the side windows had to be removed, making pressurised sprays impossible to investigate using the Malvern Spraytec system.

The Malvern Spraytec system was triggered using an external TTL signal from a bespoke Labview program. It could measure samples at a maximum rate of 2.5 kHz, which was used for all tests. A single array for droplet size distribution, average droplet size and laser transmission (a measure of spray density along the laser beam) were calculated internally by the Malvern Spraytec software using Mie scattering from the average light transmission results gathered on each of the 32 rings of the receiver at a frequency of 2.5 kHz.

3.2.4. **Refrigeration system**

In order to assess the effects that fuel waxing may have on diesel fuel spray development and droplet sizes, a system was designed and implemented which lowered the temperature of the fuel within the injector to below -10°C, which is the onset of waxing for diesel raw fuel. The refrigeration system was then used in conjunction with the Malvern system and the CVCV to assess spray droplet size distribution with fuel temperature below the fuel waxing point.

The refrigeration system for the combustion vessel was the same one that was used for the fuel pump torque characterisation rig. A smaller (25 litre) tank of a 60% ethylene glycol-water mixture was used as a buffer. This tank was cooled down overnight using the Cole Parmer chiller in a similar manner to that described in 3.1.8. The same Davies Craig recirculation electric pump was used to pump the ethylene glycol around the injector cooling jacket that formed part of the CVCV. Insulating blankets and insulating foam were installed around the tank and pipes as well as around the top of the combustion vessel (where the injector cooling jacket was located) to maintain the temperature of the antifreeze mixture and the fuel as low as possible. A diagram of the refrigeration system can be seen in Figure 3.22.

.

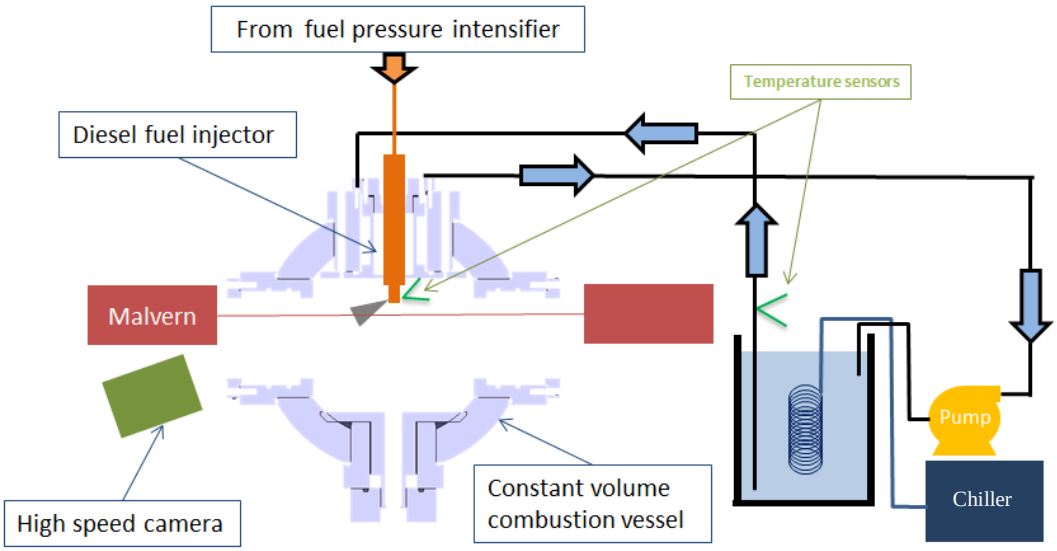

Figure 3.22: The refrigeration system around the diesel fuel injector in the CVCV

The ethylene glycol temperature was monitored using thermocouples before and after the injector cooling jacket. In order to determine the fuel temperature inside the injector, an exposed thermocouple was placed at the tip of the injector. Another thermocouple measured the temperature between the cooling jacket and the wall of the injector (see Figure 3.22).

The chiller system allowed the fuel temperature within the injector to be lowered below the waxing temperature, while still maintaining the ability to inject.

3.2.5. **Gas mixer system**

To carry out diesel combustion in the CVCV, the air temperature inside the vessel needed to be high, in the order of 400-500°C, so as to cause spontaneous ignition of the diesel fuel spray. In order to provide this temperature with sufficient oxygen for combustion, the pre-combustion of a lean mixture of gases was used, prior to the diesel fuel injection. The lean pre-combustion left sufficient oxygen for ignition and combustion of the diesel fuel spray but at an oxygen concentration below that of atmospheric air. This reduced oxygen concentration, to an extent, was not disadvantageous, as it represented combustion residuals that are always present in operating diesel engines.

Figure 3.23: The gas mixer system

To create a repeatable lean combustible gas mixture with air inside the CVCV for several repeated spray combustion experiments, a mixing rail was designed and fitted on top of the combustion vessel as shown in Figure 3.23. The system comprised of a tube with four gas entries, one outlet and a precision 0-2 bar (gauge) electronic pressure sensor. A mechanical pressure gauge and an exhaust pipe were also fitted on the mixing rail. The metering of the pre-combustion gases in the CVCV was based on the partial pressure principle that states that the number of moles and mass in a system can be determined using partial pressures as long as the chemical composition, volume and temperature are constant (ideal gas law).

Using this principle and the gas mixer system, different gases could be mixed with the air present in the CVCV at atmospheric pressure. The number of moles of gas required for the desired mixture conditions could be converted to an additional pressure to be added to the atmospheric air in the CVCV. Using the precision pressure sensor, each gas was introduced in turn in the tube at the desired pressure to be released in the combustion vessel. The process could be repeated for up to four different gases, including air.

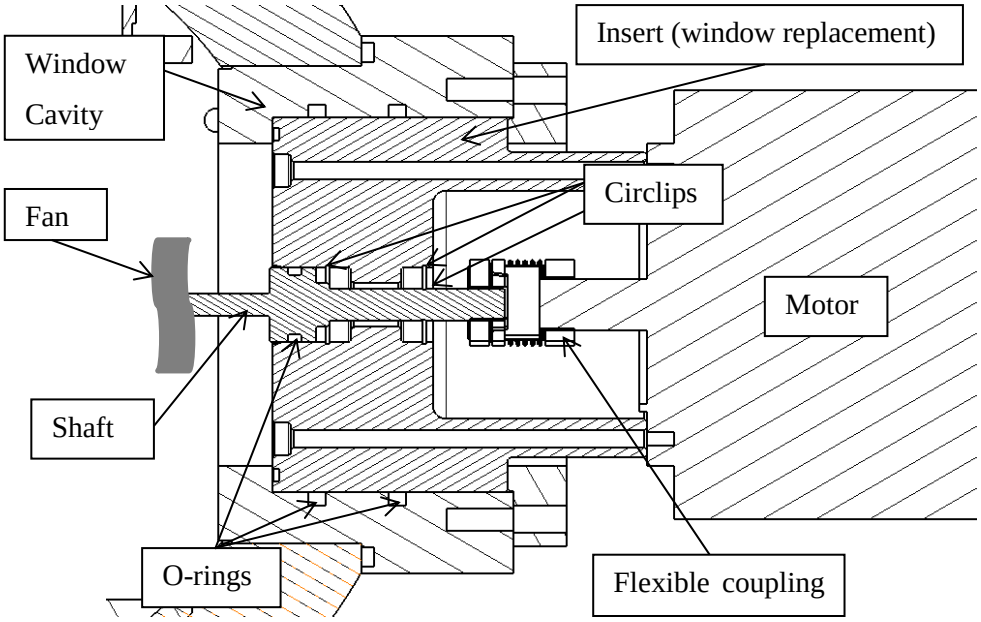

Figure 3.24: Fan mixer system

In order to enhance and speed up mixing of the gases introduced in the CVCV, one of the two smaller windows was replaced with an electric motor and fan system to allow mixing of the gases before they were ignited in the CVCV. This system consisted of a 3000 RPM fixed speed electric motor rotating a brass fan though the vessel as shown in Figure 3.24. Three O-rings and three circlips were used to ensure the pressure in the CVCV did not push the shaft in or out, or that the gases leaked through the O-rings.

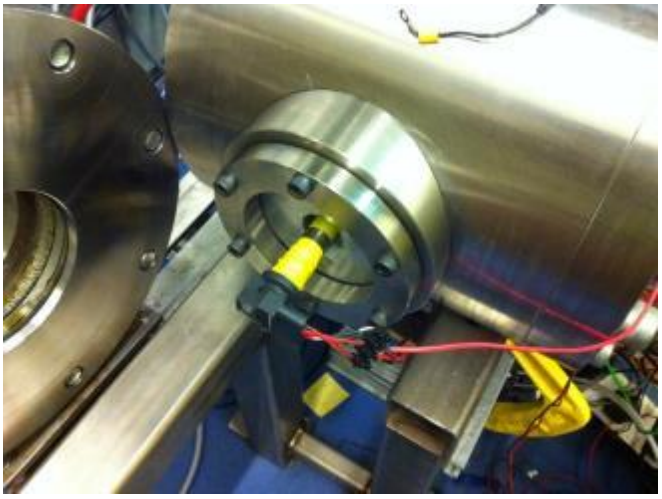

Figure 3.25: Spark plug in the CVCV

In order to ignite the pre-combustion gas mixture, a spark system was designed and implemented on the combustion vessel by a fellow PhD student Mart Mägi. This system allowed for complete control of spark timing and charge time, and delivered a spark from a spark plug located in the centre of a blank replacing the second small window, as shown in Figure 3.25.

A Labview software code triggered the spark and initiated the pre-combustion, after the gas mixing was completed. A high speed pressure sensor estimated the instantaneous gas temperature within the CVCV during pre-combustion and immediately afterwards using the ideal gas law. The ignition and combustion temperature changed too rapidly to be monitored by a thermocouple. Using the pressure trace, the diesel fuel injection was triggered at a predetermined pressure, so as to ensure repeatability of the spontaneous ignition and combustion of the diesel fuel.

3.2.6. **Exhaust emissions**

A Horiba gas analyser was used for analysis of the products of combustion in the CVCV. A ball valve connected on top of the combustion vessel could be opened, connecting the vessel directly with the Horiba system. Due to the long tube connecting the Horiba analyser to the CVCV, the vessel was pressurised with exhaust gases before the ball valve was opened to connect it to the analyser. It was found that a 5 bar initial pressure in the vessel allowed the Horiba to reach steady state and hold steady state readings for 60 seconds.

3.2.7. **Camera system**

The multiple windows on the combustion vessel allowed for extensive optical analysis of both the fuel spray and combustion events. A Photron APS-RX camera was used at a high frame rate (10000 frames/s) in black and white. A light source on the opposite window to that of the camera allowed for shadowgraph analysis of the fuel sprays.

3.3. Additives mixing procedure

Table 3.1: Raw fuel characteristics (Russell, 2014)

The additives and the raw fuel were supplied by Innospec. Information about the raw fuel can be seen in Table 3.1. Each additive was given a specific treat rate (concentration in ppm). Two blends of fuel with additives were made. The first was at the normal concentration, and the second was at 10 times the normal concentration.

The additives were mixed by weight. A certain weight of additive was measured using a balance to the nearest 0.001 gram (balance resolution). Disposable pipettes were used to transfer the additives from the bottle supplied by Innospec to a disposable beaker, where the additives were weighed. In some cases the additives were solid. When this was the case additives were heated up to 30 or 40°C to turn them into liquid, in order to weigh them in the same manner.

For experiments in the fuel pump torque characterisation rig, a series of 25 litre batches of raw fuel with 50 ppm of FM additive FM-N were made. These were made by weighing the 25 litre drum until it had exactly 25 litres of fuel and adding the carefully weighed additive. This was the 'base' fuel for the pumping experiments, as explained previously in section 3.1.9. Various other additives were then added to the 'base' fuel, one at a time, for testing.

For smaller volumes in the combustion vessel, the additive was mixed with the fuel in a 250 mL flask. Additives were weighed and added to this flask.

The spray and combustion experiments were carried out using the high pressure fuel tank described earlier, which had a 60 mL capacity. Mixing 250 mL of each fuel-additive blend was sufficient to carry out the whole series of experiments with each additive.

The emptied flasks and 5 L tanks were not re-used again to mix another additive. It was however deemed acceptable to re-use the same emptied flask and emptied tank for a higher concentration (usually 10x) of the same fuel additive, as the increased concentration of the same additive overwhelmed any fuel residue of the lower concentration additive left in the flask or tank.

Chapter 4

Pump power measurements with fuel additives

The effect of additives on the torque required to drive a high pressure fuel pump was investigated, and the results are shown in this chapter. The effects of fuel additives at different common rail pressures, fuel temperatures and fuel pump rotational speeds were investigated. Additionally, a separate study on fuel at waxing conditions (lower than -10°C for raw fuel) was conducted in the pump rig system to determine the effect of waxing on the fuel delivery system, and whether the addition of fuel additives to raw fuel had any effect in the pump torque.

4.1. Experimental methods

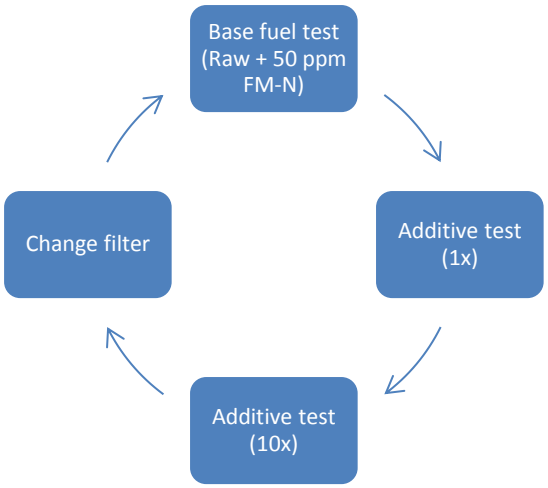

Figure 4.1: The fuel testing cycle (1x means normal additive concentration and 10x means 10 times the normal concentration)

In order to minimise contamination between different fuel-additives blends as well as the time between each experiment, an experimental protocol was devised for tests on the fuel pump torque rig.

Base fuel was tested first before any test on fuel additives (see Figure 4.1). The fuel-additive blend was then tested at its normal concentration (1x), and then at 10 times (10x) its normal concentration. The fuel filter was changed before the next additive test cycle commenced, bracketing the previous test, as shown in Figure 4.1. A table of all the additives used in the torque experiments and their normal concentrations can be seen in Table 4.1.

The fuel pump torque characterisation rig required about 4 litres of fuel per experiment. All tests with a specific fuel-additive blend were made using a single batch of 4 litres of fuel additive blend. The system was drained of its fuel between each experiment. Compressed air was used to force the remaining fuel out of the system. The system was then refilled with the next batch of either base fuel or blend of fuel-additive.

Additive type	Additive code	1x concentration (ppm)	10x concentration (ppm)
Cold flow	CF-A CF-B CF-H CF-I	150 150 150 150	1500 1500 1500 1500
Combustion improver	CI-A CI-E	250 250	2500 2500
Deposit control	DCA-A DCA-G	100 100	1000 1000
Drag reduction	DRA DRB	30 30	300 300
Friction modifier	FM-A FM-N FM-O	100 100 100	1000 1000 1000

Table 4.1: Diesel additives codes and concentrations used for torque experiments

The pump rig could run at a range of rail pressures, pump rotational speeds and fuel temperatures. Certain pump speeds had to be avoided as they corresponded to the natural frequency of the motor/pump coupling shaft (see section 3.1.9.). Therefore, four speeds were selected (10 Hz, 17 Hz, 28 Hz and 35 Hz) where investigations showed no effects of shaft resonance. These pump speeds were equivalent to engine speeds of 1200, 2040, 3360 and 4200 RPM, which are representative of low, medium and high engine rotational speeds that would be seen in typical automotive diesel engines.

Most pressures and temperatures of interest could be achieved without the chiller unit (see section 3.1.9.), but for temperatures lower than 30°C the rig required the chiller system to remove the pumping energy that heated the fuel up. For each test, the instantaneous torque required to drive the pump was recorded for 8 seconds and a time average torque value was calculated.

The common rail pressure and pump speed could be altered to a desired value almost instantaneously, however fuel temperature took a much longer time (up to several hours) to stabilise. To avoid excessive waiting time, some 8 second torque measurements were taken while fuel temperature at the pump inlet was changing slowly. Thus, a set of data could be

obtained over a wide range of quasi-steady fuel temperatures. Repeat tests showed the average to be no different from that obtained by waiting for a stable pump inlet fuel temperature.

4.2. Experiments on torque

4.2.1. **Experimental setup**

A series of tests was devised to assess the effect that an additive may have had on torque required to drive the fuel pump. Testing at multiple conditions of speed, pressure and temperature was necessary in order to determine if an additive affected the torque required to drive the high pressure fuel pump.

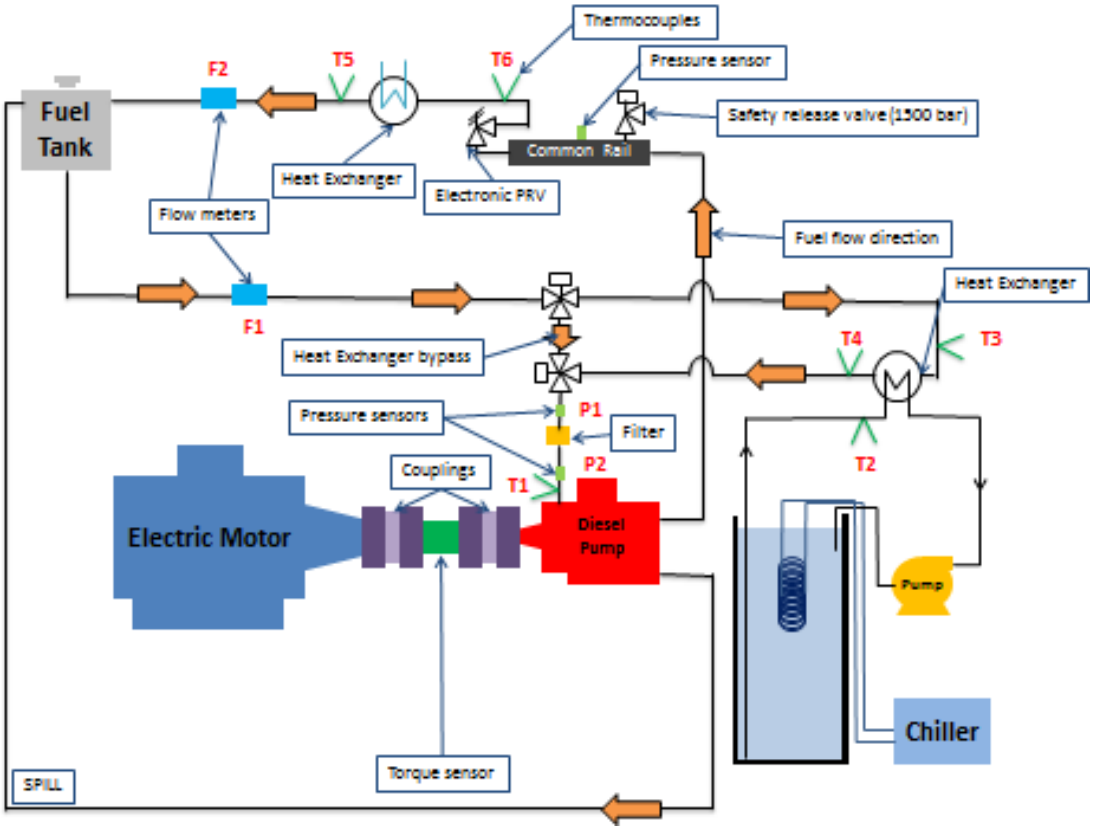

Figure 4.2: Torque tests – Fuel pump torque characterisation rig set-up.

All additives were tested at 1x and 10x concentrations (see Table 4.1) with base fuel bracketing each set of additives, as described in the experimental methods (Section 4.1.). The tests were conducted at 10, 17, 28 and 35 Hz pump rotational speed. The common rail pressures tested were 300, 700 and 900 bar. The temperatures used were 0°C (using the chiller), 30°C and 50°C. Each fuel-additive blend concentration required 36 tests to cover the above variable combinations. A diagram of the test rig and the various recording points can be seen in Figure 4.2. The data recorded included common rail pressure, coolant temperature in the chiller (T2), fuel temperature before (T6) and after (T5) the water cooled heat exchanger, fuel temperature at the pump inlet (T1), and the torque required to drive the pump. To limit the influence of day to

day changes in environmental conditions, all 36 data recordings were conducted in the same day for every fuel.

4.2.2. **Torque results on base fuel**

Before looking at the effects of different fuel additive blends on pump torque, an initial study was made using base fuel in order to assess the functionality of the fuel pump torque rig. In addition, a comparison of all base fuel tests carried out throughout the duration of the thesis was carried out to determine the shot to shot error and repeatability.

The effect of each of the control variables (common rail pressure, pump inlet temperature and pump rotational speed) on torque was investigated with base fuel. Common rail pressure was seen to be the major factor determining the torque required to drive the fuel pump. However, an increase in pump rotational speed also showed an increase in torque at a given rail pressure and fuel temperature at pump inlet. Similarly, an increase in fuel temperature decreased torque at constant rail pressure and pump speed.

During the subsequent fuel additive tests, twelve base fuel tests were conducted, bracketing each additive test, so that any drift in the rig and sensors could be detected and rectified. The twelve base fuel tests were analysed and the results are presented below. This analysis of results with base fuel showed the repeatability of the rig and the tests, but also whether contamination between various additive batches was an issue. The results show almost no contamination and very little variability between the twelve tests with base fuel.

4.2.2.1. Relationship between torque and common rail pressure

The pumping power required by the pump is given by the steady flow energy equation:

$$\dot{Q} - \dot{W} = \dot{m}h_2 - \dot{m}h_1 \quad (4)$$

The potential and kinetic energy terms were neglected as the pump inlet and outlet elevation and flow velocity differences were negligible. $\dot{Q}$ is the net heat transfer from the pump to the atmosphere in W, $\dot{W}$ is the net work transfer to the pump in W, $\dot{m}$ is the mass flow rate of the fuel though the pump in kg/s, and h is the specific enthalpy of the system at the inlet (subscript 1) and outlet (subscript 2) of the pump in kJ/kg.

Furthermore,

$\dot{Q} \ll \dot{W}$ (Confirmed by measurements later in this chapter)

At the inlet and outlet of the pump: $h = e + Pv$ and $e = C_v T$

Where e is the specific internal energy in kJ/kg, P is the fuel pressure in Pa, v is the specific volume in m^3/kg, C_v is the specific heat of the fuel at constant volume in kJ/kgK, and T is the fuel temperature in K.

Using substitution

$$\dot{W} = \dot{m}(e_2 + P_2 v_2) - \dot{m}(e_1 + P_1 v_1) \quad (5)$$

Also, $T_2 \cong T_1$ at the inlet (subscript 1) and outlet (subscript 2) of the pump, as confirmed by measurements. Thus, since $T_2 \cong T_1$ then $e_2 \cong e_1$.

The steady flow energy equation for the system becomes

$$\dot{W} = \dot{m}(P_2 v_2 - P_1 v_1) \quad (6)$$

Assuming $\dot{m}v_1 = \dot{m}v_2$ as diesel fuel is virtually incompressible, and knowing that

$$\dot{m}v = \dot{V}$$

Where $\dot{V}$ is volume flow rate in m^3/s, $\dot{m}$ is fuel mass rate in kg/s.

$$\dot{W} = (P_2 - P_1)\dot{V} + F$$

Where $\dot{V}$ is the fuel volume flow rate in m^3/s, P_2 and P_1 are the pump delivery and inlet pressures, respectively, and F represents the power losses in the pump due to tribological friction and fluid friction in the pipework and common rail. F will be largely due to hydrodynamic frictional losses at the pump bearings and the pump cam/piston interfaces; therefore, F could be expected to depend on both pump speed and pressure (normal force between rubbing surfaces). At a given pump speed, $\dot{W}$ is directly proportional to the torque required to drive the fuel pump. For a given pump speed, $\dot{V}$ will be approximately constant. Also, P_1 is much smaller than P_2, and P_1 is approximately constant. One could therefore expect a plot of pump torque against P_2 to be linear with the vertical axis intercept (i.e. where $P_2 = 0$) to be directly related to F.

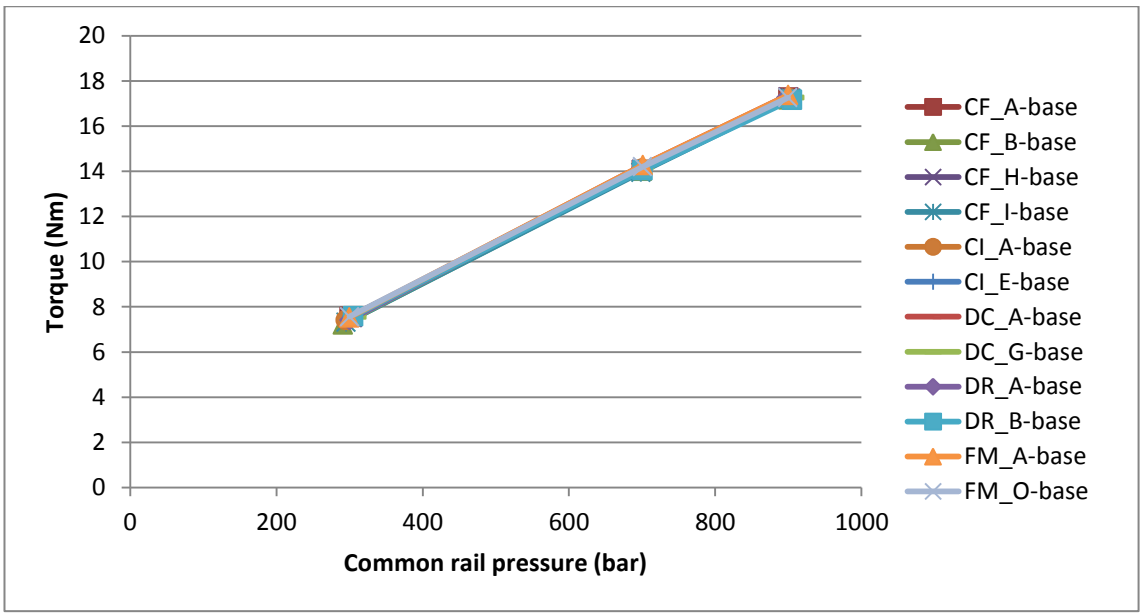

Figure 4.3: Torque vs. common rail pressure for multiple batches of base fuel at 28 Hz pump speed (1680 RPM) and 30°C fuel temperature

Figure 4.3 shows the relationship of all 12 base fuel tests between the torque required to drive the fuel pump and fuel pump delivery pressure for particular conditions of speed and temperature. As expected, the relationship is linear for all base fuel tests. Additionally, the relationship stays the same for every base fuel test, with very little variation throughout all the tests carried out during 12 months of testing.

In the case of Figure 4.3, the slope of the line indicates that a 1 bar rise in pressure required 0.0163 Nm of extra torque. Using the equation that relates torque to power $P = T\omega$, where P is power in Watts, T is torque in Nm and ω is rotational speed in rad/s, this is equivalent to 2.86 W/bar at a pump speed of 1680 RPM. In a compression-ignition engine, the common rail pressure can vary from over 300 bar to as high as 1500 bar. The power required to drive the fuel pump could therefore be multiplied by 5, depending on what the fuel pressure requirement is.

Thus, the desired fuel pressure is the primary cause of torque change. For a particular set of temperature and speed conditions, the relationship between the torque required to drive the pump and common rail pressure is linear and can be described as $T = C_1 P_2 + C_2$. Where C_1 represents the effect of delivery pressure on torque and C_2 represents the effect of internal pump friction on torque.

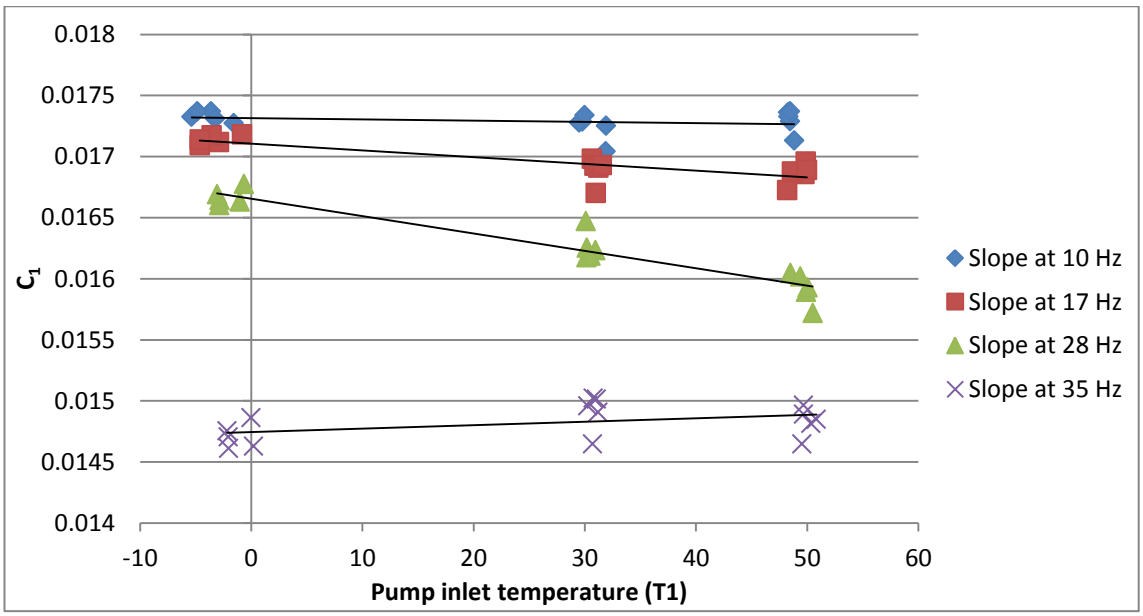

Figure 4.4: Values of C_1 vs. fuel temperature for different pump rotational speeds

Figure 4.4 shows that the rate of change of torque with pressure (C_1), is not affected significantly by the change in temperature of the fuel. This can readily be seen using the collection of values of C_1 at 28 Hz pump speed. A difference of 0.0005 Nm/bar (0.088 W/bar) can be seen when the temperature is varied by 50°C. This changes the original value by a little over 3%, which is well within the scatter of the results presented in Figure 4.4.

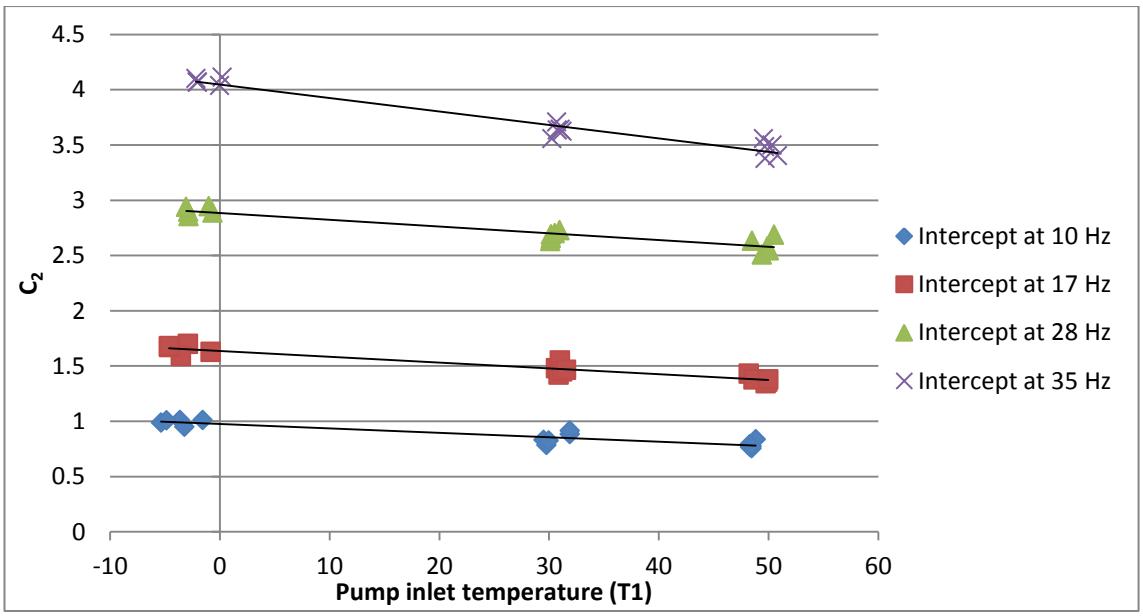

Figure 4.5: Values of C_2 vs. fuel temperature for different pump rotational speeds

C_1 varies more significantly as a function of pump speed. When the speed is changed from 10 to 35 Hz, the value of C_1 changes from around 0.0173 Nm/bar to 0.015 Nm/bar, a 13% decrease (see Figure 4.4). In other words slightly less torque is required to raise the fuel pressure at higher pump speeds than at lower ones. The reasons for this observation are not clear; one

possibility is that the large pressure pulsations in the common rail may act as a way to reduce the instantaneous pressure on the outlet port of the pump as the pump speed rises.

Similarly to Figure 4.4, Figure 4.5 shows all values of C_2 plotted against fuel temperature for all pump rotational speeds. The reader is reminded that C_2 is the intercept on the vertical axis of the torque versus pump outlet pressure (P_2) curve and, as mentioned previously, this is considered to represent the frictional losses between moving surfaces within the pump. It also includes fluid friction losses (viscous as well as turbulence losses) in the pipe circuit and common rail which will exist even when the pump outlet pressure is the same as the pump inlet pressure. Two effects are evident from Figure 4.5. Firstly, that C_2 rises appreciably with pump speed: by 23% as the pump speed was raised from 10 to 35 Hz. Secondly, there is a slight reduction in C_2 with fuel temperature at the pump inlet. Both these trends are as one would expect: a rise in pump speed increases both the fuel shear rates within the pump as well as the fuel flow velocity within the pipework, and thus the torque required to drive the pump. At 35 Hz, the value of $C_2 \cong 3.5\ Nm$ at 50°C; this corresponds to a power input to the pump of 0.77 kW. At that pump speed, an increase in the temperature from 0°C to 50°C reduces the torque by 0.5 Nm which corresponds to a reduced pump power input (0.66 kW). In contrast, the total power required to drive the pump at 35 Hz pump speed, 50°C pump inlet temperature, and 900 bar common rail fuel pressure is 3.5 kW. Therefore, when the pressure difference across the pump is zero, the pump power consumption is appreciable (e.g. 0.7/3.5 ≈ 20%)

4.2.2.2. Relationship between torque and pump rotational speed

The effect of pump rotational speed on the torque required to drive the fuel pump is shown in Figure 4.6 for a given common rail pressure of 700 bar and fuel temperature of 30°C. As one would expect, the torque required to drive the pump is only affected to a very limited degree by the rise in pump speed (note the highly expanded vertical scale in Figure 4.6). Although the frictional losses in the pump and pipework increase with pump speed, the pump outlet pressure remains the main factor deciding the torque required to drive the pump. The pump, being a positive displacement device, will require a value of torque (turning moment) proportional to the force on its plunger crowns and, therefore, proportional to the pressure at the pump outlet. Where pump rotational speed is changed from the lowest (10Hz) to the highest speed (35 Hz), which are typical low and high speeds in real engine conditions, the average torque rise is about 1 Nm. A 50 bar change in common rail pressure would have a similar effect on torque.

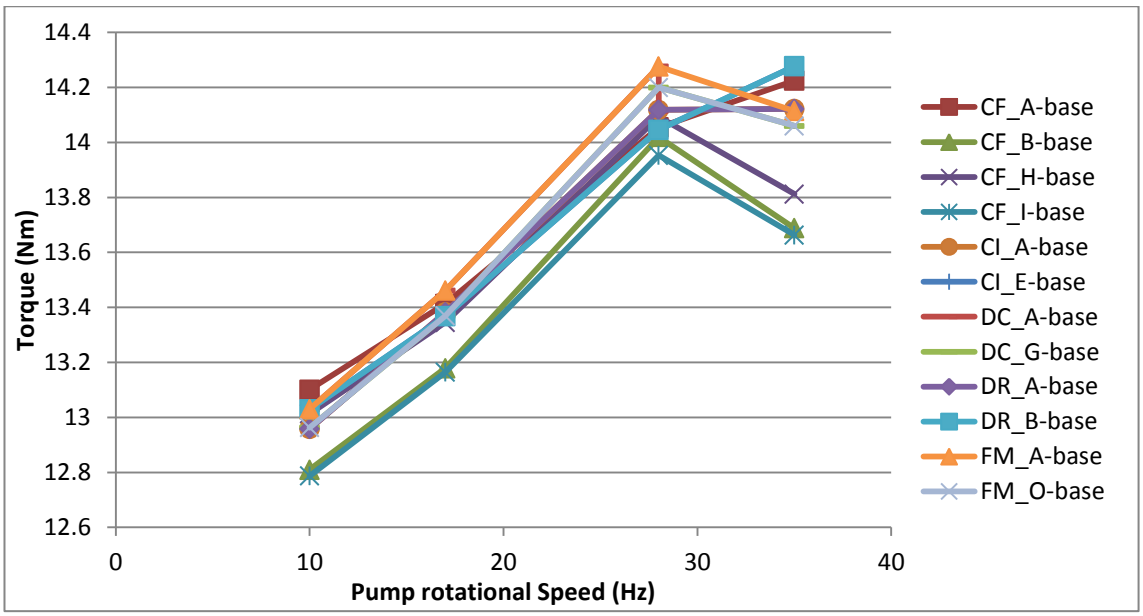

Figure 4.6: Torque vs. fuel pump speed for multiple batches of base fuel at 700 bar common rail pressure and 30°C fuel temperature

Figure 4.6 shows a non-linearity setting in between 28 and 35 Hz, particularly for base fuels occurring after cold flow (CF) and friction modifier (FM) additives. Although all the tests in Figure 4.6 were conducted with base fuels, some of the base fuels followed test with blends of additives at high concentration, which gave rise to risk of cross contamination. The peculiar behaviour in Figure 4.6 is consistent throughout all sets of fuel inlet temperature and common rail pressure conditions tested. It is thought to be due to cross contamination from the additive sample to the next base fuel.

It has been found that at the highest tested pump speed of 35 Hz, the reduction of torque due to CF additives is more significant, as discussed in section 4.2.3.2. The base fuels tested before CF-B, CF-H, CF-I all occurred after a test on 10x of CF additive (see Figure 4.1). There is a strong likelihood that part of these additives were not flushed out sufficiently during the cleaning process, and that they mixed with the subsequent base fuel to form a blend of additive that had an effect in reducing torque at 35 Hz, where the reduction is most significant. In the case of the base fuels for CF-I and CF-B, the reduction is more global, occurring for all speeds, pressures and temperatures.

A slight non-linearity can also be seen for the base samples before FM-A and FM-O, but the values for torque at 35 Hz are always well within the standard deviation of all base tests.

4.2.2.3. Relationship between torque and fuel temperature through the pump

Finally, the change in torque with fuel temperature was investigated for all base fuels. As expected, the relationship is once again linear with a decrease in torque as fuel temperature increases (see Figure 4.7). The change in torque brought by the change in pump inlet fuel temperature is minimal compared to the effect of common rail pressure, or pump rotational

speed. However, the temperature has a linear relationship with torque independent of the fuel pressure.

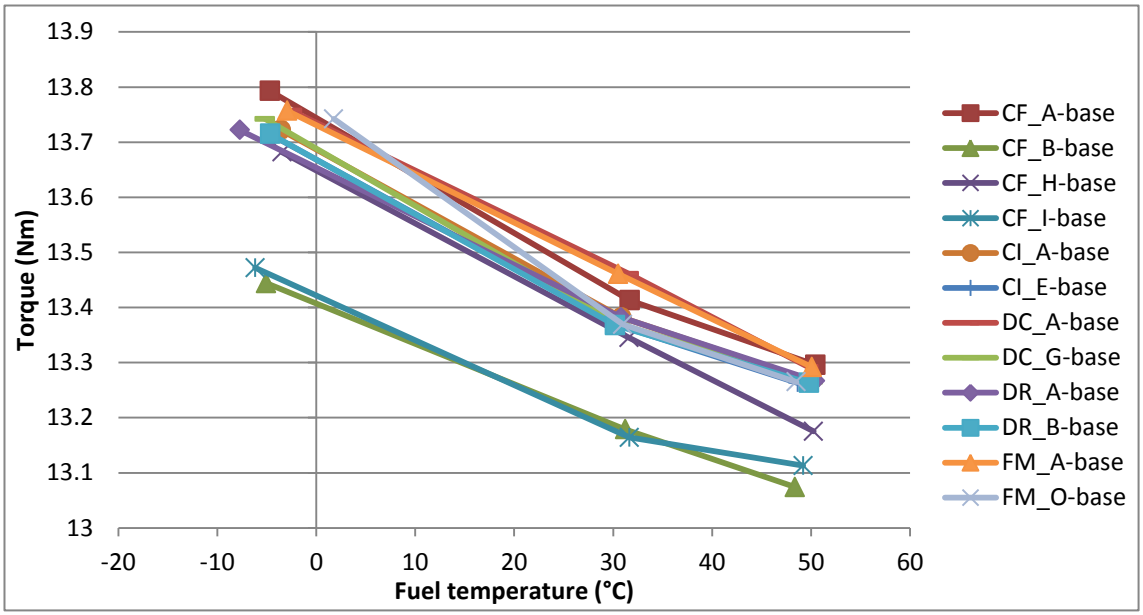

Figure 4.7: Torque vs. fuel temperature for multiple batches of base fuel at 700 bar common rail pressure and 17 Hz pump rotational speed

The small drop in torque with increasing temperature can be explained as being mainly due to the reduction of the fuel dynamic viscosity. The reduction in viscosity causes a reduction in the shear stress ($\tau = \mu \frac{du}{dy}$) between rubbing surfaces within the pump subject to hydrodynamic lubrication. The flow frictional losses within the pipework also reduce when the fuel viscosity reduces.

In the boundary lubrication regime, the fuel additive reacts with the two rubbing surfaces, forming a mono-molecular coating protecting the surfaces from scuffing and wear. When temperature is increased, the chemical reactions linking the FM additive molecule and the metal surfaces occur more often, resulting in a faster build-up of the protective molecular layer. Therefore, as fuel temperature increases, the FM additive in base fuel (50 ppm of FM-N) is more effective in reducing the frictional losses due to boundary layer lubrication (Williams, 1994). This effect is small compared to the effect due to the reduction of the fuel's dynamic viscosity. Only at extreme temperatures (above 200°C) would the molecules become damaged, resulting in a poorer boundary lubrication regime (Williams, 1994).

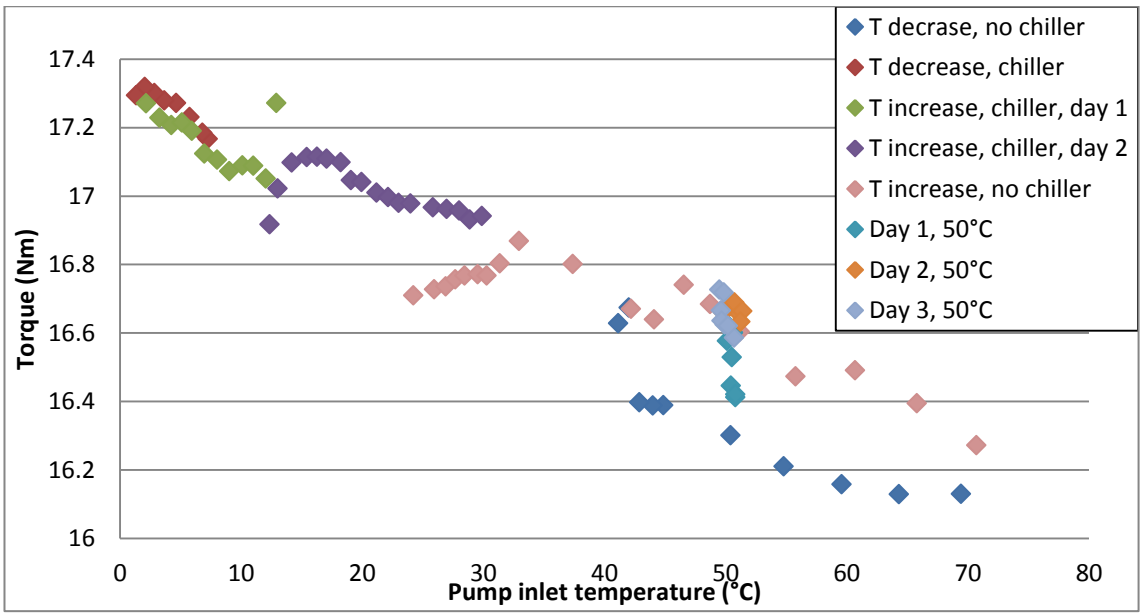

Figure 4.8 Torque vs. transitional pump inlet fuel temperature of raw fuel with 50 ppm of FM-A at 900 bar common rail pressure, 35 Hz pump speed

In order to assess the linearity of temperature with torque, further tests were carried out at intermediate temperatures (Figure 4.8). These were conducted using a different FM (100 ppm FM-A to raw fuel) instead of the 50 ppm FM-N normally present in base fuel to ensure that the linearity was not due to the 50 ppm FM-N added to raw fuel. These tests also assessed multiple ways of reaching cold temperatures, and looked at whether there was an effect when the fuel was heating up or cooling down. The results were consistent with previous findings, confirming the theory that the increase in temperature reduces the viscosity of the fuel, thus reducing friction losses due to shear stress.

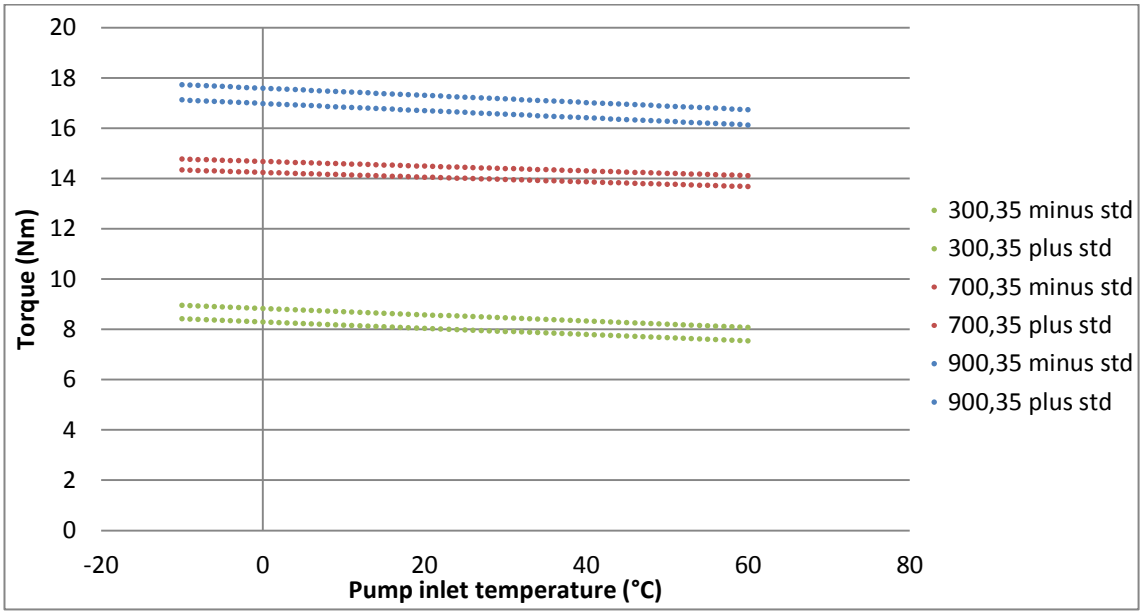

Figure 4.9: Torque vs. pump inlet temperature at 35 Hz pump speed – base standard deviation.

From the analysis carried out in this chapter, it was possible to determine the average base fuel behaviour by averaging the twelve identical base fuel tests carried out throughout the thesis. The standard deviation of those twelve instances for each data point was recorded, and it was decided that the mean base value +/- one standard deviation was to be the window of error for base tests (see Figure 4.9). When comparing tests involving mixtures of base fuel with additives, this window was used to diagnose additive effect from general error of the base fuel testing. The base fuel upper and lower limits appear as dashed lines on all subsequent graphs when comparing various blends of additives in the pump torque rig. An example of base standard deviation windows can be seen on Figure 4.9.

4.2.3. **Torque results with fuel additives**

All additives in the list shown in Table 4.1 have been tested using the protocol described in section 4.1. In general, all additive blends with base fuel have shown that fuel additives have little or no measurable effect on the torque required to drive the high pressure pump, regardless of the conditions of common rail pressure, pump inlet fuel temperature, and pump rotational speed.

Results involving each group of additives are shown below in graphs mapping torque against the fuel inlet temperature for three pressures at a specific pump rotational speed. Results are also shown in graphs mapping C_2, the intercept of the vertical axis of the common rail pressure, against torque. C_2 is a measure of frictional losses within the pump (see section 4.2.2.1.) and the rig circuit. As a measure of the reliability of the data, the average standard deviation obtained from all base fuel tests has been drawn as dotted lines on all subsequent figures.

4.2.3.1. Friction modifiers

Three friction modifier (FM) additive blends were tested in the diesel fuel pump torque characterisation rig. The results were compared against base fuel, which is itself a blend of FM-N and raw fuel. The results show a small improvement in the zero pressure equivalent torque (C_2) for high concentration of FMs. This improvement is not systematic, and does not follow a trend, suggesting a very limited improvement due to the FM additive.

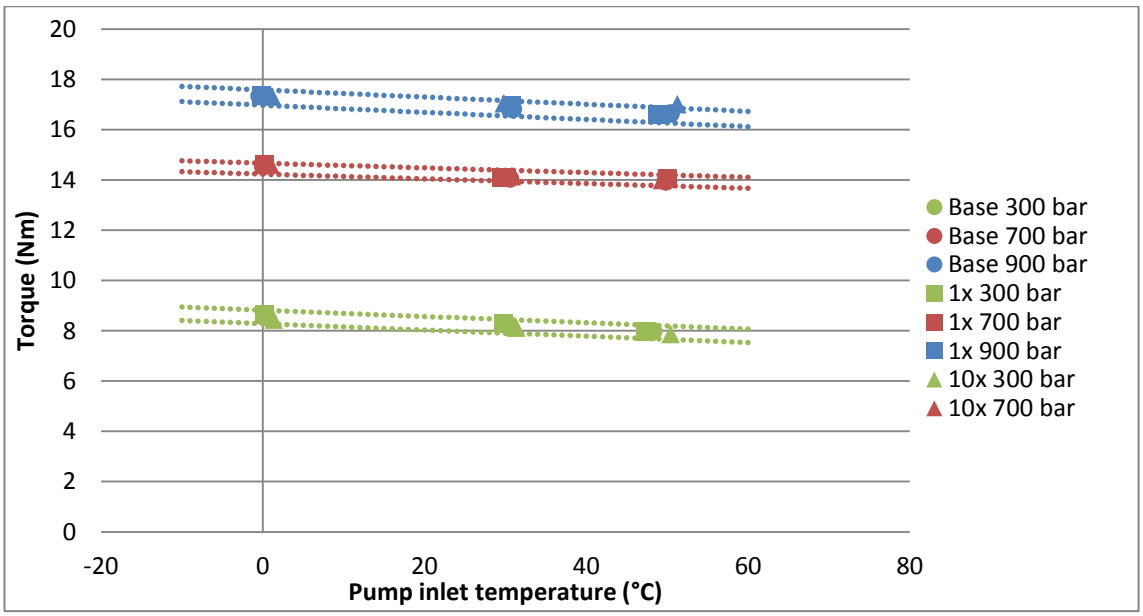

Figure 4.10: Torque vs. pump inlet temperature at 35 Hz pump speed for additive FM-O and its base.

The values of torque at 1x or 10x concentration of FM-O seen on Figure 4.10 are similar and fall within the standard deviation of the base fuel tests on the rig. This particular graph is representative of all FM additive tests for all four speed conditions at which the test was conducted. FM additives have no measurable effect on the torque required to drive the fuel pump when compared with base fuel.

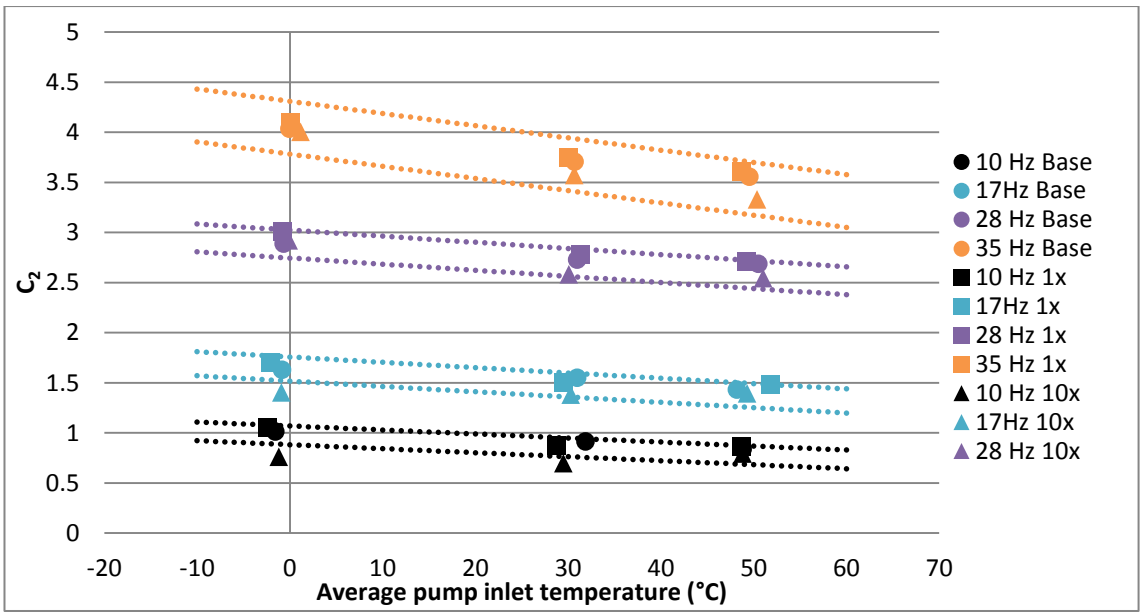

Figure 4.11: Values of C_2, the zero pressure equivalent torque vs. temperature for additive FM-O

Figure 4.11 and Figure 4.12 show the value of the intercept of the torque vs. common rail pressure curve (C_2) for additives FM-N and FM-O. For all tests on FM additives, C_2 has shown a small reduction in torque at low to medium pump rotational speeds for normal (1x) and high (10x) additive concentration. The drop in C_2 for certain pump rotational speeds does not occur

all the time. For this reason, it is difficult to draw solid conclusions as to whether the additives in higher concentration had definite improvements on pump efficiency.

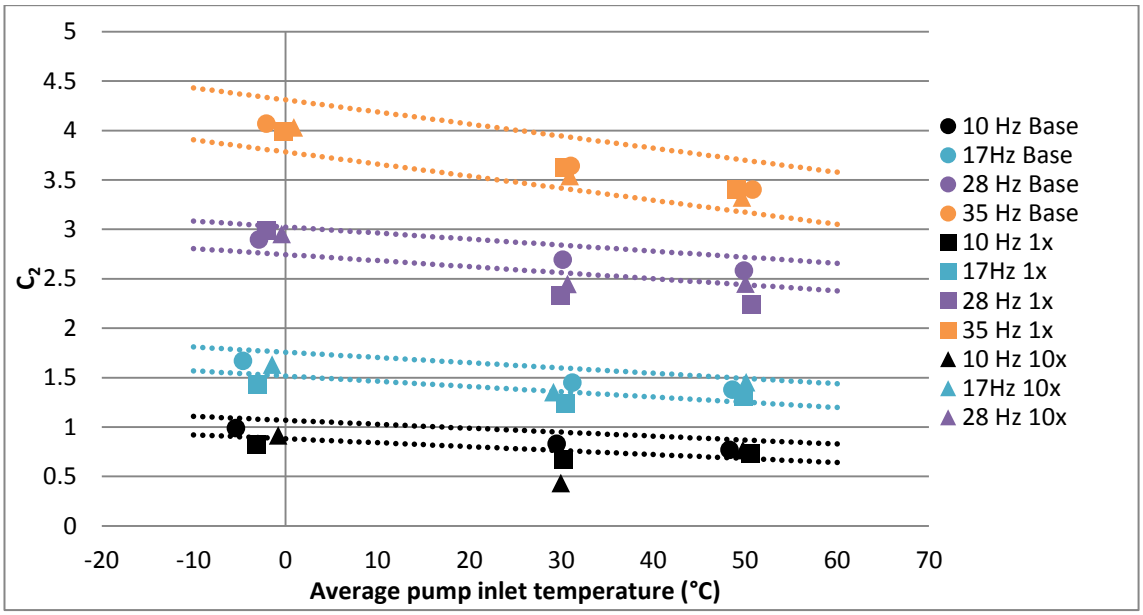

Figure 4.12: Values of C_2, the zero pressure equivalent torque vs. temperature for additive FM-N

As discussed in the literature review, FM additives work by coating the surfaces inside the pump in order to avoid damage to contacting surfaces when boundary lubrication occurs. As long as enough additive is provided to supply the surfaces with additive molecules at the same rate that additive molecules are removed from the surfaces, then surface damage can be expected to be limited. The addition of more additive should not help to reduce further the power required to run the fuel delivery system because the additive molecules are designed to react or adsorb with the metal surfaces and, once the metal surface is coated, further surface coating ceases.

In this case, because 50 ppm of FM-N is added as part of the base fuel, there is already a good supply of additive molecules to the pump surfaces. When the pump rotates at lower speeds, the addition of more FM further reduces the value of C_2, suggesting that 50 ppm of FM-N is below the optimal amount of additive to offset the removal of surface molecules through pump operation.

Because the results do not show a clear improvement for one particular additive concentration, it can be said that no clear difference between the 1x and 10x additive concentration can be seen. This suggests that once enough additive is added to maintain the boundary layer lubrication coating, no further improvement could be obtained by supplying a fuel with a higher concentration of FM additive.

Furthermore, no particular additive has shown greater improvement over the others, suggesting that as long as the additive is supplied in a concentration of 100 ppm, the additive chemistry does not play too important a role in a pump similar to the one used for those tests.

4.2.3.2. Cold flow additives

The four cold flow (CF) additives provided by Innospec were investigated at 30°C and 50°C using the method described in section 4.2.3. However, blends with additive CF-A were tested at several cold temperatures from 5°C to -5°C for various common rail pressures and pump rotational speeds. The purpose of the tests on additive CF-A at a sub-zero temperature was to investigate the effect of wax formation in fuel delivery systems, the effect waxing may have on torque; as well as how CF additives affect the torque required to operate a high pressure diesel fuel pump. The results from the cold experiments will be discussed in detail in the next section 4.3.

The fuel blends with CF additives were tested in the sequence: CF-A, CF-H, CF-B and CF-I, one after the other. To save changeover time, these experiments, as well as the cold tests discussed in the next section 4.3. below, were carried out using the same batch of CF additive. As a consequence, each blend of fuel with CF additive spent a significant amount of time in the pump rig (~30 test hours, including the cooling down period vs. the usual approximate 3 hours for blends with other types of additives).

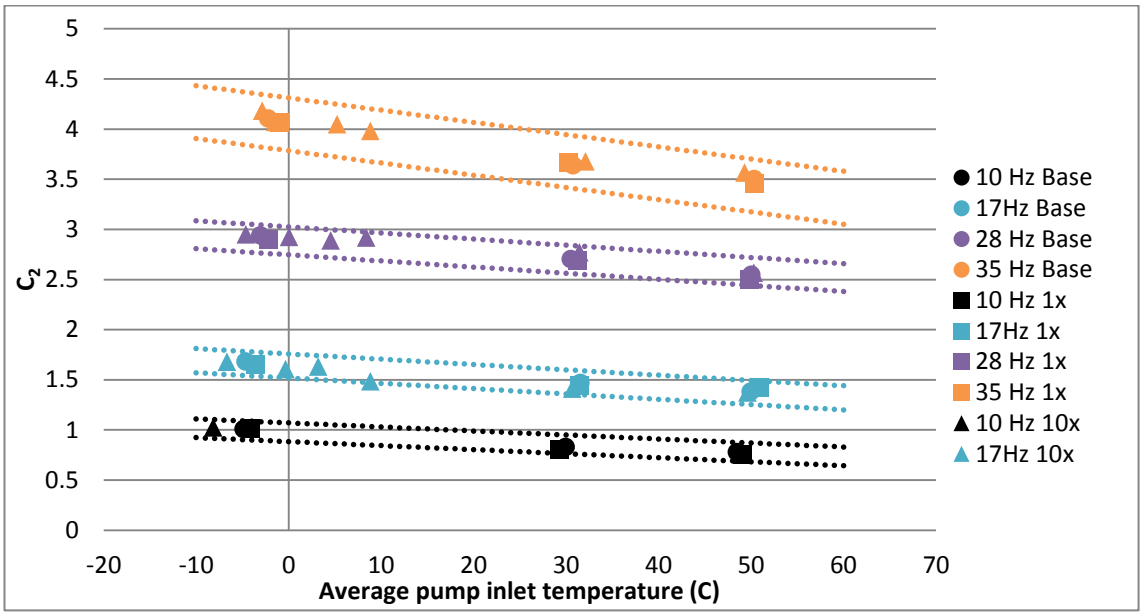

Figure 4.13: Values of C_2, the zero pressure equivalent torque against temperature for additive CF-A

The first fuel blend with CF additive CF-A (see Figure 4.13) showed no measureable change compared to base fuel in both the torque required to operate the fuel pump and the value of C_2. The absence of any discernible effect led to the decision to investigate the effect of waxing and CF additives further in the pump delivery system, as will be discussed in section 4.3.

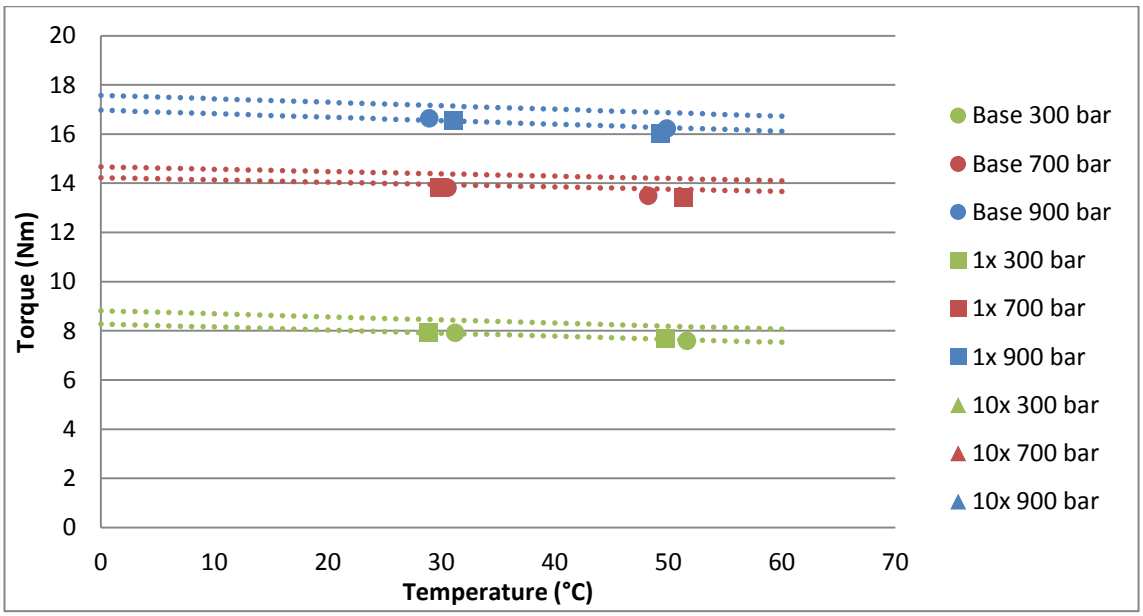

Figure 4.14: Torque vs. pump inlet temperature at 35 Hz pump speed for additive CF-H and its base

The other three CF additives (i.e. other than CF-A) were tested at 30°C and 50°C only. Results showed that for additives CF-H and CF-B, the torque required to drive the pump was generally slightly lower for all conditions of common rail pressure and pump rotational speed (Figure 4.14). As this reduction is observed on the zero pressure equivalent torque (C_2) for experiments on fuel blends with both CF-H and CF-B (see Figure 4.15), it can be concluded that losses were reduced in pumping, pipework and common rail friction.

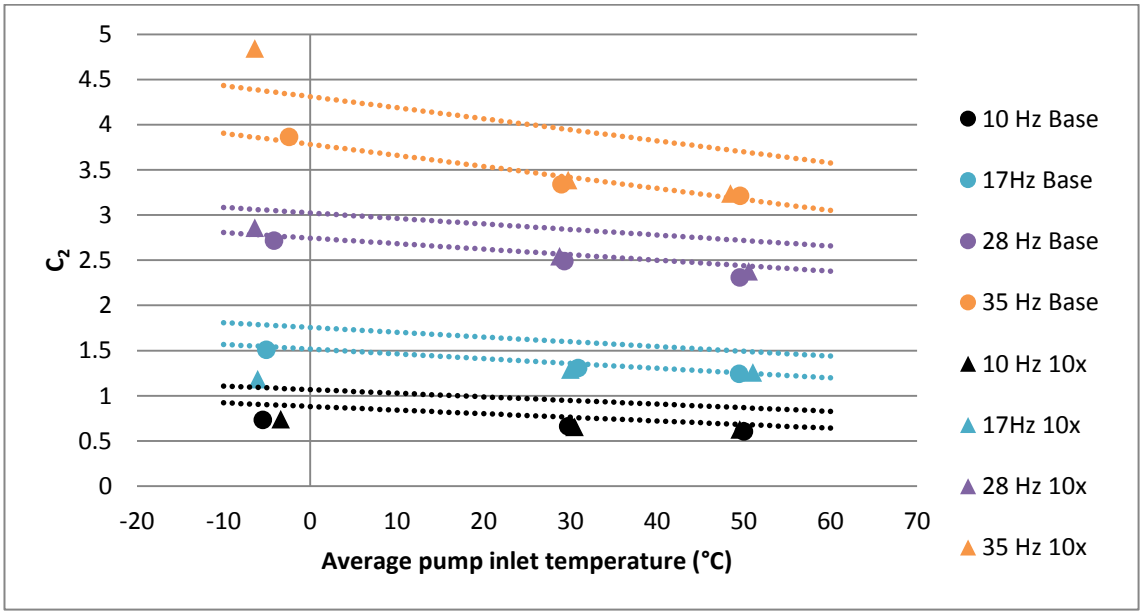

Figure 4.15: Values of C_2, the zero pressure equivalent torque against temperature for additive CF-B

CF additives act by preventing the wax nuclei, or wax crystals that naturally form in the fuel from growing and agglomerating, as discussed in the literature review. It is believed that the reduction in power loss may be due to an overall decrease in fuel viscosity or surface tension with additives CF-H and CF-B, rather than the formation of fuel waxing. As discussed earlier

(see section 4.2.2.2.), the reduction in torque due to additive CF-H and CF-B was also seen in the base fuels tested before the fuels with additives CF-B and CF-I respectively, probably due to cross contamination.

4.2.3.3. Deposit control additives

The results with deposit control additives DCA-A and DCA-G have shown no change in the torque required to operate the fuel pump compared to base fuel.

Molecules of deposit control additives (DCAs) are attracted to deposit particles and thus prevent the deposit particles from agglomerating. DCAs also coat metallic surfaces so as to prevent deposits from being attracted to the surfaces. However, in contrast to FM additives, DCAs form a weaker bond to metallic surfaces. This is because FM additives are designed to maintain their bond under conditions of high stress and shear where two metal surfaces are rubbing each other. In contrast, DCA additives are designed to work on metallic surfaces which are not usually in contact with others (such as injector nozzles, or the top of engine pistons).

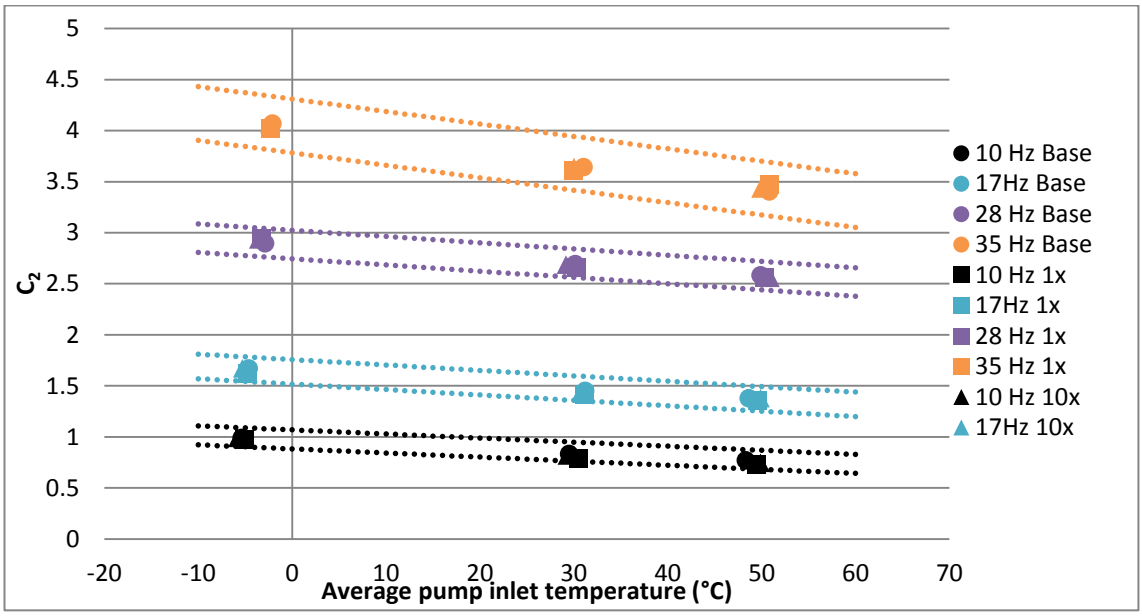

Figure 4.16: Values of C_2, the zero pressure equivalent torque vs. temperature for additive DCA-A

Figure 4.16 shows that DCA additives have no effect on the zero pressure equivalent torque (C_2) when compared with base fuels.

4.2.3.4. Drag reduction additives

DR-A and DR-B, two drag reduction additives, were tested in the pump rig. Drag reduction additives (DRAs) are known to be damaged by pumping. When used in fuel transporting pipelines, DRAs need to be added after the fuel has passed through a pump, in order to replace damaged molecules. Drag reduction additives are fragile, and the very long molecular chains

from which they are formed break easily if the fuel is put under enough stress imposed by high pressure, shear stress, or temperature.

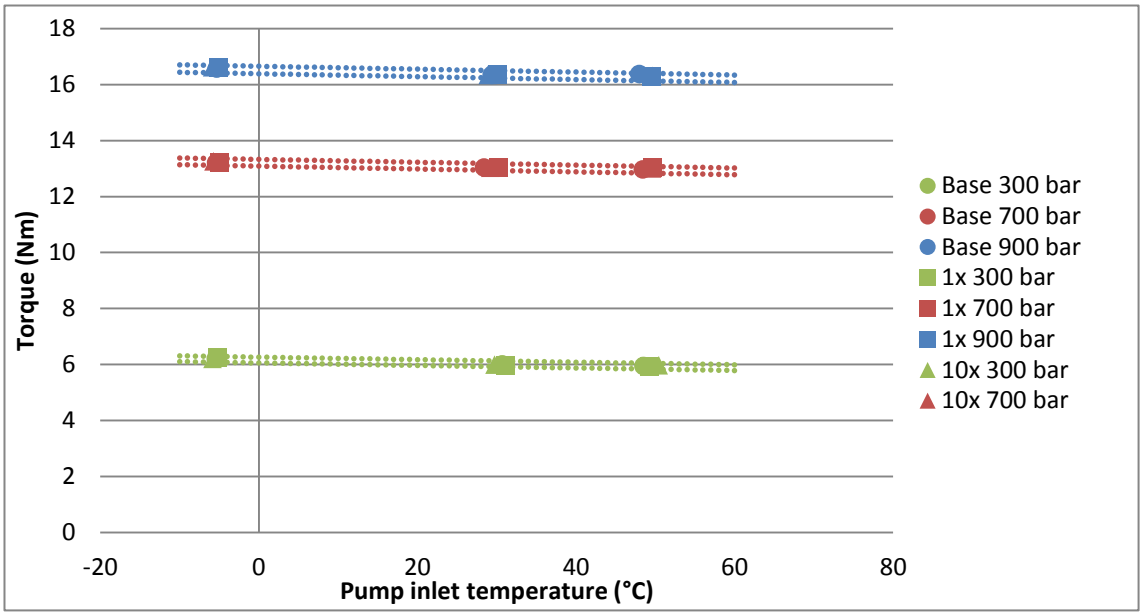

Figure 4.17: Torque vs. pump inlet temperature at 10 Hz pump speed for additive DR-A and its base

Figure 4.17 shows that DR-A and DR-B have had no effect on the torque required drive the high pressure fuel pump. This is believed to be because they were damaged by their passage through the pump.

4.2.3.5. Combustion improvers

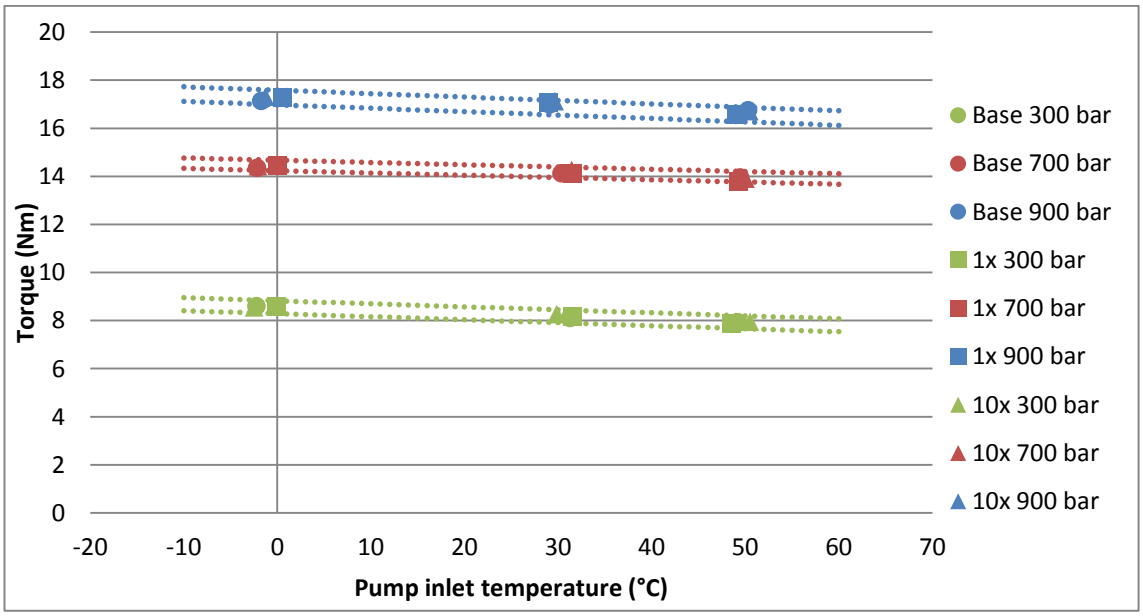

Figure 4.18: Torque vs. pump inlet temperature at 35 Hz pump speed for additive CI-A and its base

Combustion improvers CI-A and CI-E were also shown to have no measurable effect on the torque required to drive the fuel pump or the frictional losses between moving surfaces in the

pump (C_2), as seen on Figure 4.18 and Figure 4.19. Similar results to those shown in Figure 4.18 and Figure 4.19 were obtained for other pump speeds.

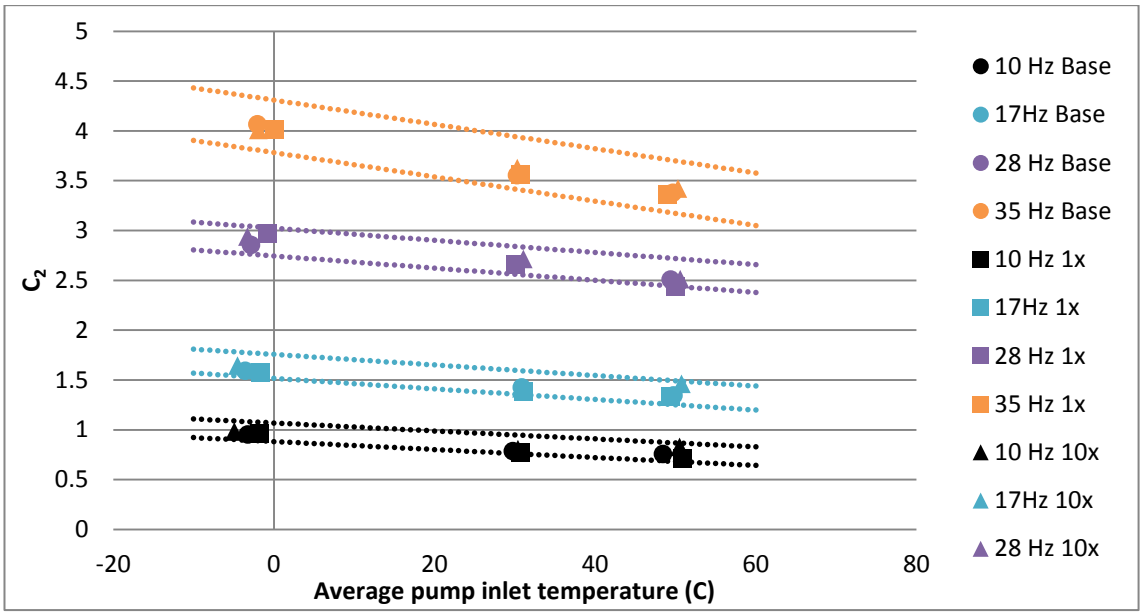

Figure 4.19: Values of C_2, the zero pressure equivalent torque vs. temperature for additive CI-A

4.3. Experiments at sub-zero temperatures

In order to study the effects of fuel waxing on pumping power, a series of additional tests was designed using the fuel pump torque characterisation rig. Using a blend of cold flow (CF) additive CF-H and base fuel, the temperature of the fuel was lowered below the waxing point (around -10°C) of the base fuel.

4.3.1. **Initial study on a cold flow additive (CF-H)**

For this series of tests, the chiller was used to cool down the ethylene glycol solution in the cooling tank from room temperature to its minimum temperature of about -21°C. The process of reaching -21°C took approximately one day. The fuel was then run through the chiller system and cooled down with the heat exchanger located before the fuel pump (see Figure 4.20).

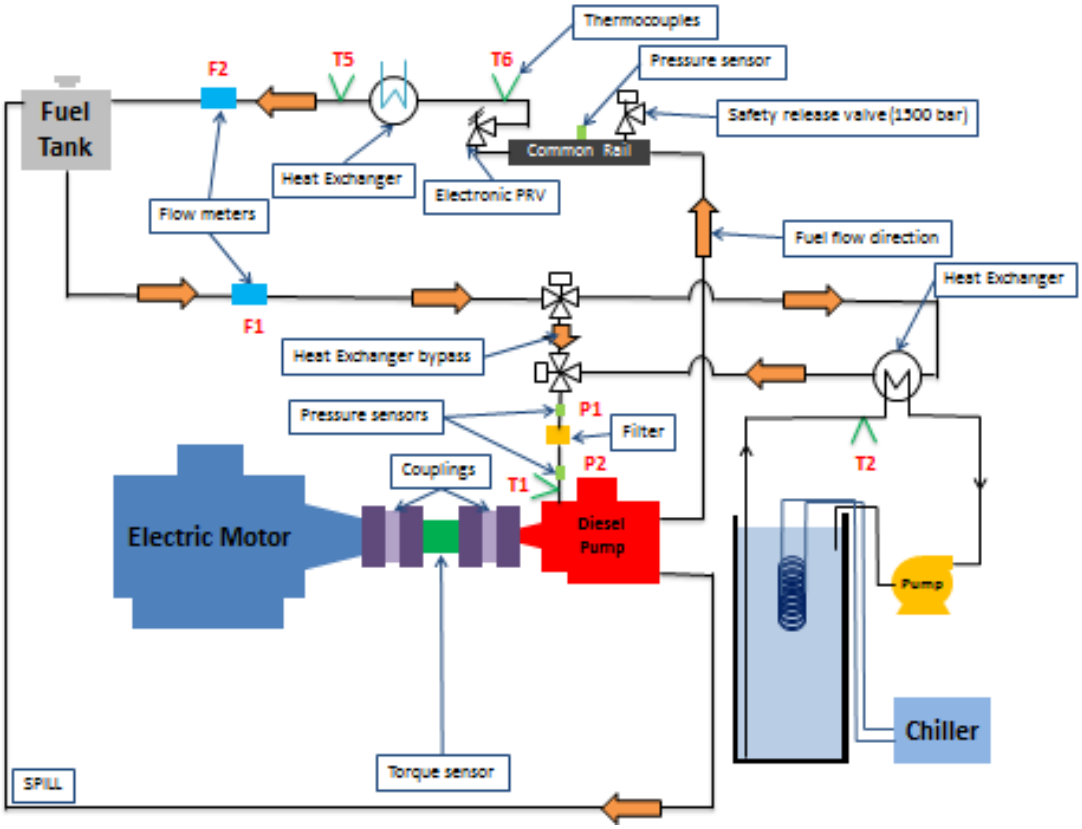

Figure 4.20: CF-H cold tests – Fuel pump torque characterisation rig set-up.

The set-up used for the cold tests experiments is shown in Figure 4.20. Eight second sets of data were recorded every minute for a prolonged amount of time (over 2 hours) as the fuel was pumped around, through the heat exchanger. The diesel fuel pump speed was fixed at 10 Hz (1200 RPM equivalent engine speed) and the common rail pressure was set to 700 bar. In some of the tests, the common rail control valve (PRV) was left open or bypassed so as to minimise the pumping power and energy dissipation into the fuel, in order to reach fuel temperatures as low as possible.

The reader is reminded that the main problem with waxing fuel in modern engines, operating in extremely cold conditions, is filter obstruction or blockage. This occurs because the waxing crystals are too large to pass through the 5-50 micron fuel filter, and start forming a solid film blocking the filter. In order to measure the extent of filter blockage, the pressure drop across the filter was monitored. The chiller temperature, fuel temperature and fuel flow rate were also monitored, so as to determine at which temperature waxing occurred, and the effect waxing fuel may have had on the fuel flow rate.

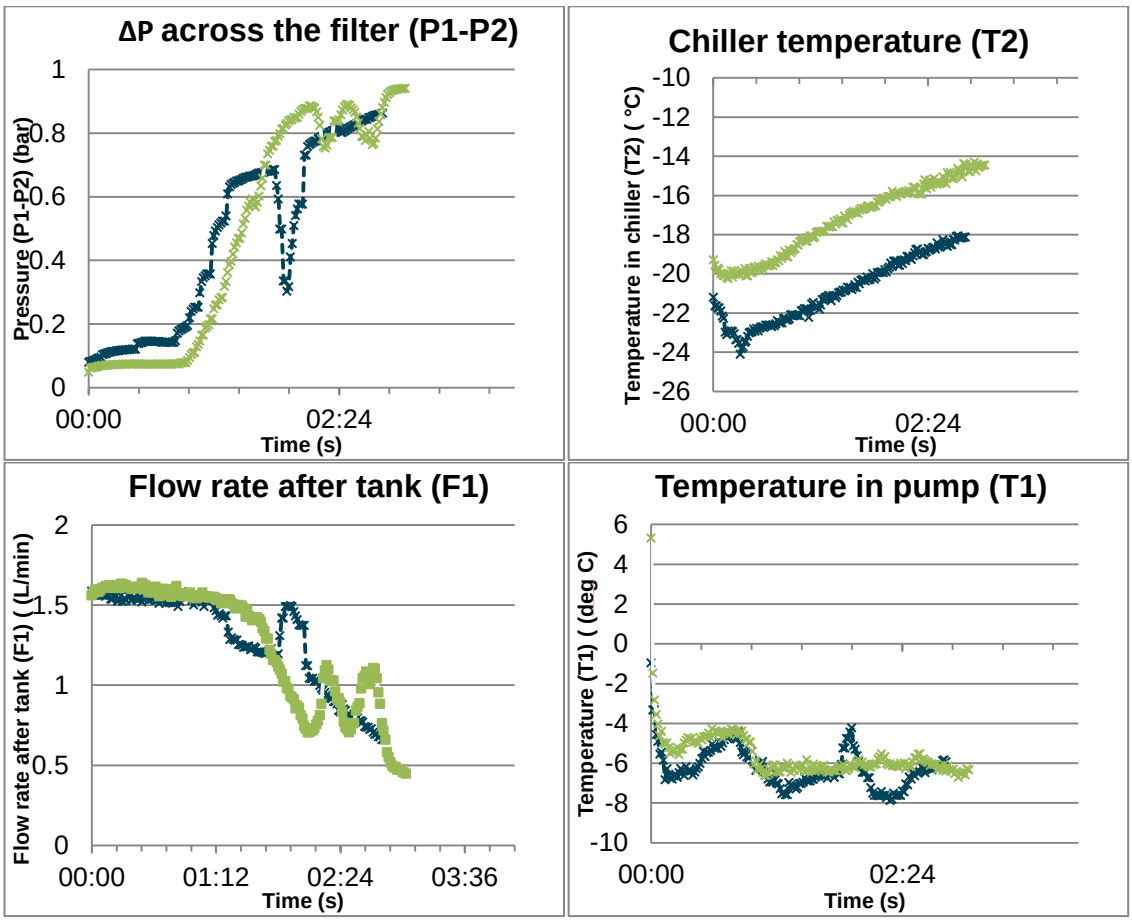

Figure 4.21: CF-H additive blend behaviour at open common rail (blue – 10x CF-H; green - Base)

The initial test was carried out using a blend of CF additive CF-H at 10x concentration with base fuel. The test was bracketed with base fuel tests. The results from this test are shown in Figure 4.21.

Chiller temperature (T2) dropped initially as the temperature-stratified ethylene glycol in the chiller tank was stirred and mixed due to the inflow and outflow from the tank. The subsequent constant rate of temperature increase in the chiller suggests that for both fuel tests, the heat removal rate from the fuel was not affected by the additive.

Initially, the temperature at the fuel pump inlet (T1) reduced as the fuel was rapidly cooled down by the heat exchanger. As wax started to form, the pressure across the fuel filter (ΔP) rose rapidly for both fuel blends, hampering fuel circulation through the system. As a consequence, the fuel flow rate (F1) dropped. The fuel was cooled down further by the heat exchanger (due to the reduced flow rate), resulting in a further decrease in the fuel inlet temperature to the pump (T1).

However, as the temperature of the fuel continued to reduce below -10ºC, a new phenomenon occurred, that is, wax began to form on the internal surfaces of the heat exchanger. This had two effects on the system. Firstly, the wax coating acted as an insulator in the heat exchanger, preventing fuel from being cooled down as efficiently as previously, bringing T1 to a minimum

temperature. Secondly, the chemical composition of the leftover liquid fuel changed as the heavy paraffins in the liquid fuel formed into wax crystals, leaving a liquid fuel with a different fuel composition. This prevented extra wax from forming, and allowed the system to keep running as the fuel filter was only partly blocked.

Then, the pressure drop across the filter (ΔP) reduced because the wax in the filter started to melt, partly because the waxing of the heat exchanger reduced fuel cooling and partly because of some throttling in the common rail heating up the fuel. This increased the fuel flow rate (F1) and restored heat exchanger efficiency as the wax layer melted. The cycle then started over again, as depicted on Figure 4.21.

This behaviour, involving cycling wax formation and melting, occurred several times per hour. In most cases, the filter eventually fully blocked due to wax build-up in the filter, and fuel flow rate fully dropped to zero. The fuel pump torque characterisation rig was stopped when the filter blockage was too severe, so as to limit damage to the pump from fuel starvation.

Similar results were found when the common rail pressure was set to 700 bar. Because the fuel was pressurised in the common rail, the fuel temperature in the tank was greater than when the common rail was open. As a result, the decrease in heat exchanger efficiency due to internal wax coating was less significant when the minimum T1 was reached, resulting in smaller oscillations of T1 during the wax cycling behaviour. Additionally, these higher minimum temperatures did not allow for wax to build up in the filter, so filter blockage did not occur. The tests were stopped after a 3 hour run.

The wax coating cycling pattern was specific to the pump rig system used for this project and may not be reproducible in real vehicle situations. Wax in a vehicle forms uniformly in the fuel tank, as the outside temperature drops. Furthermore, wax formation in an engine is a slow process (taking hours) where wax nuclei form and grow progressively and then bond together to form large wax crystals over time. In contrast, in the pump rig system, the wax formation was localised at the heat exchanger walls and almost instantaneous. The results from Figure 4.21 show that CF additives were ineffective in preventing wax accumulation in the heat exchanger. The data suggests that wax nuclei and crystals grew too quickly to sizes too large to pass through the filter, before the CF additive had the time to prevent wax crystals from forming.

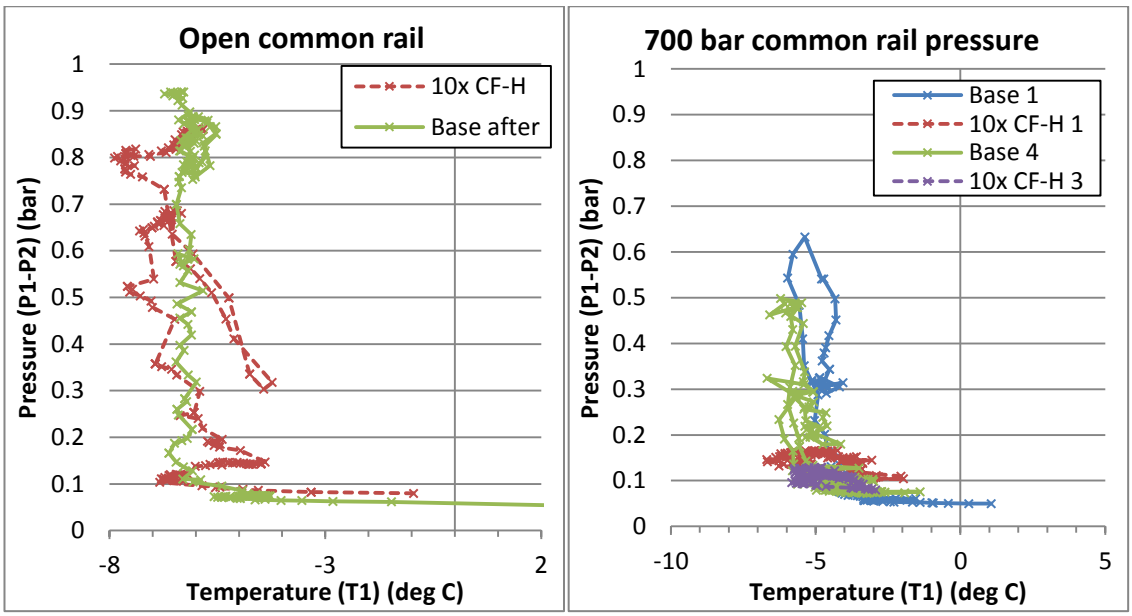

Figure 4.22: Pressure difference across the fuel filter vs. fuel temperature

Figure 4.22 shows the effect of temperature on filter blockage for tests on CF-H and base fuel. The onset of waxing for diesel fuel in the system occurred at the same pump inlet temperature T1 (around -6°C), regardless of the additive or the common rail pressure. This could be explained by the wax coating cycling pattern. This minimum value of T1 was determined as the point where the finite layer of wax present on the heat exchanger walls decreased the efficiency of the heat exchanger to a point where the fuel could not be cooled down any further. Once all of the wax for the given amount of fuel (4 litres) was formed, the heat exchanger efficiency dropped. It is assumed that if fresh fuel had been supplied continuously, then wax would have kept forming until the filter was fully blocked.

Figure 4.23 shows that, as long as fuel was still able to flow through the fuel filter, the torque required to operate the fuel pump was not affected as the fuel passing through the filter behaved as normal fuel. The torque only varied when the filter was blocked to a point where the positive displacement pump was starved of fuel, preventing the operating pressure in the common rail from being reached.

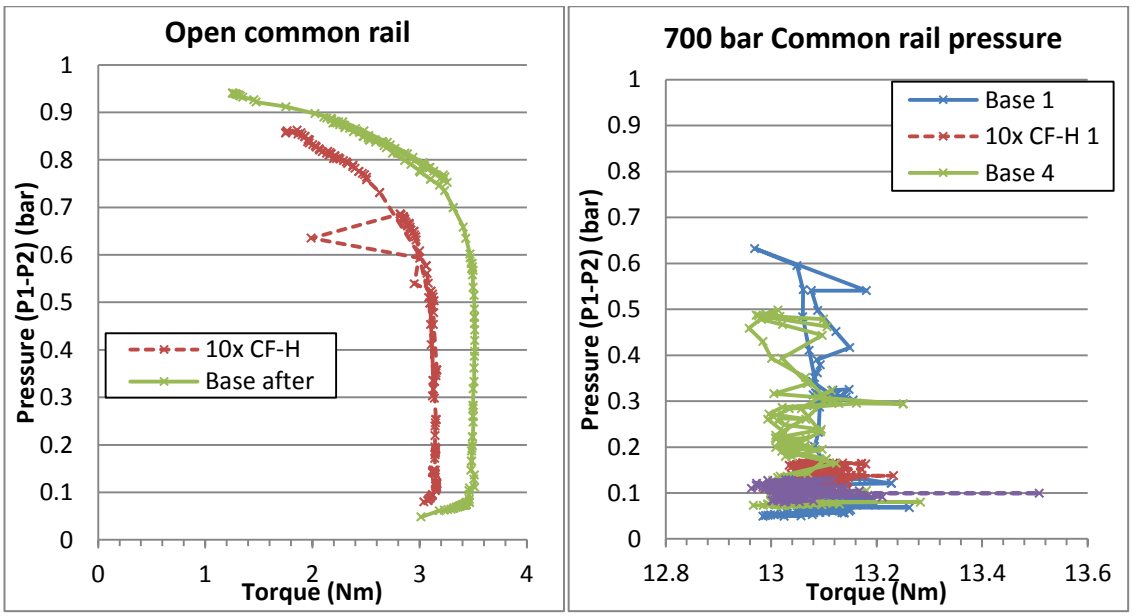

Figure 4.23: Torque vs. pressure drop across the filter

On Figure 4.23, the 0.5 Nm difference in torque required to operate the fuel pump between fuel with and without additive is believed to be due to a change in fuel viscosity. Pressure and torque built up as a result of fuel passing through the common rail orifice. The difference in the fuel's viscosity changed the pressure build-up in the common rail, which affected the torque. When the pressure in the common rail was set to 700 bar, both fuel blends behaved in the same way, which confirmed that the effect was not wax-related.

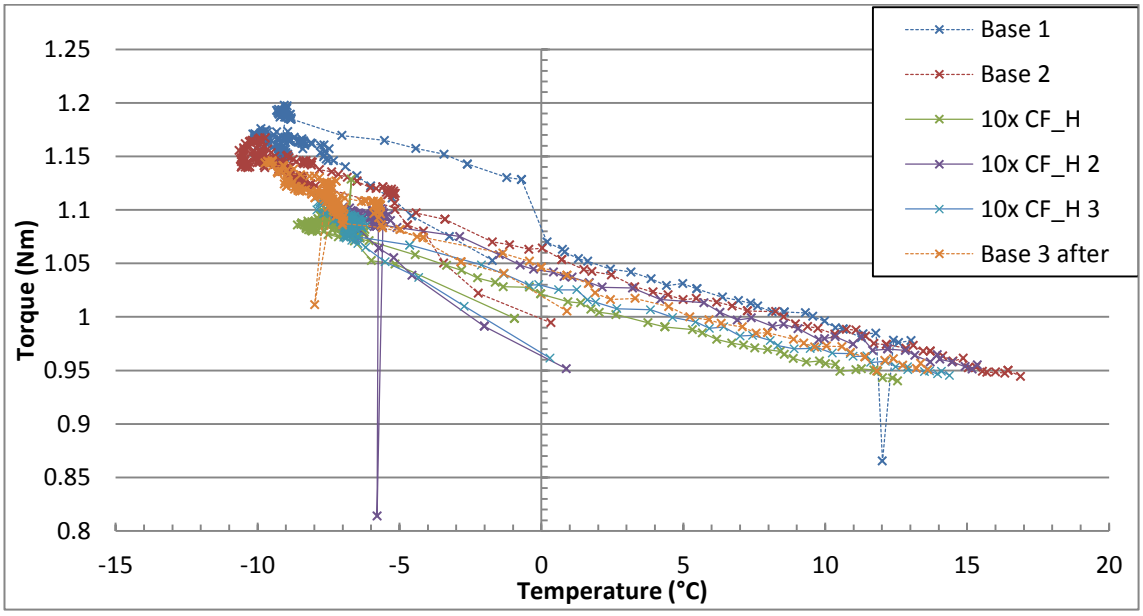

Figure 4.24: Fuel temperature before the pump (T1) vs. torque required to drive the pump with no fuel filter and bypassed common rail

Further tests, the results of which are shown in Figure 4.24, were carried out to confirm that wax had no effect on torque, as well as to investigate the effect of wax inside the diesel fuel pump. The fuel filter was removed, preventing blockage from occurring, and the common rail

was bypassed, so as to prevent damage to the electronic PRV. The results showed that the torque required to operate the pump was directly proportional to the pump inlet temperature, regardless of whether the fuel was above or below waxing temperature. The linear decrease in fuel viscosity with increasing fuel temperature resulted in a linear decrease in the shear stresses in the pump, common rail and pipework, thus requiring less torque.

Therefore, fuel waxing, whether in the fuel filter or in the pump, had no negative effect on the torque required to operate a fuel pump. The torque was only affected when the fuel supply to the pump was prevented due to filter blockage, resulting in fuel starvation of the pump, which lowered the pressure reached in the common rail, and therefore the torque. Under these circumstances a commercial vehicle engine would not be supplied with fuel at the correct pressure and it is likely that it would stop operating.

4.3.2. **Effects of waxing diesel fuel in the heat exchanger**

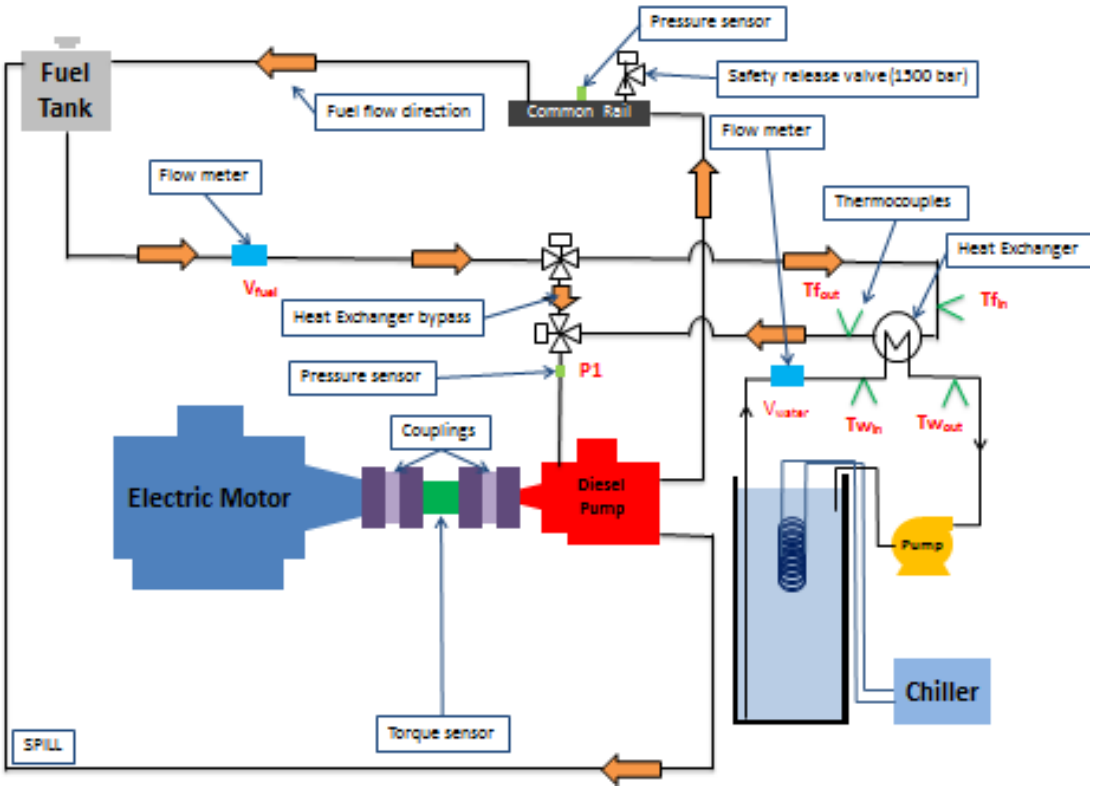

Figure 4.25: Diesel fuel pump torque characterisation rig set up for heat exchanger study

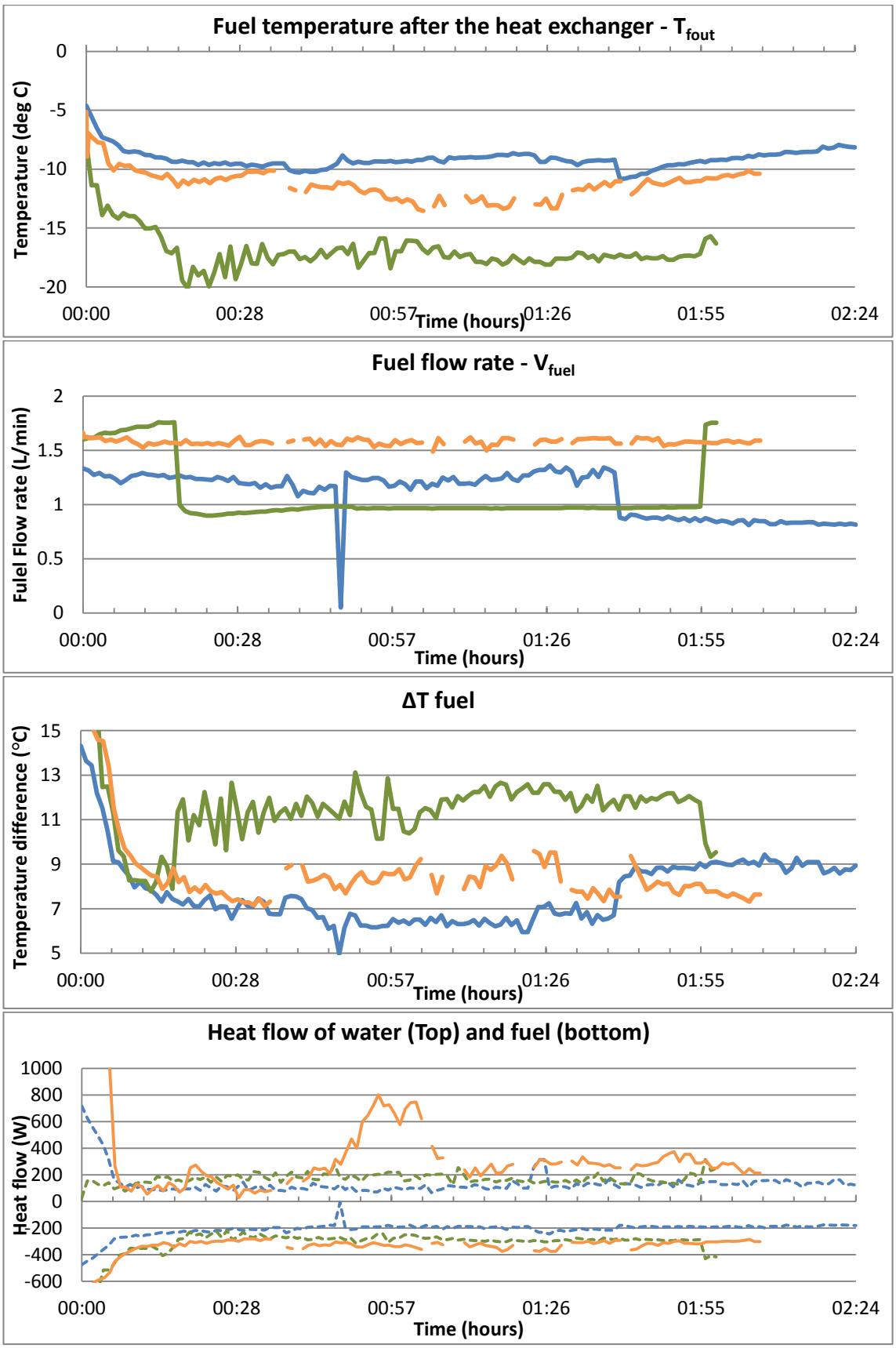

Figure 4.26: Diesel fuel pump torque characterisation rig behaviour around the heat exchanger (orange – Base; Light blue – 10x CF-H, Green – 10x CF_A)

In order to be able to confirm the wax coating cyclic behaviour, a series of tests was carried out to confirm the drop of heat transfer through the heat exchanger when waxing occurred. To do this, the energy transfer across the heat exchanger was experimentally determined. The following fuels were used: base fuel, a blend of base fuel with 10x CF-H and a blend of base fuel with 10x CF-A, another CF additive.

In order to determine the value of energy flow $\dot{Q}_w$ to the ethylene glycol side of the heat exchanger and $\dot{Q}_f$ on the fuel side of the heat exchanger, the coolant and fuel flow rates, and temperatures in and out of the heat exchanger, were recorded, as seen in Figure 4.25. The fuel filter was removed from the system to ensure that any change in fuel flow rate was caused by wax forming in the heat exchanger rather than the filter blocking with wax. The common rail was bypassed in order not to damage the electronic PRV with unfiltered fuel. A long test was carried out as previously, while recording the flow rates and temperatures of the fuel and the coolant. The energy flow equation was used as follows:

$$\dot{Q} = \dot{v}\rho c_p \Delta T \quad (7)$$

Where $\dot{Q}$ is the energy flow in W, ρ is liquid density in kg/m^3, c_p is the fuel heat capacity at constant pressure in kJ/kgK, ΔT is the change in temperature in K, and $\dot{v}$ is the volume flow rate in m^3/s.

Figure 4.26 shows the energy flow characteristics on the two sides of the heat exchanger, including fuel flow rate, fuel temperature after the heat exchanger, and the fuel temperature

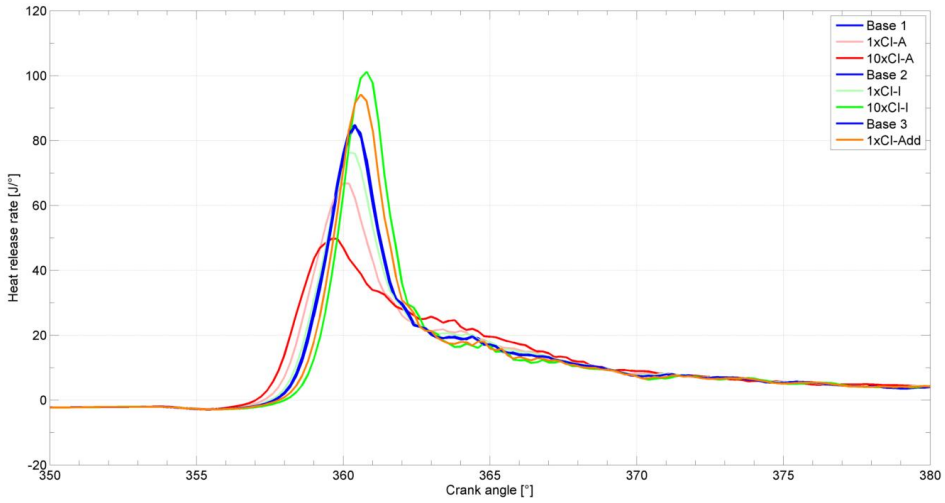

were observed as the waxing and non-waxing behaviours within the heat exchanger.

Base fuel (in orange in Figure 4.26) waxed very quickly (within the first 15 minutes), seen as a quick drop in fuel temperature out of the heat exchanger in Figure 4.26. After about 45 minutes of testing, the energy flow on the ethylene glycol side increased, suggesting a melting of wax,

possibly as a result of the layer of wax reducing the heat exchanger efficiency. Within minutes however, the layer of wax melted, which reversed the process.

The blend of additive CF-A (in green in Figure 4.26) also waxed within 15 minutes, reflected as a drop in fuel flow rate, and an increase in temperature difference. The energy flow is not visibly affected in Figure 4.26 by this process, but the sudden change in flow rate can only be due to an added restriction due to wax formation in the heat exchanger. The blend of additive CF-H took about 1 hour and 45 minutes to form wax in the same manner as additive CF-A.

For all three blends of diesel fuel, the results from Figure 4.26 have proven the presence of localised waxing of fuel in the heat exchanger, whether it is through a change in heat exchanger efficiency (base fuel) or through a restriction of flow in the heat exchanger (blends with CF additive). The proof of localised waxing in the heat exchanger further validated the waxing cycling theory.

4.3.3. **Cold flow additives in the fuel pump torque characterisation rig**

Cold flow additives CF-A, CF-B and CF-I were tested with additional instrumentation on the pump rig to determine whether CF additives other than CF-H behaved similarly. Figure 4.27 shows the experimental setup. The tests were run for at least 1.5 hours, or until the fuel filter was fully blocked by wax. Every minute, an 8 second sample at 10000 samples per second was recorded from all of the instrumentation shown in Figure 4.27. The pump speed was set to a constant 10 Hz (equivalent to 1200 engine RPM). The common rail pressure was monitored while the common rail electronic pressure relief valve (PRV) was left open (open common rail). Further tests were also carried out at 700 bar pressure. The chiller system was used to cool down the fuel as in previous experiments.

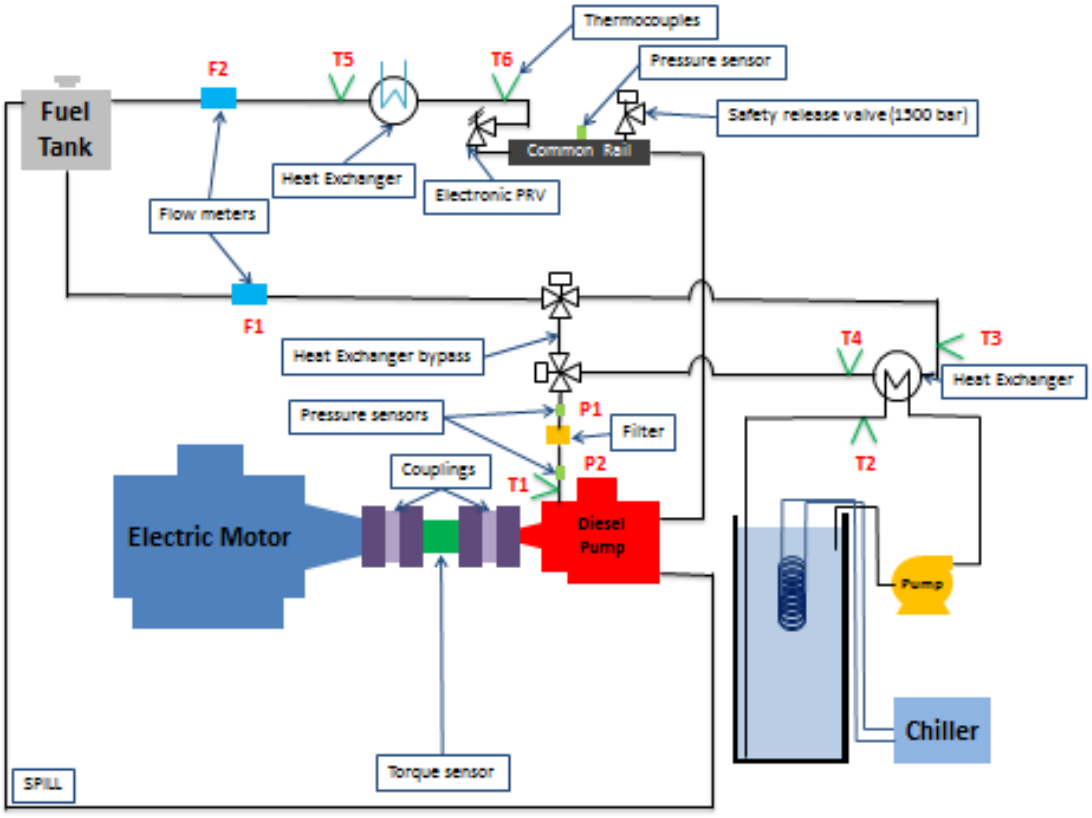

Figure 4.27: Fuel pump torque characterisation rig setup for further tests on CF additives

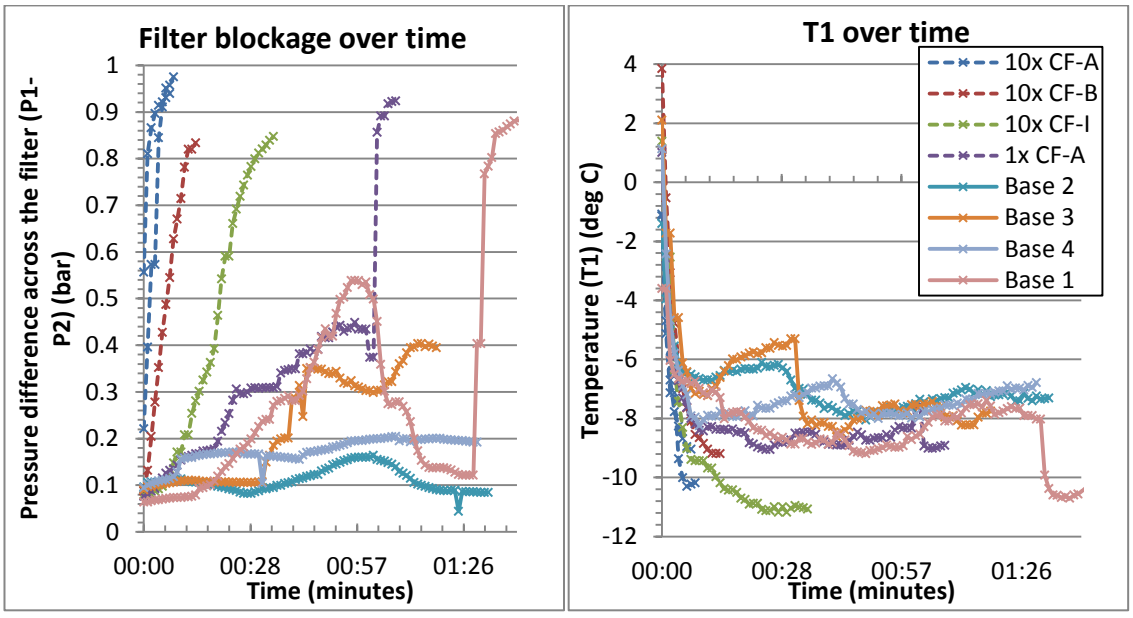

Figure 4.28: Filter blockage with open common rail of various CF additive blends

The results on fuel blended with a variety of CF additives can be seen in Figure 4.28. Surprisingly, from these sets of results, it is evident that the addition of CF additives in the pump rig had a strong negative impact on filter blockage. The addition of any diesel fuel blended with CF additive at higher (10x) concentration resulted in the filter being fully blocked within 30 minutes. A fuel blend of 1x of additive CF-A also had the effect of blocking the filter

prematurely. The results from all base fuel tests showed the wax coating cycling pattern (as seen previously for base fuel and blends with additive CF-H). With the exception of base fuel 1, all base fuel tests were stopped after about 1.5 hours without having blocked the filter.

It is known from previous sections that wax forms rapidly on the heat exchanger's internal walls, unlike in a vehicle where wax formation occurs over time throughout the fuel tank, pipework, and engine fuel system. It is believed that the accelerated formation of wax in the rig heat exchanger did not allow sufficient time for the CF additive to bond with the wax nuclei and small crystals in the pump rig. Therefore, the wax crystals could rapidly grow large enough to block the fuel filter. For these reasons, it is believed that the CF additives provided no benefit in preventing waxing in the pump rig.

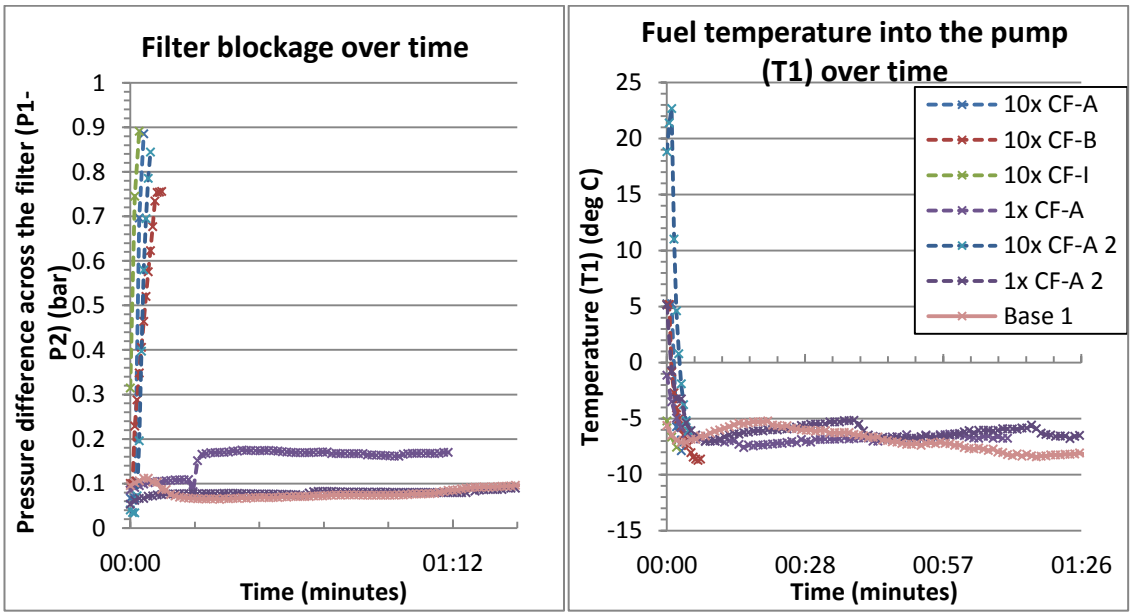

Figure 4.29: Filter blockage at 700 bar common rail fuel pressure of various CF additive blends

The results shown in Figure 4.29, where the system's common rail is pressurised to 700 bar, show very similar results to those seen with an open common rail, with the exception that, unlike previously, the blend with additive 1x CF-A did not block the filter. This behaviour suggests that, like 10x CF-H in the initial tests, 1x CF-A in this instance reached a stable enough concentration not to fully block the filter or coat the heat exchanger. The lower concentration of additive does not add enough molecules to the system to allow full solidification of the fuel/additive agglomeration.

4.4. Conclusions from pump power studies

It has been found that in a fuel delivery system resembling that of an engine, the torque required to operate a fuel pump is mostly governed by the required fuel pressure, and that the relationship between the two is linear. It is therefore possible to extrapolate this linear relationship to intercept the torque axis at zero pressure. This torque value, at zero pressure,

represents the frictional losses inside the pump due to lack of lubrication, as well as fluid friction losses in the pump, pipework and common rail. The fuel temperature and the pump rotational speed both had an effect on this frictional torque, with pump speed having a larger effect on this frictional torque than the fuel temperature.

The results have shown that the friction torque increase from a low engine speed operation to a high engine speed operation (10 to 35 Hz) is about 3 Nm, whereas the torque decrease resulting from cold (0°C) to hot (50°C) diesel fuel is 0.5 Nm. Nevertheless, these frictional losses were found to be almost negligible compared with the ~14 Nm needed to pump fuel from, say, 1 to 700 bar at 28 Hz.

It has been also found that, for all additives, the frictional torque and, therefore, the torque required to drive the pump is not affected significantly by the additives.

In principle, FMs were expected to reduce the torque required to drive the fuel pump. However, it was not possible to carry out tests without any FM additive, for concern over damaging the pump. Therefore, it was not possible to confirm the effect of FM additives on frictional torque. Simply adding more FM additive would not have provided the answer to this question, as, once some FM additive is used, the internal pump surfaces become coated and further addition of FM additive are ineffective.

The behaviour of waxing fuel was investigated by exposing the flowing fuel to sub-zero temperatures by means of a heat exchanger. Behaviour not typical of an actual car engine was observed. This was due to the fact that the same small quantity of fuel (4 litres) flowed around the system multiple times, and that the diesel fuel was cooled down much more rapidly than in a car engine. This resulted in the wax coating undergoing a cycling pattern which was explained in detail in this chapter by investigating in some detail the energy flows through the heat exchanger.

The relationship between torque required to operate the pump and fuel inlet temperature was found to be linear regardless of whether the fuel begun the waxing process or not. This linear relation held regardless of the CF additive in diesel fuel.

In general, CF additives, especially at high concentration, made the fuel wax more quickly in the fuel pump torque characterisation rig. This was not an expected result. It is believed that this was due to the rapid cooling of fuel in the heat exchanger, unlike in an engine, where fuel is cooled more slowly by the ambient temperature dropping progressively. In commercial fuels, CF additives are known to positively and significantly affect the waxing behaviour of fuels in commercial vehicle engines, and to heavily reduce the CFPP.

Chapter 5

Cold spray investigations in combustion vessel

Much is already known about the effects on fuel spray behaviour of variables such as fuel injection pressure, injector nozzle diameter, fuel temperature or ambient gas density. Physical aspects of the diesel fuel, especially viscosity and surface tension, also have an effect on spray behaviour, and, particularly, droplet size.

As mentioned in the literature review, diesel fuel additives make up such a small percentage of the overall raw fuel concentration (less than 0.1% per additive) that they do not play a significant role in altering the physical properties of a fuel, such as viscosity, density or surface tension. For this reason, it is unlikely that the addition of fuel additives would have a significant effect on diesel fuel spray behaviour. Instead, experimental data suggests that environmental conditions (injection pressure, fuel temperature, gas density, etc…) and fuel physical properties dictate the fuel spray behaviour (Elkotb, 1982).

The effect of fuel temperature on spray characteristics is widely known. As fuel temperature decreases, the fuel viscosity increases, creating larger fuel droplets (section 2.1.). However, little is known as to what happens to the spray behaviour, and, most particularly, to droplet size distribution, when the fuel temperature falls below its cold filter-plugging point (CFPP) and wax crystals begin to form. In an engine, anti-wax additives are used to prevent wax from agglomerating into large crystals. One could therefore suggest that wax crystals may affect fuel spray characteristics, and that the use of an additive to prevent wax crystals from agglomerating may have a beneficial effect on spray characteristics.

The effect of fuel wax on spray characteristics was investigated experimentally and the results are presented in this chapter. Fuel sprays with no additives and sprays with cold flow (CF) additives were studied at sub-zero ºC temperatures, below the onset of fuel waxing.

The aim of the experiments was to determine whether wax had a significant effect on spray characteristics, and whether the addition of CF additives modified spray characteristics when the fuel temperature was below the fuel waxing point.

5.1. Experimental methods

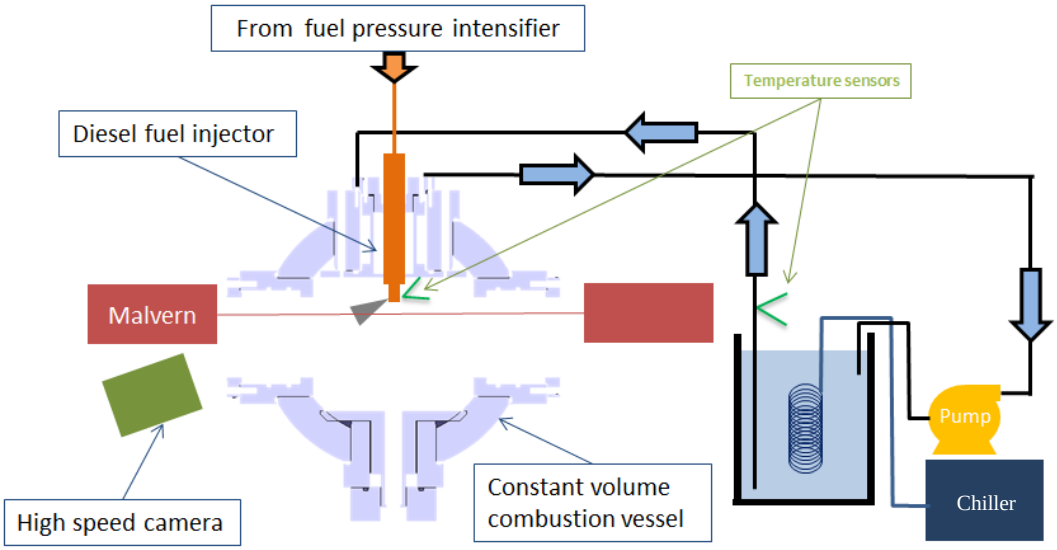

Figure 5.1: Setup of combustion vessel for spray experiments

The spray experiments were carried out within the constant volume combustion vessel (CVCV). A diagram of the spray characterisation setup can be seen in Figure 5.1. A custom built two-hole Delphi injector was used for all spray experiments. The use of only two holes, diametrically opposite to each other, retained some of the injector internal flow symmetry while at the same time improving optical visibility for droplet sizing and spray characterisation. An injector cooling jacket was used, which was supplied by cold water/ethylene glycol mixture from a chiller. This arrangement allowed for the injector and the fuel within it to be cooled down to temperatures around -13°C (the chiller unit and flow circuit are shown in Figure 5.1). More than 24h were required for the water/ethylene glycol mixture to reach the desired waxing temperatures in the injector due to the large heat transfer to the injector cooling jacket from the combustion vessel walls. Details of the chiller system can be found in Chapter 3.

Two separate analyses were carried out: the measurement of droplet size distribution using the Malvern Spraytec, and spray image analysis using shadowgraphy.

5.1.1. **Droplet size distribution experimental methods**

When carrying out droplet size measurements, the Malvern Spraytec laser beam was aligned orthogonally to the injector spray. The laser beam was arranged to pass diametrically through the centre of one of the two injector nozzle spray cones, 5 mm from the nozzle hole. The combustion vessel was kept at ambient pressure, filled with air at room temperature.

To reach the lowest possible temperature (below the onset of waxing, around -10°C), the chiller was left switched on overnight, prior to a test day. The chiller was turned off on the test day so that tests were carried out while the temperature of the chiller and the fuel slowly increased during the test day. The temperature of the injector tip was recorded using an exposed junction thermocouple. Twenty injection events were carried out for each injector tip temperature. The temperature variation between all twenty injections was found to only vary by a maximum of 1°C. The injector tip temperature values tested varied, for each additive blend, between approximately -13°C (the coldest attainable temperature by the system) and -2°C (the temperature reached at the end of the day by the system through energy absorbed from the atmosphere).

Four fuel batches were used for droplet size distribution experiments. Base fuel was investigated first, followed by additive CF-I at 10x concentration. A fresh batch of base fuel (denoted base') was then run again, followed by additive CF-A at 10x concentration.

Each spray event lasted 2 ms, and was captured for 10 ms by the Malvern Spraytec system. Observations of the Spraytec laser beam transmission showed that the 10 ms period of recording was sufficiently long to include and capture the full spray event of 2 ms duration.

5.1.2. **Experimental methods on imaging tests**

In order to assess the physical effect of fuel temperature on the spray, spray visualisation experiments were carried out. Two sets of images were taken on base fuel at fuel tip temperature of -11.6°C and at fuel tip temperature of 12°C (room temperature). One of the two sprays of the two-hole injector was optically captured using shadowgraphy, with the high speed camera sampling at a frame rate of 10000 images per second. For the shadowgraphy visualisation experiments, the spray duration was changed to 4 ms so as to ensure that the entire transient spray event would be captured by the camera. The individual spray images were then averaged over twenty spray events using software (MATLAB).

5.1.3. **Commissioning of the spray system**

A preliminary test was carried out at 600 bar injection pressure to determine how many spray events were necessary to obtain a stable Sauter mean diameter. The results for these preliminary tests are illustrated in Figure 5.2. The results show that the average Sauter mean diameter reaches a steady value after about twenty injection events, except for the tests at 300 bar injection pressure where the SMD is considerably less stable even after thirty injections. However, all other pressures show a consistent trend for average Sauter mean diameter after twenty injection events at room temperature. For this reason, the injection settings chosen for all tests were 600 bar pressure, with twenty repeat injections.

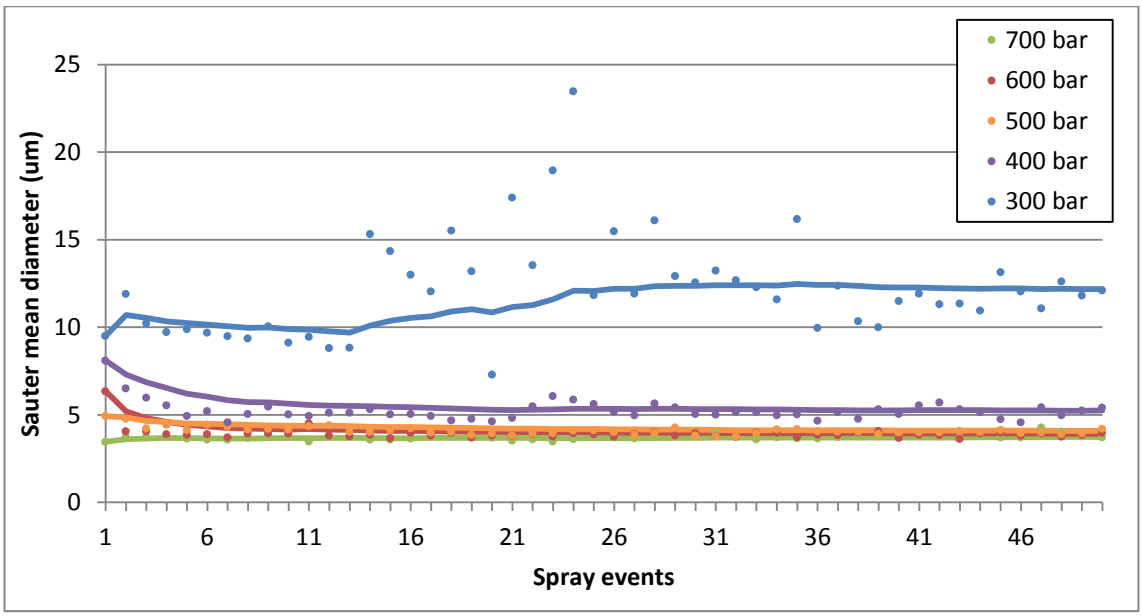

Figure 5.2: Spray Sauter mean diameter at 2.8 ms after start of injector trigger signal vs. accumulating number of injection events

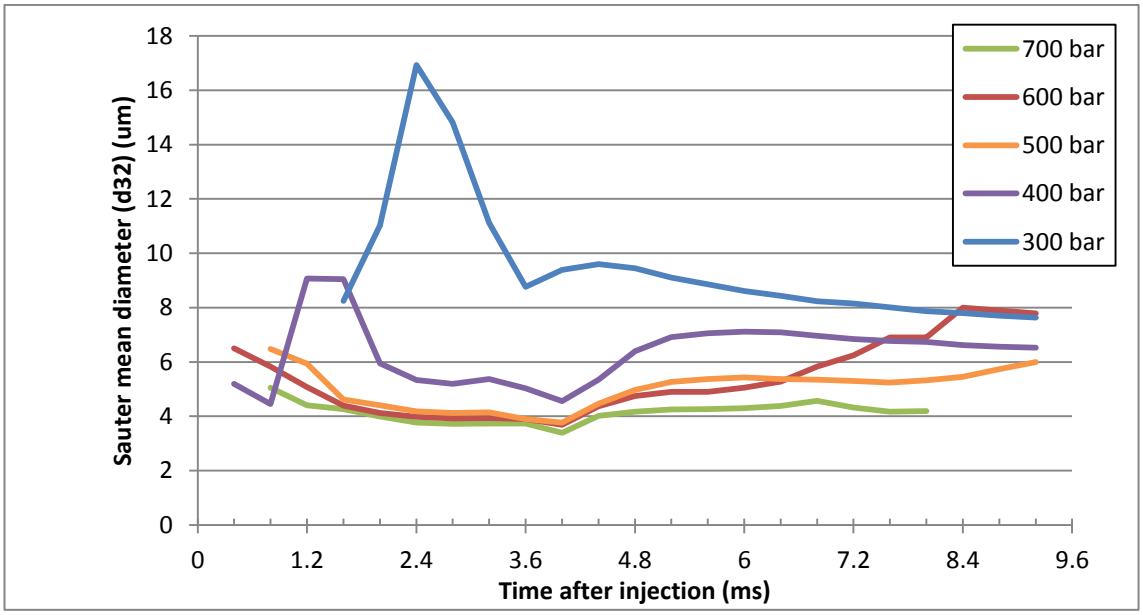

Figure 5.3: Spray Sauter mean diameter (average of 50 injection events) vs. time after injection

Figure 5.3 shows the average Sauter mean diameter recorded for a full injection period. The diameter appears to be more stable for pressures above 500 bar. At the beginning of the spray (particularly at lower pressures), the diameter shows high values during the main fuel spray event. These high values appear to be associated with the transient establishment of the fuel spray, following the start of injection and arrival of the initially large droplets to the Malvern laser beam.

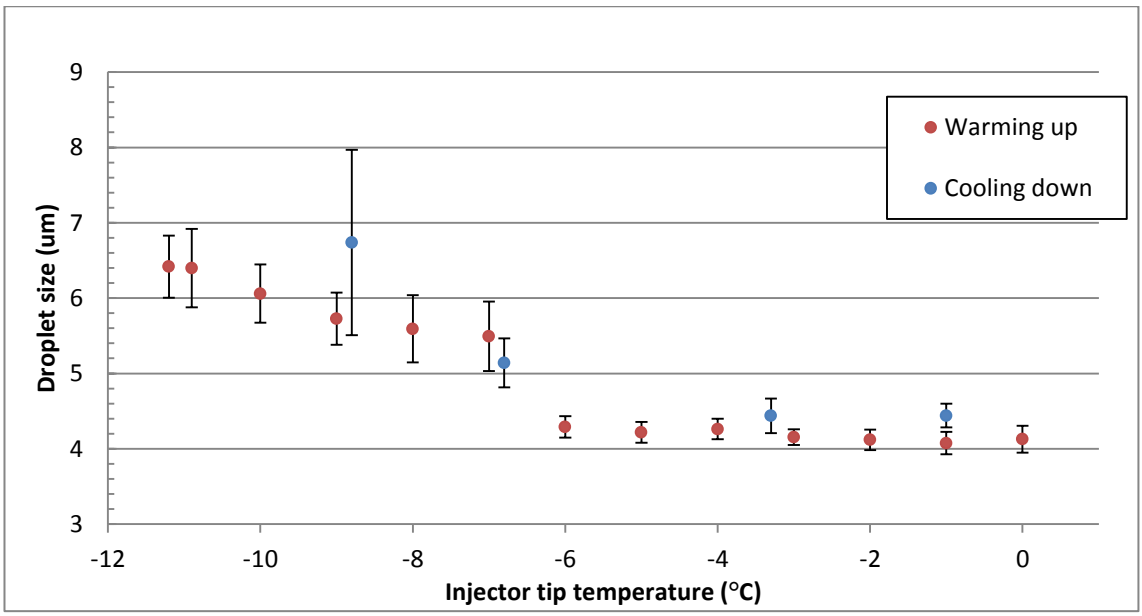

Figure 5.4: Comparison of average droplet size of 50 spray events vs. injector tip temperature while warming up and cooling down the system

Figure 5.4 shows preliminary results using the base fuel, carried out in order to assess the effect on droplet diameter of the temperature of the fuel within the injector. This figure shows that as the fuel temperature was reduced to around -6ºC and under, the mean droplet diameter increased, which was interpreted as the effect of the commencement of the formation of wax crystals. Above around -6ºC, the fuel temperature seemed to have little effect on Sauter mean diameter (with a diameter approximately constant at 4 µm).

5.2. Imaging on base fuel spray

Figure 5.5 and Figure 5.6 show spray images with base fuel at 12°C and at the much lower temperature of -11.6°C respectively. Note that -11.6°C injector tip temperature is below the cold filter plugging point (CFPP) of the base fuel, where wax is expected to have formed. Two main differences can be seen from these images.

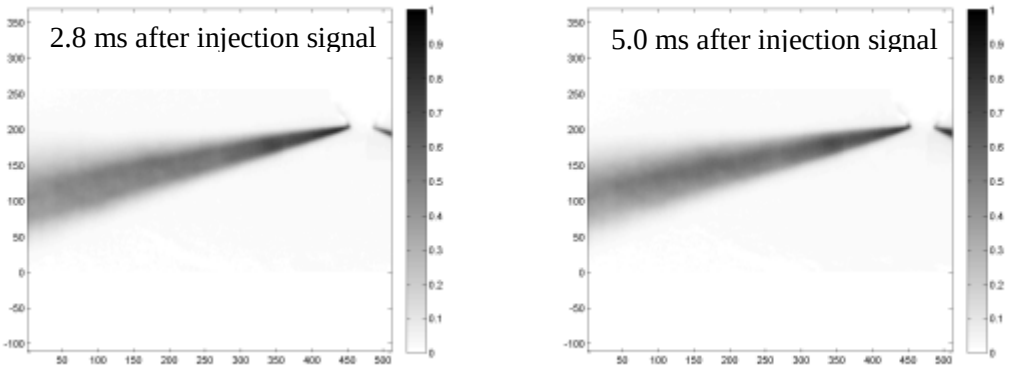

Figure 5.5: Base diesel fuel spray images at 12°C fuel injector tip temperature

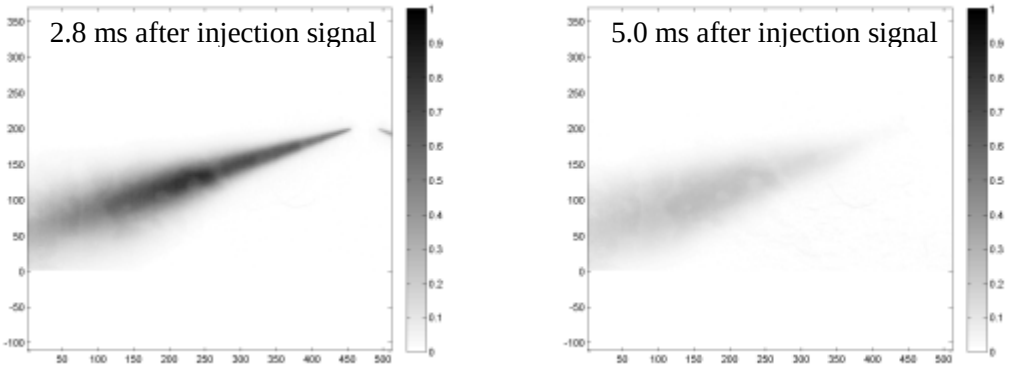

Figure 5.6: Base diesel fuel spray images at -11.6°C fuel injector tip temperature

Firstly, it was observed that when fuel was sprayed below its waxing point, the physical spray duration was shorter than when it was sprayed at 12ºC temperature. At -11.6°C, the fuel spray lasted for approximately 3.6 ms, compared to 4.6 ms at 12ºC. This reduction of 1 ms in physical spray duration at -11.6°C temperature was mostly due to a further delay of about 1 ms in the appearance of the spray after the injector electronic signal. The spray images from Figure 5.5 and Figure 5.6 show that, at 5.0 ms after the injector signal, the spray for -11.6ºC injector tip temperature started to diminish compared to the case when the injector temperature was at 12ºC.

Secondly, it was observed that, at 12ºC, the spray appeared to be denser, which is an observation confirmed by the lower light transmission values measured with the Malvern Spraytec system.

At a -11.6°C injector tip temperature, the fuel being fed to the injector was cold enough to form wax crystals. Wax formation involves the freezing of the heavy components of diesel fuel into wax crystals, which then grow and agglomerate to form larger wax crystals visible macroscopically. It is assumed that, once wax started to form, both a potential partial blockage of the injector and a slower needle operating response reduced the period of physical spray appearance.

The observed uneven spray optical density (i.e. high density spray at the core) during the injection event (2.8 ms) at -11.6ºC may have been linked to the fact that, at –this temperature, the fuel viscosity rose, increasing the value of spray droplet size. As a consequence, the spray was observed to be longer, have a smaller cone angle, and poorer atomisation. In contrast, the high density spray at 12°C is short, and spray atomised more evenly shortly after the injector tip, as seen in Figure 5.5.

5.3. Droplet size analysis

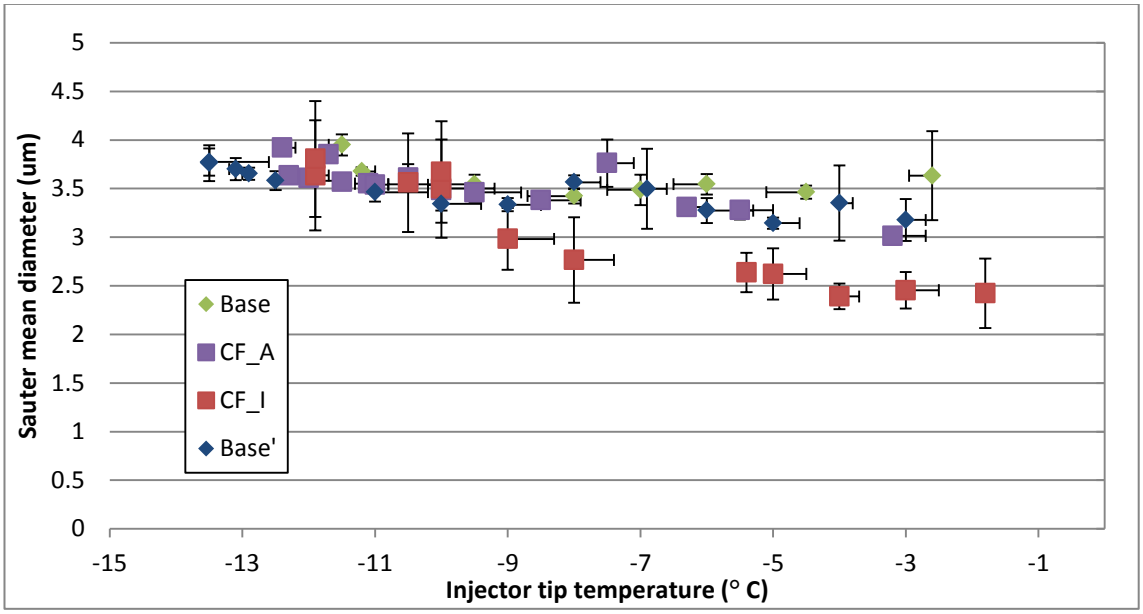

Figure 5.7: Average of Sauter mean diameters of twenty sprays during injection (1.6 ms to 3.6 ms) vs. injector tip temperature for all fuels

Using the light transmission measurements from the Spraytec system, it was determined that the spray, over a temperature range of -2ºC to -14ºC, was stable for a time window of 2 ms during the spray event (1.6 ms after the injection signal to 3.6 ms). The results can be seen in Figure 5.7. The spray Sauter mean diameter was measured at various temperatures, ranging from -2ºC to -14ºC. At each temperature, a set of 20 spray injections was performed and, for each spray, the mean SMD was calculated over the 2 ms time interval. Then, the overall SMD for the 20 injections was determined for each temperature in the range, about every 1°C.

For all experiments shown in Figure 5.7, the average SMD of all fuels varied between 2.4 and 4 µm. These values for SMD are very close to those found in literature on high pressure sprays of 600 bar used here.

For all fuel additive blends, the average SMD increased as temperature decreased. As the temperature of the fuel fell, its viscosity increased, which is known to cause an increase in the size of the fuel spray droplet. The apparent increase in droplet size was small, with a 0.6 µm increase over about a 10°C drop in temperature, except for the additive blend of 10x of CF-I, which showed an increase of about 1.5 µm in SMD for the same 10°C drop in temperature.

It is speculated that adding 10x of additive CF-I (1500 ppm, or 0.15% by mass) to base fuel may have altered the viscosity-temperature relationship of the fuel, much like a viscosity modifier (ATC, 2007). This change in viscosity only had an effect in reducing the average SMD at higher non-waxing temperatures. It appears that any viscosity effect of a high concentration of additive CF-I is a side effect to its intended purpose of preventing the agglomeration of wax crystals in order to control waxing. Additive CF-A follows the same trend as that of the base fuel.

Below the onset of waxing of base fuel, which is about -10°C, Figure 5.7 indicates that the relationship between Sauter mean diameter and injector tip temperature remained unchanged. This was the case for base fuel as well as fuel blends with CF additives and suggests that wax in fuel had no additional or special effect on the droplet size of a fully formed spray of diesel fuel.

The reason that the nucleation and agglomeration of wax crystals in fuel appear to have no effect on diesel sprays is probably because the binding forces of the wax crystals are weaker than the high pressure shear forces exerted on the fuel as it is sprayed through the injector orifice. Thus, droplet size, even at temperatures below the CFPP, appears to be governed by the fuel's viscosity, which varies with temperature.

5.4. Light transmission analysis

The Malvern Spraytec system recorded the amount of laser beam light transmitted through the spray; that is, the residual amount of incident light arriving at the detector after some of it was refracted by the spray. The detector was positioned in the line of sight of the laser beam, approximately 0.5 m from the laser transmitter outlet. The system continuously monitored the transmitted light so as to ensure that the diesel spray was not too dense and that sufficient light was refracted by the spray and reached the receiver rings. The amount of transmitted light was made available to the operator via the Spraytec software. The light transmission curve of the spray against time, as seen in Figure 5.8, also allowed the operator to determine the start and end times of a stable spray. Droplet size was measured throughout a 8 ms period, following the digital trigger to the injector, as shown in Figure 5.8. However, Figure 5.8 shows that only the period from 1.6 ms to 3.6 ms after the injection trigger signal corresponded to a stable spray interrupting the system laser beam. Before and after this 2 ms time window, the spray was forming and dispersing respectively.

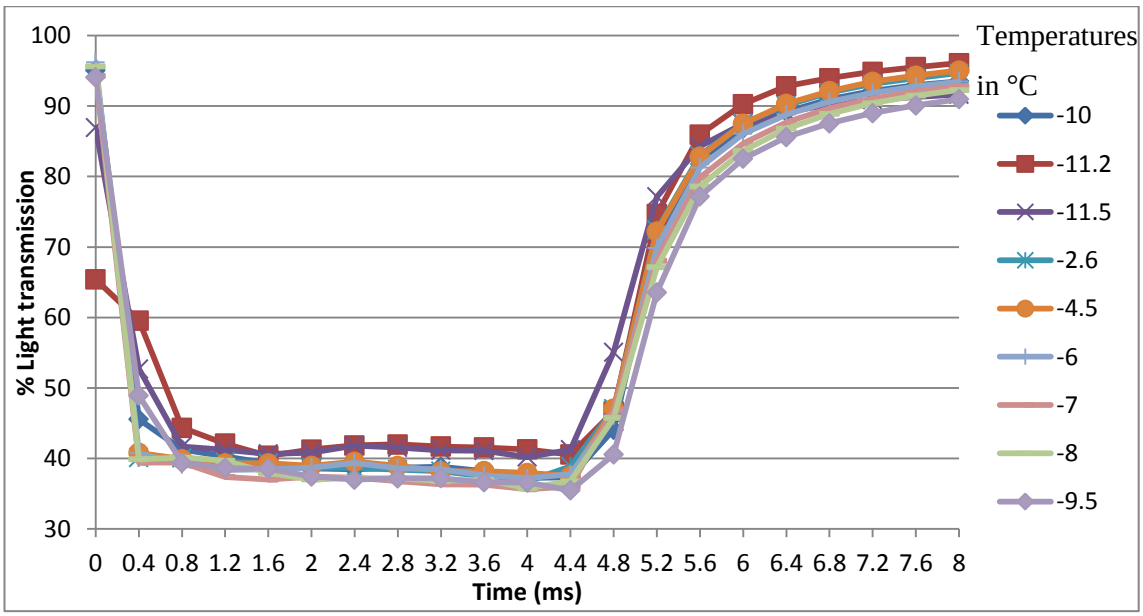

Figure 5.8: Average light transmission of base fuel sprays at multiple temperatures over time

The spray durations can be seen in Figure 5.8 as a drop in light transmission (around 40%) during the spray period. In general, the spray duration stayed constant at around 3 ms. However, for the coldest injector tip temperatures of -11.2°C (delayed spray start) and -11.5°C (premature spray ending), the spray duration was found to be shorter. During the 3 ms period of stable spray, it is believed that the large fuel pressure overcame the fact that there were wax crystals present in the fuel, as explained in the previous section 5.3. and that this resulted in no apparent effect of wax crystals on the spray characteristics.

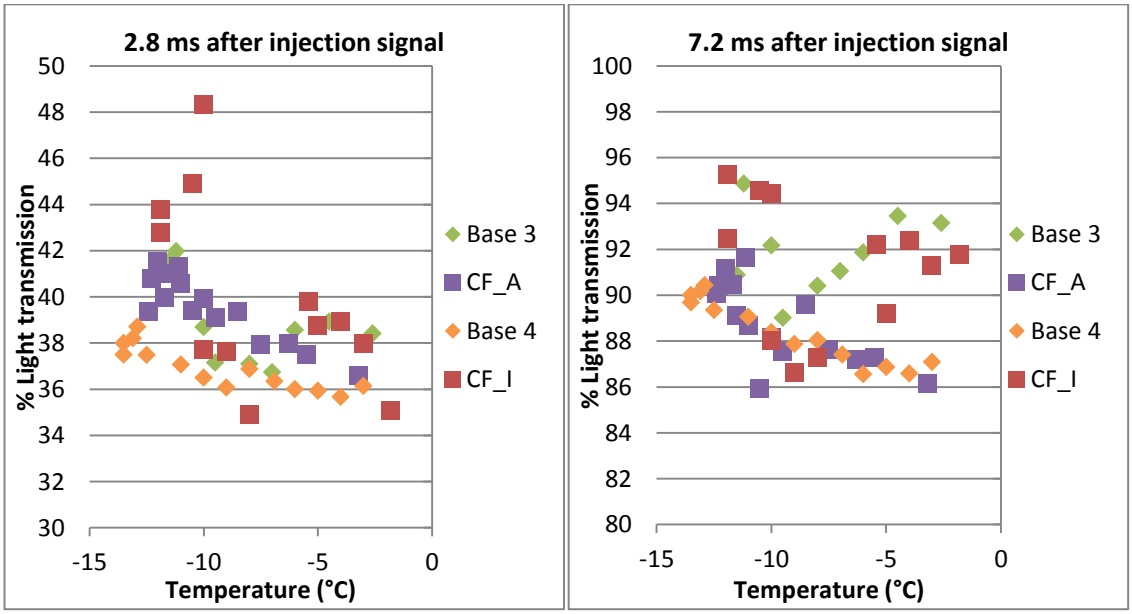

Figure 5.9: Light transmission of different blends of additives against temperature 2.8 ms and 7.2 ms after the injection signal

If one takes a closer look at Figure 5.8 and Figure 5.9, these suggest that there may have been a slight rise in light transmission as fuel temperature decreased for both base fuel and fuel blends

with CF additives. However, this small rise in transmission does not appear to be consistently related to the type of additive (as Figure 5.9 shows no discernable pattern from one specific additive type). Therefore, the blends of diesel fuel with CF additives appear to have behaved in a similar way to base fuel with regards to light transmission, during the stable spray period. Furthermore, CF additives appear to have had no effect on the light transmission of the leftover fuel mist after the spray (7.2 ms after injection signal), as shown on Figure 5.9.

5.5. Droplet size distribution analysis

In addition to the Sauter mean diameter and laser light transmission, the Malvern Spraytec system recorded the particle size distribution every 0.4 ms during each spray event.

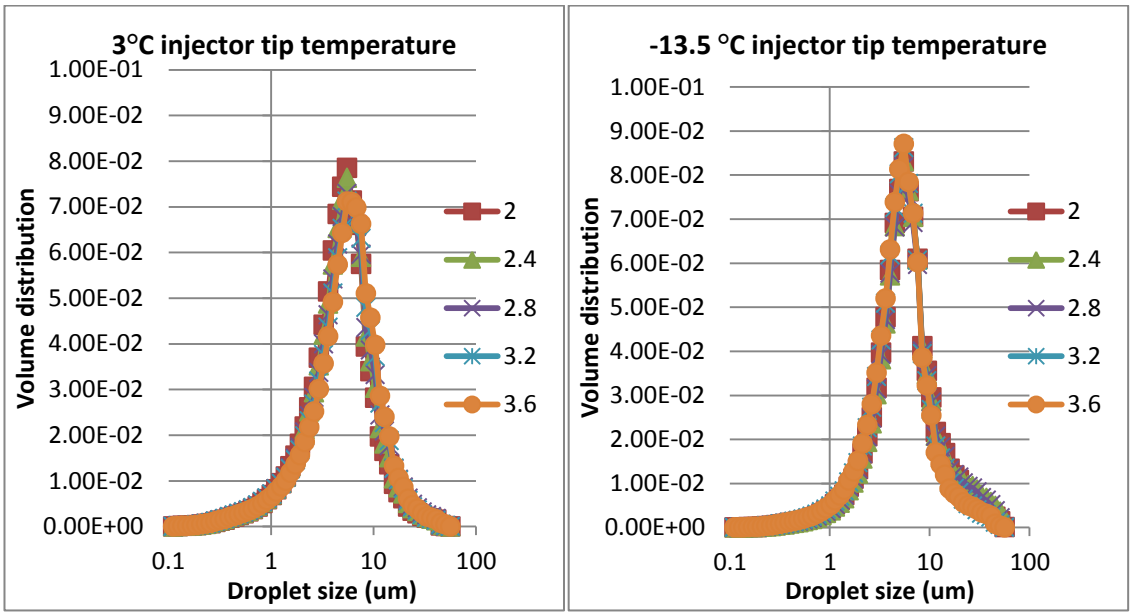

Figure 5.10: Average droplet size distribution of base fuel sprays for five different sampling times (in ms) during the spray event

Figure 5.10 shows the average droplet size distribution of base fuel sprays sampled by the system at different times during the 2 ms stable spray period (see Figure 5.8) at two injector tip temperatures of 3°C and -13.5°C (which is below the fuel's onset of waxing at -10°C). As can be seen, during the 2 ms stable spray period, the droplet size distribution of base fuel did not vary significantly. During the stable spray period, the spray was supplied at a constant pressure and the injector valve was fully opened. Thus, the fuel flow rate out of the injector nozzle can be expected to have been constant throughout that 2 ms period (save the short opening and closing periods of the start and end of this 2 ms period). The average droplet size distribution appears, from Figure 5.9, to have stayed unchanged during this stable spray period.

Figure 5.10 also shows that the droplet size distributions of the sprays for the base fuel at spray tip temperatures of -13.5°C and at 3°C are very similar. Figure 5.10 suggests that there is a

small probability that, at the -13.5°C temperature, the distribution had a slightly narrower droplet size distribution.

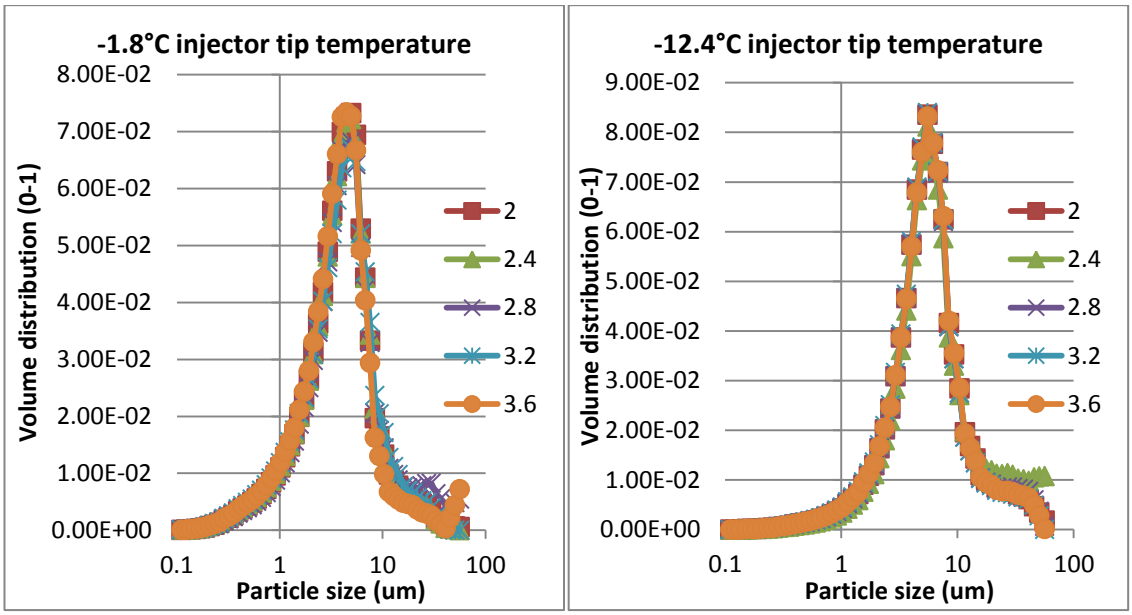

Figure 5.11: Average droplet size distribution of sprays of a blend of 10x CF-A for five different sampling times during the spray event

Figure 5.11 shows a similar set of curves for a blend of base fuel with 10x additive CF-A. The results appear to be similar to those shown in Figure 5.10 for the base fuel without additive. At the injector tip temperature of -12.4°C, the fuel additive blend was above the CFPP of the fuel, and it appears that the wax present had not formed into nuclei large enough to pose a plugging problem to fuel filters. Despite this, the curve is similar to that of base fuel at -13.5°C in Figure 5.10, suggesting that any wax crystal formation at these temperatures (around -13.5°C) appear to have no major influence on droplet size distribution.

5.6. Conclusions from spray investigations

In general, it has been found that wax crystals which are too large to go through a standard diesel fuel filter have no effect on the spray atomisation regime, or any spray characteristics. In order to create wax, diesel fuel has to be brought to low sub-zero temperatures (in the fuel used, below -10°C). This increases the fuel viscosity, which is believed to be the main cause of the rise in the average droplet size observed in the experiments (Figure 5.10 and Figure 5.11). The droplet size distribution curves, as well as transmission and imaging graphs, also support the view that the fuel spray is not significantly affected by large wax crystal agglomeration present in the injected fuel.

CF additives allow the wax crystals to stay small in size and pass the CFPP test (see section 1.1.3.). It has been found that the addition of CF additives to the base fuel has no effect on the steady state spray characteristics. This further confirms the fact that large wax crystals, which

are problematic in the fuel filters of internal combustion engines, have no significant effect on any of the spray characteristics of diesel fuel.

In an engine, large wax crystals would find their way to the filter and block fuel flow so that the fuel cannot reach the common rail or injector. The likelihood is that the filter will be blocked if the fuel is not treated with CF additives. However, wax crystals can also form past the filter, in the common rail and fuel injector, in a vehicle left standing overnight at low sub-zero temperatures. The results in this chapter indicate that the spray characteristics are unlikely to be affected significantly. As the vehicle engine warms up, the heat transfer from the combustion process then allows the injector tip to stay hot, making any injected fuel warmer than its CFPP, and thus wax-free. The findings of this chapter indicate that the wax in fuel is only likely to be problematic in blocking the fuel filter.

Chapter 6

Combustion experiments on combustion modifier additives

The addition of combustion modifier (CI) additives to diesel fuel is known to affect the ignition delay in an engine, which in turn affects some aspects of the overall engine performance (see 2.2.2.). In order to assess the effect of some combustion modifier additives on combustion it was decided to conduct combustion experiments on raw fuel (baseline tests) as well as blends of raw fuel with three combustion modifier additives: CI-A, CI-I and CI-ADD.

Combustion tests were carried out in the constant volume combustion vessel (CVCV) using pre-combustion of hydrogen-air mixtures to reach the necessary ambient temperature for diesel auto-ignition. Single injections of high-pressure diesel fuel blends were combusted and the instantaneous pressure in the CVCV was analysed.

Combustion tests were also carried out in a research single cylinder engine. Once again, the in-cylinder instantaneous pressure was analysed for different blends of additives over an ensemble of 100 engine cycles. Exhaust gases from the engine bed tests were analysed for particulate matter and other regulated emissions.

By analysing the data from these experiments, it was possible to assess the effect of three combustion modifier additives on diesel combustion, as well as the effects that the addition of these additives to diesel fuel may have on particulate matter and other exhaust gas emissions.

6.1. Experimental methods

6.1.1. **Diesel combustion in the constant volume combustion vessel**

The constant volume combustion vessel was used for combustion experiments with additives. In order to enable auto-ignition in the combustion vessel, a pre-combustion event consisting of a lean hydrogen-air mixture was used. The pre-combustion event provided ambient conditions of

temperature, pressure and oxygen concentration which allowed the subsequent spray of diesel fuel to auto-ignite and be combusted. The hydrogen-air mixture was introduced into the vessel via the gas mixer system (see section 3.2.5.) using partial pressures as a means to control the mixture composition. This lean mixture was ignited using a conventional automotive spark plug. The combustion event led to a rise in pressure and temperature inside the vessel. Diesel fuel was sprayed into the hot gases in the vessel using a high pressure direct injection diesel injector, triggered using software. Then, the diesel fuel auto ignited. A fast response piezoelectric pressure sensor and a low speed gauge pressure sensor were used together to determine the heat release rate of both consecutive combustion events, individually.

The direct injection diesel injector was fitted in a cavity at the top of the vessel. It was a six-hole injector, identical to the one that was used in the diesel research engine (see later). A two-hole version of the same injector was used for the imaging work carried out initially and discussed later in this section. The combustion vessel normally has four windows arranged orthogonally. Three of the four windows were replaced by aluminium blanks, modified to accommodate extra instrumentation, and lower the risk of unnecessary damage to the transparent windows. A diagram of the vessel viewed from the top can be seen in Figure 6.1. The left side window of the vessel was replaced with an aluminium blank fitted with a spark plug, which was used to ignite the hydrogen mixture. The right side window was replaced with a fan to allow mixing of the hydrogen-air pre-combustion mixture and to ensure that the hydrogen combustion occurred homogeneously. This enabled a more uniform spread of the reactant gases, ensuring the same local concentration of leftover oxygen throughout the vessel. The front window was blanked as it was not required, but the rear window was kept in place, so that some combustion images could be taken using the natural light emission from the burning diesel fuel spray.

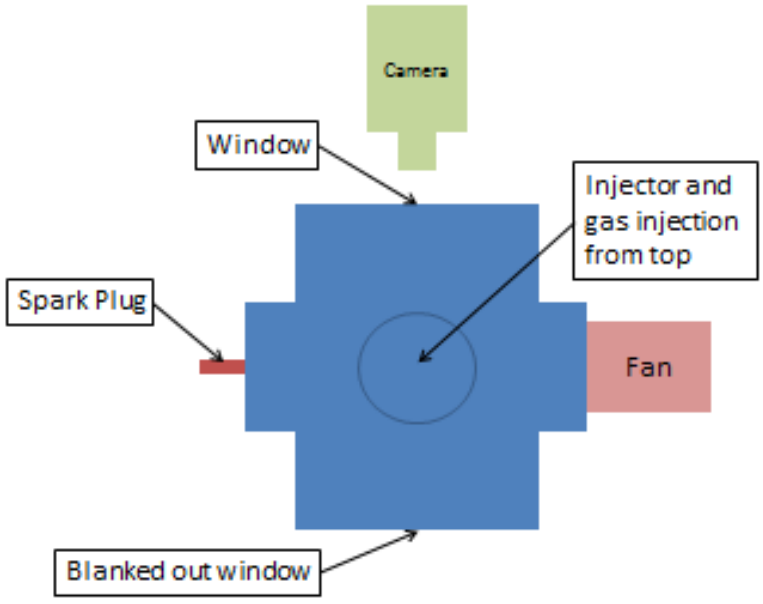

Figure 6.1: Top view of combustion vessel for combustion experiments

The pre-combustion events consisting of a hydrogen-air mixture had to be controlled as precisely as possible, in order to ensure that any discrepancies found in the combustion characteristics came from the diesel combustion rather than the pre-combustion event. To do so, the addition of the hydrogen gas into the vessel as well as the mixing procedure was controlled precisely. This ensured a constant equivalent ratio, and mixing in the vessel. To facilitate mixing, the gas mixer system (see section 3.2.5.) was placed above the combustion vessel. A sensitive 0-2 gauge pressure sensor on the mixer system was used to measure precisely to the nearest 0.02 bar (1% of maximum gauge pressure) the partial pressures of every successive amount of gas added to the combustion vessel. The procedure was as follows:

- The vessel was first allowed to fill up with ambient air to atmospheric temperature and pressure (~1 bar absolute air). It was then sealed off from the atmosphere.
- Pure hydrogen gas was then added in the vessel to the required amount (+0.432 bar hydrogen absolute pressure) using the sensitive pressure gauge.
- The vessel was then topped up to 3 bar absolute (+1.568 bar) pressure with atmospheric air.
- The fan was then switched on for a full 60s to ensure thorough mixing of the hydrogen with air, and then switched off.

The amount of hydrogen added was such as to ensure that the final 3 bar (absolute) mixture had a hydrogen-air equivalence ratio of 0.4, thus leaving sufficient oxygen after the pre-combustion event for auto-ignition of the diesel spray. A full diagram of the combustion vessel rig and its instrumentation can be seen in Figure 6.2.

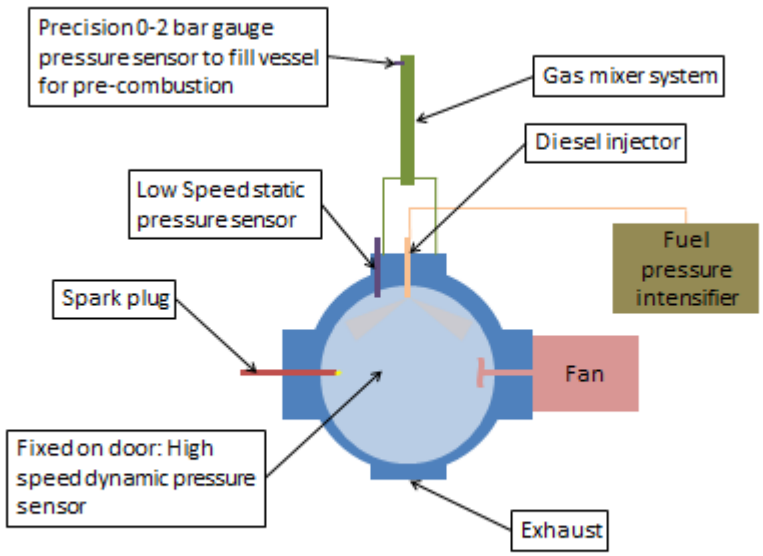

Figure 6.2: The combustion vessel setup for combustion experiments

After mixing, the rest of the combustion procedure was carried out using bespoke software written in Labview. The spark plug was energised by the software, triggering the hydrogen/air combustion. The pre-combustion raised the vessel pressure to, typically, 12 bar. The software then monitored the vessel pressure's gradual decrease (due to energy loss by heat transfer to the walls) until it reached 8 bar gauge pressure, at which point the software automatically caused the injection of diesel fuel at 700 bar injection pressure for 2 ms.

The pre-combustion event, at an equivalent ratio of 0.4 used up 40% of the oxygen present in the vessel, lowering the oxygen content of the gas products present in the vessel to 12.6% by volume (compared to the normal atmospheric volume fraction of 21%). This oxygen content was equivalent to 43% exhaust gas recirculation (EGR) in engine conditions, which is not uncommon in modern diesel engines. It was calculated that the hydrogen/air combustion would result in a vessel pressure (after adiabatic combustion) of a theoretical 16.2 bar and 1471°C products temperature. The 8 bar gauge pressure of the remaining products of the hydrogen with air combustion was calculated to correspond to 600°C ambient temperature, assuming ideal gas behaviour. These conditions of pressure and temperature were sufficient for diesel auto-ignition.

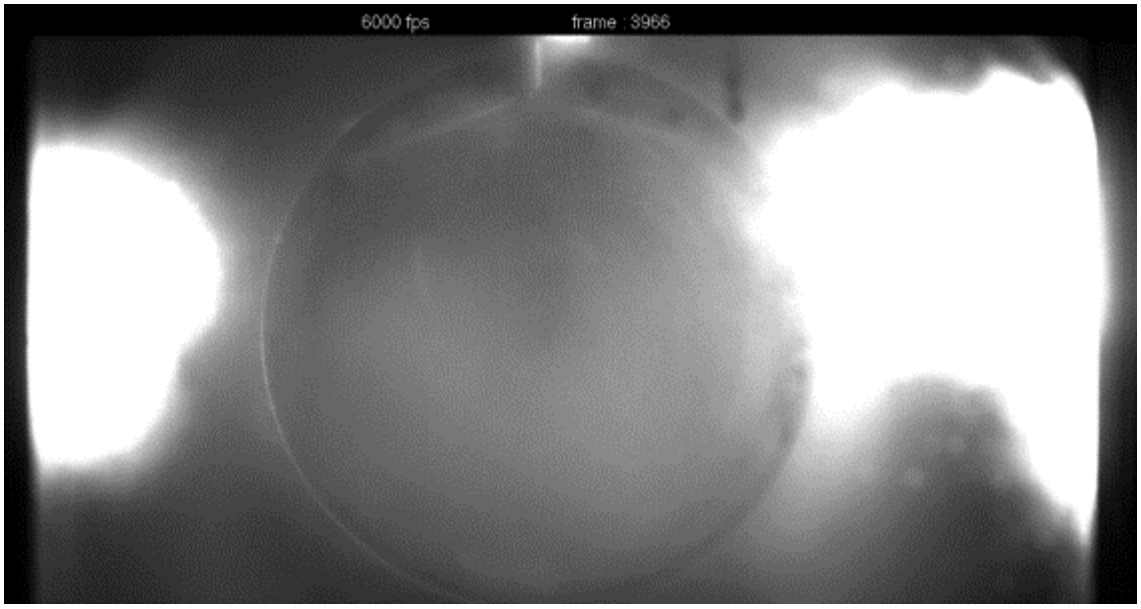

Figure 6.3: Diesel auto-ignition in the combustion vessel during stable spray conditions

In order to measure the small and very quick changes in pressure associated with the combustion, a high response rate piezoelectric pressure sensor was used. This pressure sensor was located on the front door panel, orthogonally to the injector, about half way down the height of the vessel. Because of the high drift in the slow-varying pressure for this sensor, the slow-varying pre-diesel ignition pressure was measured by a separate piezo-resistive pressure sensor located at the top of the vessel. Although able to also measure fast changing pressures, this sensor was much less precise in dynamic measurements than the piezoelectric sensor. Positions of both sensors can be seen on the diagram in Figure 6.2. To summarise, the piezo-

electric sensor was used for fast changing dynamic pressures, while the piezo-resistive sensor was used for the slower changing pre-combustion product pressure, for control purposes.

At the end of each diesel fuel injection event, the products of the diesel combustion were evacuated through the exhaust at the bottom of the vessel. To facilitate the process, a 5 bar supply of atmospheric air was passed through the vessel from the top, to help push the reactant gases towards the exhaust. Furthermore, the fan was turned on to create turbulence and ensure that no gases from the previous combustion event remained trapped within the fan cavity in the vessel. The emptying and purging process lasted for a full 5 minutes.

Emptying the vessel of its products in such a manner meant it was not necessary to open the vessel between each combustion event. Thus, ten combustion events were carried out for each fuel-additive concentration of combustion improver (CI) additive. The vessel door was only opened between each type and concentration of additive. The vessel was then cleaned thoroughly on the inside by hand first with acetone, then with soapy water.

Initially, the vessel was set up to measure the exhaust gases and particulates from the reactants of the combustions. However, preliminary testing showed that the products of one combustion event were not large enough in quantity to be detected by the Horiba exhaust gas analyser, due to the fact that the product's concentrations were too small. Similarly, the Cambustion DMS 500 particulate analyser could not detect any particulates from the reactant gases. This is believed to be due to the particulate matter in the gases being attracted to the surfaces of the large cold walls of the vessel by means of thermophoresis. Exhaust gas and particulate analysis were however conducted during the engine bed tests described in the next section.

Combustion tests were conducted on three different combustion modifier additives: CI-A, CI-I and CI-ADD at the normal concentration (labelled 1x) and 10 times the normal concentration (10x). Raw fuel (without friction modifier (FM) additive unlike in Chapter 4, also called base fuel in the current chapter) was tested before each new additive, to ensure that the addition of a high concentration of additive had not contaminated the system.

6.1.2. **Engine bed tests on combustion modifier additives**

Additional experiments were carried out on an engine bed specifically designed for combustion research. The engine used was a 4-stroke direct injection single cylinder compression-ignition engine modified from a commercial Ford Duratorq CD132 130PS engine. Engine specifications are listed in Table 6.1.

Engine head model	Ford Duratorq
Engine bottom end model	Ricardo Hydra
Number of cylinders	1
Cylinder bore	86 mm
Crankshaft stroke	86 mm
Swept volume	499.56 cc
Compression ratio	15.8:1
Maximum cylinder pressure	150 bar
Peak motoring pressure at test conditions	360 bar
Piston design	Central ω-bowl in piston
Oil temperature	353 ± 2.5 K
Water temperature	348 ± 2.5 K
Fuel injection pump	Single-cam radial-piston pump (BOSCH CP3)
High pressure fuel rail	Solenoid controlled, max 1600 bar (BOSCH CRS2)
Injector	6-hole solenoid controlled (DELPHI DF1 1.3)
Electronic fuel injection system	1 µs accuracy (EMTRONIX EC-GEN 500)
Shaft encoder	0.2 CAD resolution

Table 6.1: Engine specifications (Hellier, et al., 2012)

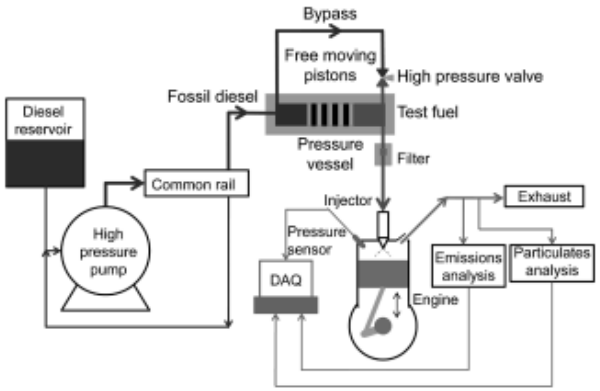

Figure 6.4: The low volume high injection pressure fuel system (Hellier, et al., 2012)

In order to allow easy change between additive samples, the research engine was fitted with a previously designed and manufactured low volume high injection pressure fuel system. The system was designed and developed by Dr. P. Hellier. The system is comprised of two free pistons. One end is pressurised by fossil diesel using a traditional high pressure pump. The free piston movement allows the other side of the pressure vessel to be pressurised, where the small quantity (100-250 mL) of test fuel is located. The sealing pistons prevent mixing of the test and fossil fuels. This allowed for tests to be carried out on a full system without the need to mix a large quantity of each concentration of additive. Finally, to prevent any blockages in the injector, a 1 µm sintered filter element was used after the sample fuel tank, and before the injector. The injector used was the same six-hole injector used in the previous combustion

vessel tests. Each hole was 154 µm in diameter. A schematic of the low volume high injection pressure fuel system is given in Figure 6.4 (Hellier, et al., 2012).

The naturally aspirated engine drew in air at atmospheric pressure and temperature and had a compression ratio of 15.8:1. In-cylinder pressure was measured every 0.2 crank angle degrees (CAD) using a piezo-electric pressure transducer (Kistler 6056AU38) and charge amplifier (Kistler 5011) and logged with a PC data acquisition card (National Instruments). Various temperatures were also measured using K-type thermocouples and logged using the same data acquisition card. The net apparent heat release rate was then derived from the in-cylinder pressure measurements during post-processing (MATLAB) (Hellier, et al., 2012).

The engine exhaust gases were sampled 180 mm downstream of the exhaust valves to determine the concentration of gaseous species using an automotive gas analyser system (Horiba MEXA 9100 HEGR) and also size and mass particulate distribution using a differential mobility spectrometer (Cambustion DMS500). The Horiba exhaust gas analyser measured NOx concentrations by chemiluminescence, CO and CO2 concentration with non-dispersive infrared, O2 concentration with paramagnetic analysis and levels of unburnt hydrocarbons with flame ionisation detection. More information on these processes can be found in section 2.2.3.1. Particulate sampling was made via a heated line and a dilution cyclone. Exhaust gases were first diluted at 4:1 and then again at 100:1 with air. The heated line and both dilution cyclones were kept at a constant temperature of 328 K (Hellier, et al., 2012).

Figure 6.5: The Ford Duratorq engine

For each measurement with a new concentration of additive, pressure and temperature data was recorded by the PC data acquisition card, the exhaust gas analyser and the particulate analyser over 100 engine cycles. Similarly to the tests in the combustion vessel, each blend of diesel fuel with combustion modifier additive was tested at normal (1x) and 10 times the normal concentration (10x), and was bracketed with raw (base) fuel with no additives. For these tests,

the engine speed was kept constant at 1200 RPM. The injection timing was set to 7.5 crank angle degrees before TDC and the injection pressure was kept to a constant 450 bar. The injection duration was varied and controlled to achieve a constant IMEP of 4 bar. A picture of the engine used for this set of tests can be seen in Figure 6.5.

6.2. Heat release analysis with a combustion vessel

In addition to base fuel, five different fuel blends with three combustion modifier additives at different concentrations were used in the constant volume combustion vessel.

- Additive CI-A is a diesel ignition improver. An addition of 250 ppm of additive CI-A was expected to provide a cetane number increase of 2-3 CN (Cooney, 2012).
- Additive CI-I is a gasoline anti-knock additive. It increases the RON, or octane number, by 1-2 when added at 5000 ppm (Cooney, 2012). Additive CI-I prevents knocking. When added to diesel fuel, it acts as a combustion inhibiter, essentially providing a cetane decrease of 1-2 CN. This is because anti-knock additives use up radicals during the pre-combustion stage, preventing branching from occurring as quickly as normal, in direct contrast to diesel ignition improvers which break down creating extra radicals during compression-ignition. Additive CI-I is made up of organic compounds.
- Additive CI-ADD, is also a gasoline anti-knock additive, but uses organo-metallic compounds in order to achieve the same RON increase/CN decrease as CI-I. Thus, metal particles and oxides are released in the exhaust gases when using fuel blends with this additive. This makes CI-ADD a potentially harmful additive to use, as was TTL (Tetraethyl lead) in old blends of gasoline fuels with additives. Nowadays, in most markets, gasoline is not allowed to be blended with metallic additives, especially TTL, hence the name "unleaded fuel". 7000 ppm of additive CI-ADD will provide an increase of 1.5 to 2.5 RON (Cooney, 2012).

The order of all combustion tests, as well as the concentration of fuel additive blends is displayed in the table below.

Additive blend	Additive code	Concentration (ppm)
Base fuel – no additive	Base	
Base fuel + Ignition Improver	CI-A (1x)	250
Base fuel + Ignition Improver	CI-A (10x)	2500
Base fuel – no additive	Base	
Base fuel + Anti-knock additive	CI-I (1x)	1000
Base fuel + Anti-knock additive	CI-I (10x)	10000
Base fuel – no additive	Base	
Base fuel + Anti-knock additive	CI-ADD (1x)	7000

Table 6.2: Order and concentration of fuel additive blends for combustion experiments

6.2.1. **Signal processing and heat release analysis in the combustion vessel**

The various blends of diesel fuel with additive were sprayed into the combustion vessel in suitable conditions of elevated pressure and temperature, and auto-ignited following the pre-combustion of hydrogen in air. The combustion event created two distinct pressure rises, one due to the pre-combustion of hydrogen with air in the combustion vessel, the other due to the auto-ignition of diesel fuel in the combustion vessel. A typical pressure rise graph for a combustion event can be seen in Figure 6.6.

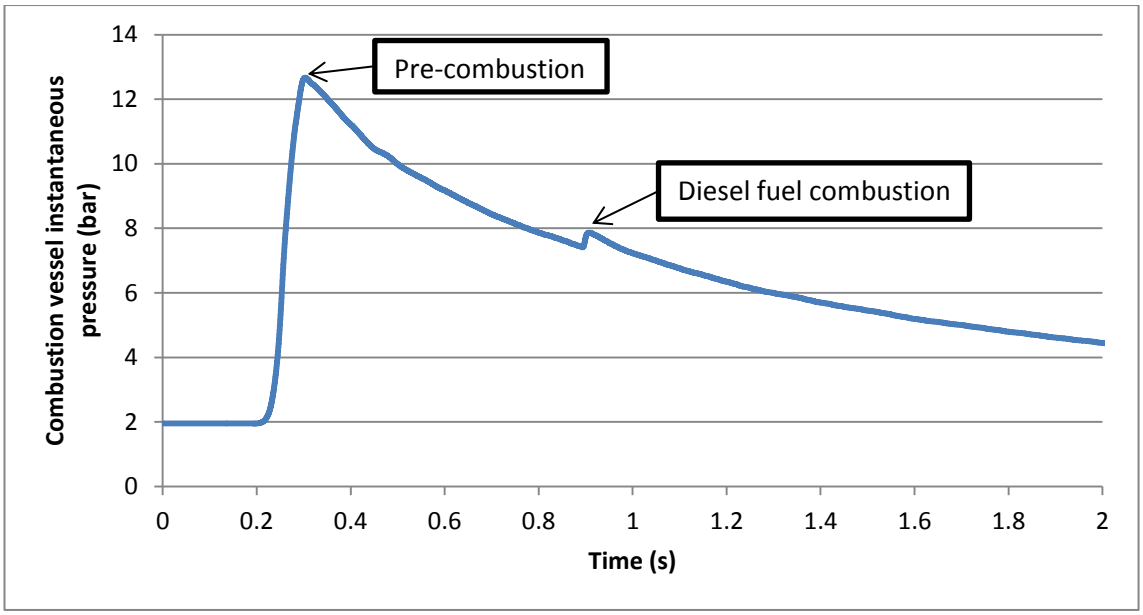

Figure 6.6: Instantaneous vessel pressure against time of a base fuel combustion event

The rise in instantaneous vessel pressure due to the diesel combustion was much smaller in magnitude than the rise due to the hydrogen combustion in air. In a typical automotive engine, the combustion chamber is less than a litre in volume and the diesel fuel spray, when combusted, consumes the majority of the air in the cylinder. In the 23 litre control volume vessel, the spray was concentrated on the central region of the vessel and only consumed a small fraction of the 23 litres of air in the vessel. As a result the diesel combustion was localised to the centre of the vessel, and only contributed a small pressure rise of typically up to 0.5 bar.

From the instantaneous pressure rise curve in the vessel, the heat release rate of the diesel combustion was calculated using the heat release rate equation (equation 2):

$$\frac{dQ_n}{dt} = \frac{\gamma}{\gamma - 1} p \frac{dV}{dt} + \frac{\gamma}{\gamma - 1} V \frac{dp}{dt}$$

The equation simplifies, as the vessel volume is constant:

$$\frac{dQ_n}{dt} = \frac{\gamma}{\gamma - 1} V \frac{dp}{dt} \quad (8)$$

Where $\frac{dQ_n}{dt}$ is the heat release rate in W, V is the combustion vessel volume, 0.023 m^3, $\frac{dp}{dt}$ is the derivative of instantaneous pressure with respect to time, and γ is the heat capacity ratio of air in the vessel, taken as 1.4.

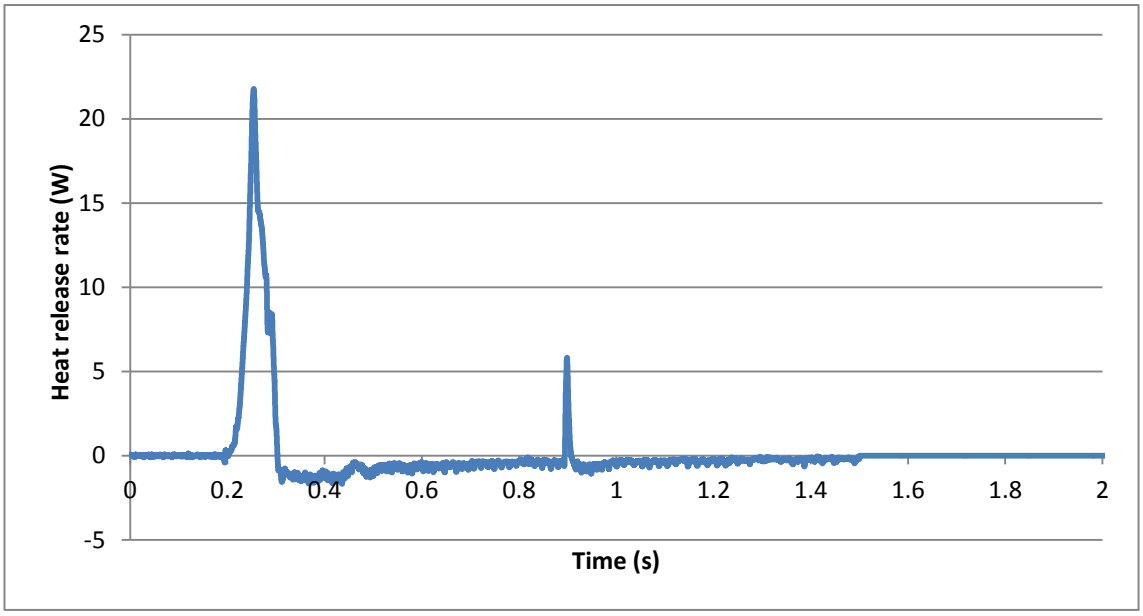

Figure 6.7: Heat release rate of a base fuel combustion event

An example of a full heat release rate curve can be seen in Figure 6.7, but only the second peak, which relates to the diesel fuel combustion, is of interest. The first peak relates to the hydrogen pre-combustion.

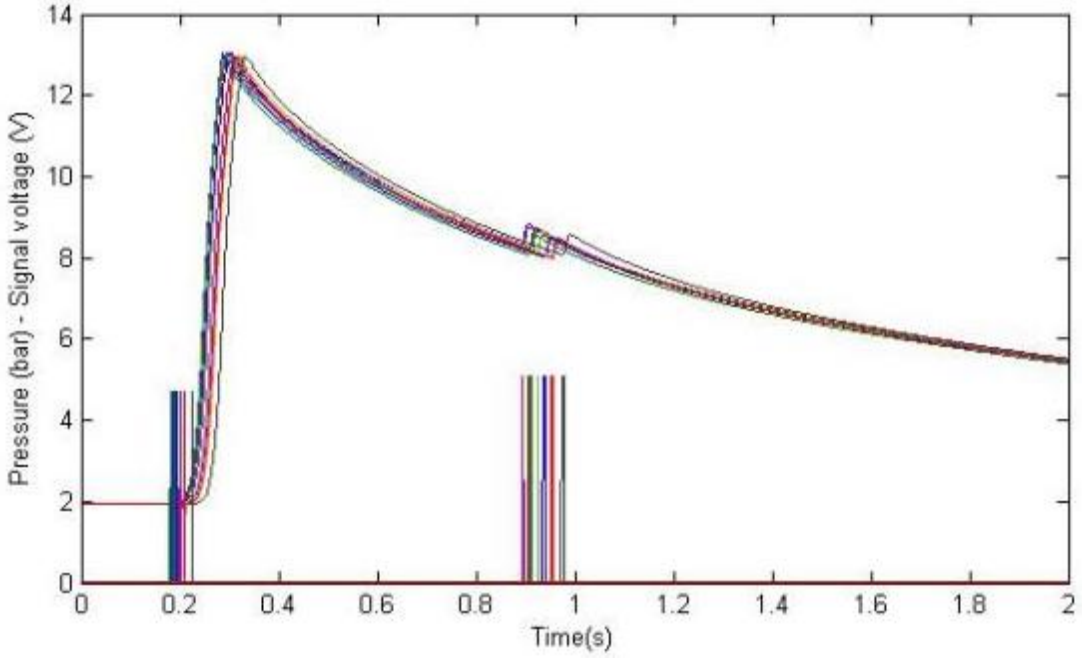

Figure 6.8: Raw pressure trace of all ten combustion events from one base fuel test with spark and injection trigger signal traces. Legend: One combustion event per colour.

In order to be able to compare the different combustion events with each other, the trigger signals for the spark and for the diesel injector were recorded. Figure 6.8 shows the instantaneous pressure from 10 repeat combustion events with base fuel, including these triggers. As can be seen, the injection signals do not occur at the same time for each combustion event. The reason for this is that, for consistency, the diesel fuel injection event was initiated when the gas pressure after pre-combustion had decayed to 8 bar. As the gradient for this pressure decay varied, as a result of test to test heat transfer variability, the start of diesel injection also varied from test to test.

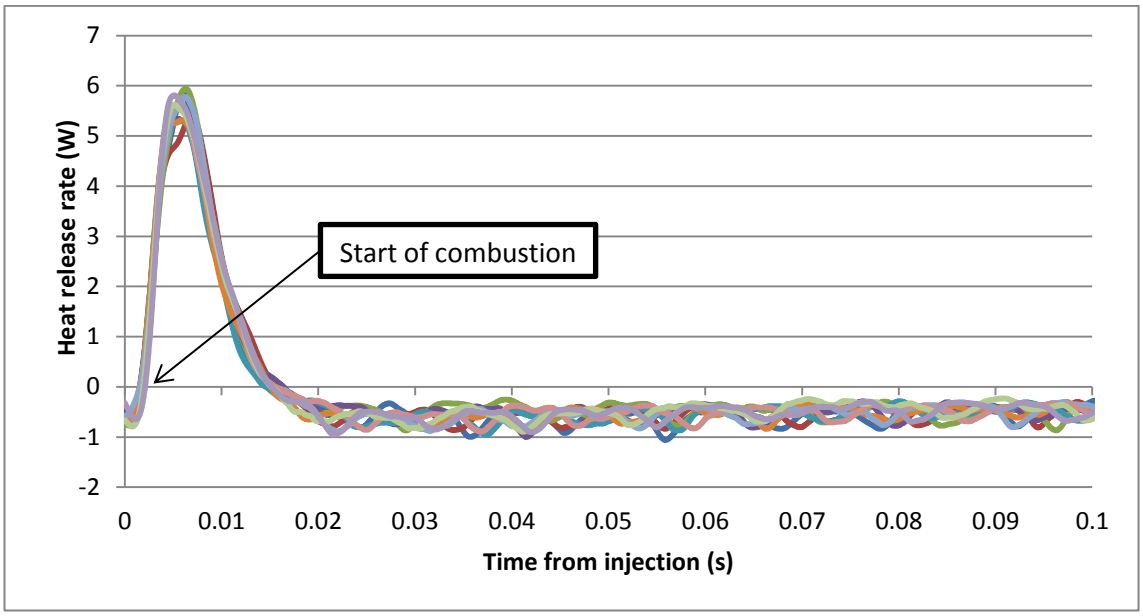

Figure 6.9: Heat release rate of all ten combustion events from one base fuel test aligned with the timing of their diesel spray signal. Legend: One combustion event per colour

Thus, in order to compare the heat release rate for all 10 combustion events, the injection signal was used as a starting point for diesel combustion. For the 10 combustions in Figure 6.8, the heat release rate is shown on Figure 6.9 with the 10 starts of injection synchronised. The start of auto-ignition was calculated as the time when the heat release rate crossed the x-axis. From the data, it was possible to find out the time from start of injection to the start of auto-ignition. This length of time is known as the ignition delay.

6.2.2. **Analysis of pre-combustion settings**

In order for diesel to auto-ignite in the combustion vessel, a mixture of hydrogen in air at 0.4 equivalence ratio was ignited in the combustion vessel to raise the pressure and temperature of the ambient gases prior to the main diesel combustion event. More details about the mixing method of the hydrogen in air, as well as the pre-combustion conditions are described in section 6.1.1. and summarised in Table 6.3 below.

Condition	Setting
Combustion vessel internal pressure	3 bar absolute (2 bar gauge)
Equivalence ratio of hydrogen gas with air	0.4
Oxygen present in vessel after combustion	12.6%
Spark duration	5 ms
Hydrogen partial pressure	0.432 bar (absolute)
Air partial pressure	3-0.432 bar (absolute) = 2.568 bar
Methodology	1 bar absolute air in vessel (atmospheric pressure) Add 0.432 bar H_2 Top up to 3 bar absolute (2 bar gauge) air

Table 6.3: Pre-combustion conditions

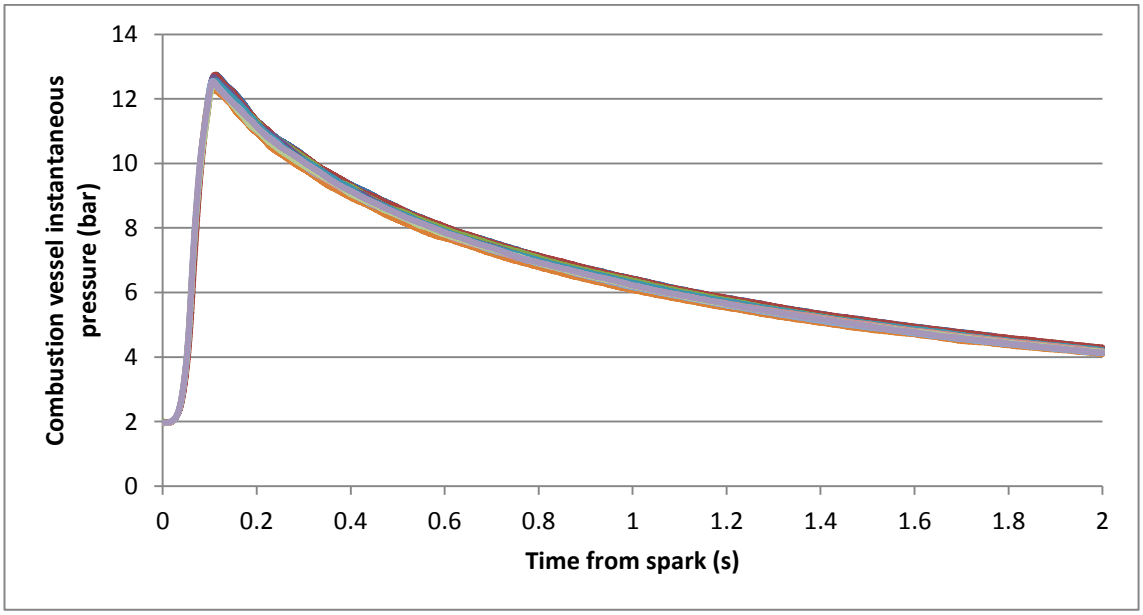

Figure 6.10: Instantaneous vessel pressure against time for multiple events of hydrogen in air ignition. Legend: One combustion event per colour

To determine the repeatability of the pre-combustion event, an analysis of the pressure trace of the hydrogen combustion with no diesel injection was carried out (see Figure 6.10). As expected, the hydrogen combustion was observed to raise the instantaneous pressure in the vessel to more than 12 bar. The exact maximum pressure achieved differed from combustion to combustion, but the standard deviation of the maximum pressure was within 0.2 bar, and always above 12 bar gauge (13 bar absolute). This means that assuming ideal gas behaviour of the combustion gases as contents, the temperature in the vessel reached at least 950ºC, a temperature above the ignition point of diesel fuel. The high speed data acquisition system started recording data as soon as the spark was triggered. This allowed for a near perfect superimposition of all hydrogen combustion events, as seen on Figure 6.10.

Following every pre-combustion event, the rate of pressure decrease varied, which led to a slight variation in ambient pressure at diesel fuel auto-ignition. The rate of pressure decrease depended on how well the hydrogen and air were mixed together before the spark triggered the

combustion as well as the rate of energy loss from the combustion gases to the vessel internal surfaces.

6.2.3. **Effect of some combustion modifiers on the ignition delay in the combustion vessel**

The ignition delay was calculated from the heat release rate curve as described in section 6.2.1. for all blends of diesel fuel with combustion modifier (CI) additives. Figure 6.11 shows the ignition delay for all the combustion events carried out in the vessel against peak heat release rate.

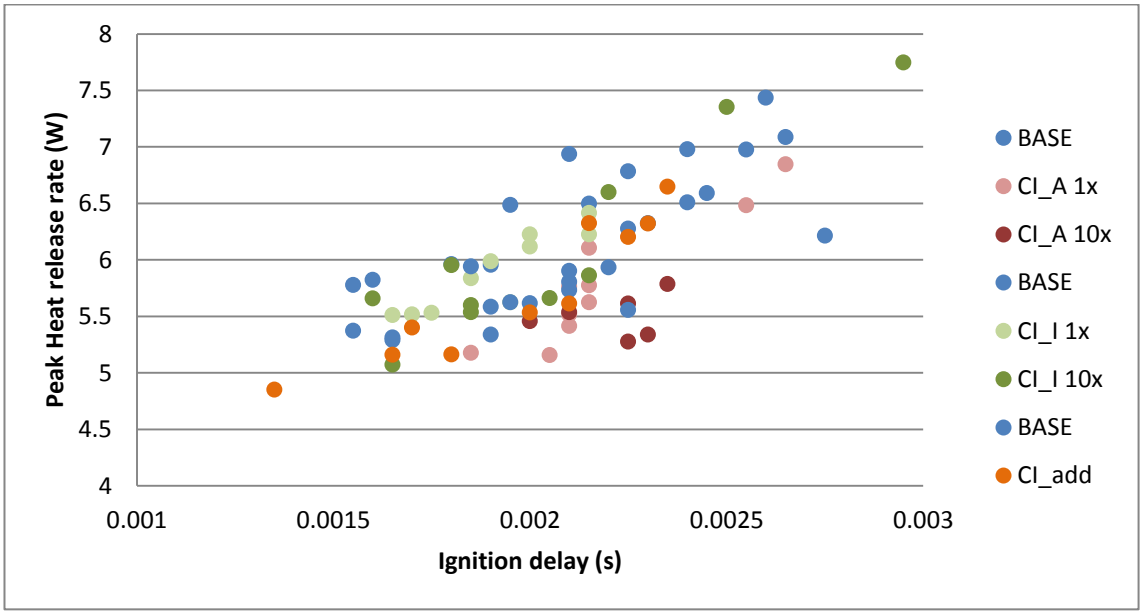

Figure 6.11: Ignition delay vs. peak heat release rate

Figure 6.11 shows that no blend of additive had any noticeable effect on ignition delay. In general, the ignition delay varied from 1.35 ms to 2.95 ms, regardless of the additive blend. In fact, the shortest ignition delay was seen with a blend of additive that should theoretically increase the ignition delay relative to base diesel fuel's ignition delay (CI-ADD, an anti-knock additive). Similarly, one of the longest ignition delays recorded was from a blend of diesel fuel with additive CI-A at 1x concentration. Additive CI-A, an ignition improver, is known to increase the cetane number, and thus shorten ignition delay.

The shot to shot variability of the ignition delay of diesel combustion in the combustion vessel is such that no conclusions can be drawn from the ignition delay information. The most tested blend, base fuel, shows a wide spread of ignition delays from 1.55 ms to 2.75 ms in 30 combustions with a standard deviation of 0.3 ms (~16% of the mean ignition delay of 2.1 ms). The blends of the same base fuel with ignition improver additives show similar spreads for ignition delay.

As expected, when ignition delay increases, the peak heat release rate also increases (Figure 6.11). This is because the increased delay allowed the diesel fuel more time to premix with the ambient air before auto-ignition, resulting in a greater release of energy.

The diesel combustion parameters were dependant on the pre-combustion conditions of hydrogen and air, which varied somewhat between tests. This changed the ambient temperature and pressure in the vessel at the time of fuel injection, which in turn affected the fuel ignition parameters and the ignition delay. It may be that any changes in ignition delay as resulting from the addition of combustion modifier additives were too small; they were swamped by the errors in recording ignition delay in the constant volume combustion vessel.

Finally, for the combustion vessel experiments, only ten combustions for each blend of base fuel with CI additive were averaged for calculation of the ignition delay (due to time constraints). When calculating the ignition delay in an engine, many more ignition events are usually averaged so as to reduce averaging errors (in the UCL laboratory, 100 engine combustion cycles are usually averaged for the calculation of the ignition delay).

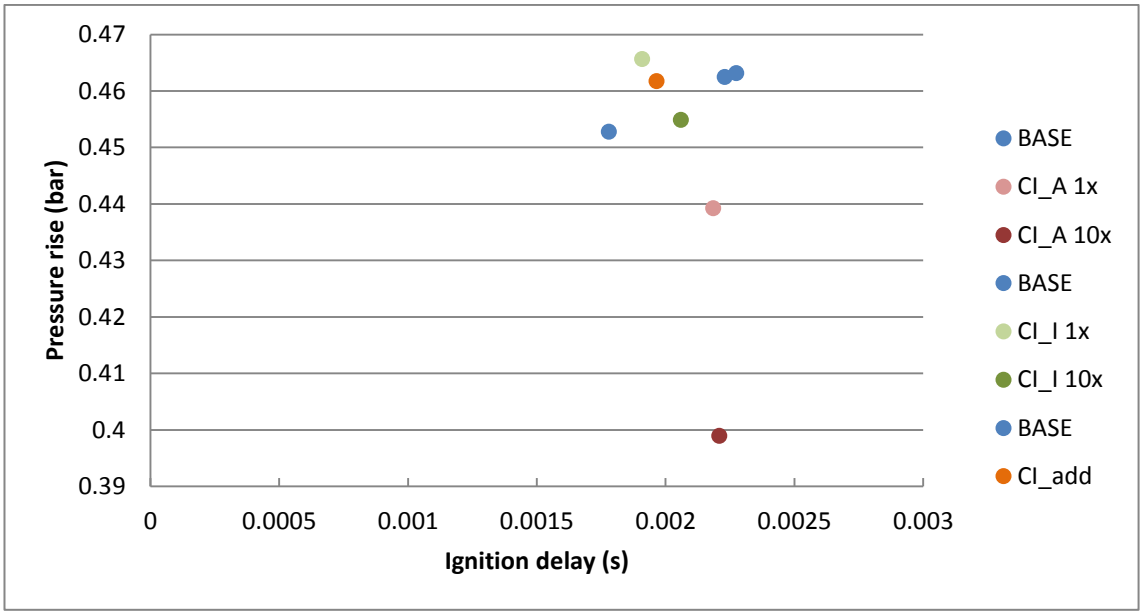

Figure 6.12: Ignition delay vs. peak pressure rise from diesel combustion (peak pressure of diesel combustion minus pressure at start of injection) – average per additive blend

As shown in Figure 6.12, combustions with blends of base fuel with ignition improver additive CI-A produce a lower pressure rise than all other blends, as well as a lower peak heat release rate. The reason for this is unknown.

To summarise, no significant differences from base diesel fuel were measured with the addition of combustion modifier additives. This appears to be the result of several factors:

- A low number of tests with each CI additives, due to time constraints.

- The need for pre-combustion in order to auto-ignite diesel meant that less oxygen was present in the vessel.
- The injector used was unsuited to the large 23 L vessel, with the spray only making use of a small fraction of the oxygen in the CVCV. This meant that the diesel combustion was lean and localised, leading to a pressure rise that was small and difficult to measure accurately (less than 0.5 bar).

The vessel is much more suited to spark triggered premixed combustions, where the stoichiometry can be monitored and controlled. Also, the vessel, with its excellent optical access is well suited to the observation of diesel combustion spray and flames, rather than to the quantitative analysis of heat release or to the analysis of combustion pollutant products.

6.3. Combustion modifiers in a laboratory engine

The same five blends of diesel fuel with combustion modifier (CI) additives were used to carry out additional tests on the UCL single cylinder research engine facilities described in section 6.2.1. The testing procedure was the same as the one described in Table 6.2, where all combustion modifier additives were bracketed with base fuel. As described in the methods section of this chapter (section 6.2.1.), the engine speed, common rail pressure, engine temperature and start of injection were all kept constant (see Table 6.1). The injection duration was varied to achieve an IMEP of 4 bar at a constant engine speed of 1200 RPM. Thus, it was possible to compare the combustion characteristics for each blend of diesel fuel with CI additives for a common engine power output.

6.3.1. **Ignition delay of diesel fuel with combustion modifier additives**

The ignition delay was calculated using the rate of heat release curve (Figure 6.13) which was calculated using in-cylinder pressure and in-cylinder volume (through the use of a crank angle sensor). The calculation method is described earlier in this chapter (see section 6.2.1.). In this case, diesel fuel was always injected 7.5 crank angle degrees (CAD) before top dead centre (TDC). The results displayed in Figure 6.13 and Figure 6.14 show the average heat release rate curve against CAD and the premixed burn fraction against the ignition delay in CAD after TDC for all 80 tests carried out on the research engine respectively.

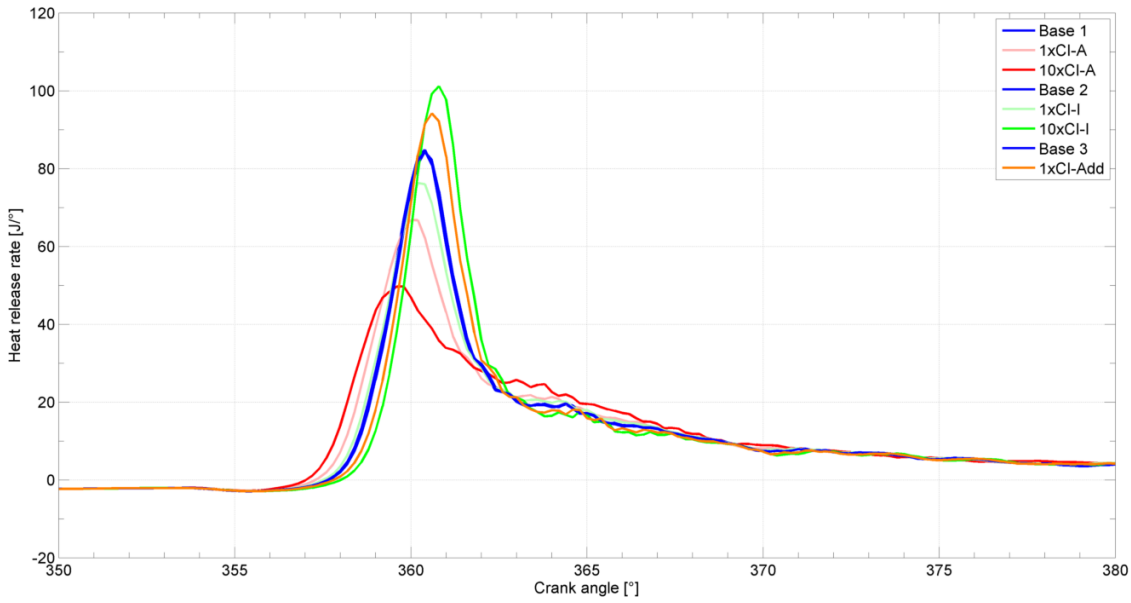

Figure 6.13: Average heat release rate vs. crank angle degrees of various additives in an engine (CI-A additive is a diesel ignition improver; CI-I is an anti-knock-gasoline octane enhancer; and CI-Add is a metallic anti-knock additive)

The average heat release rate against crank angle degrees for all blends with CI additives and their associated base tests can be seen in Figure 6.13. When fuel is injected into the combustion chamber of the engine, the heat release rate reduces slightly, as heat energy is used by the system to evaporate the fuel when it mixes with the air in the chamber. During mixing and branching (the breaking down of hydrocarbon molecules to form radicals), the system provides energy to the combustion reactants. Combustion is defined as the point when heat release rate becomes positive, which means the chemical reaction taking place in the combustion chamber provides energy and heat to the system. The initial sharp rise and fall in the heat release rate coincides with the pre-mixed phase of the diesel combustion where the gases already present in the chamber all ignite at once. The diffusion burning phase is then seen as a sharp change in the heat release rate slope. Figure 6.13 shows that the heat release rate trace is heavily affected by the addition of CI additives. With combustion improver additives, the ignition delay is shorter, which reduces the peak heat release due to less pre-mixing. The opposite is true of anti-knock additives.

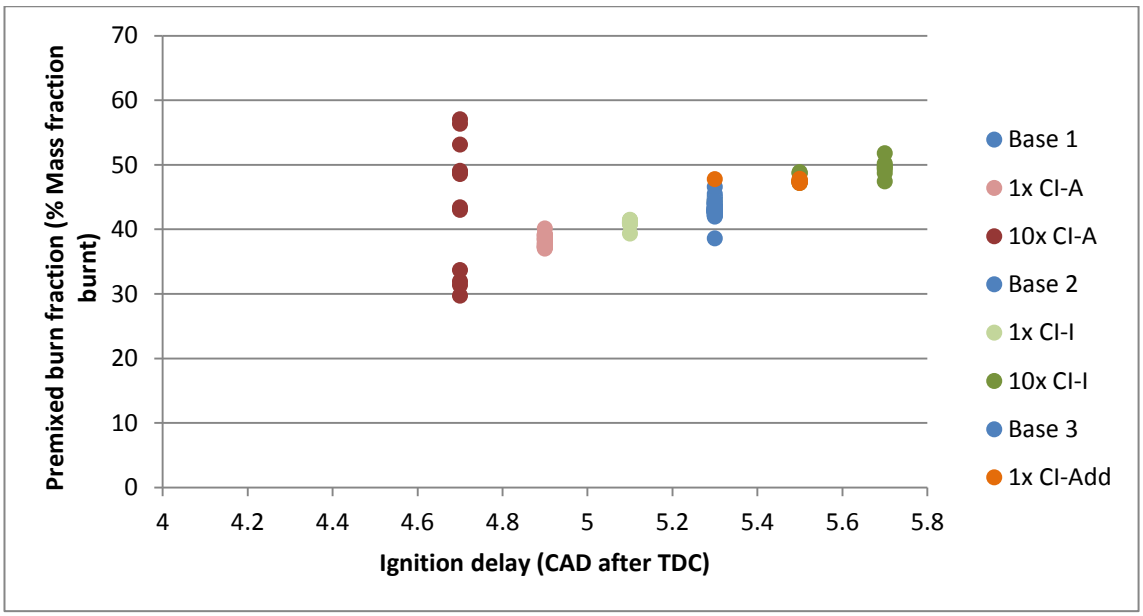

Figure 6.14: Premixed burnt fraction vs. ignition delay (CI-A additive is a diesel ignition improver; CI-I is an anti-knock-gasoline octane enhancer; and CI-Add is a metallic anti-knock additive)

Figure 6.14 shows that as the ignition delay increases, the fuel has more time to mix before auto-ignition, which is seen as an increase in the premix burn fraction. In general, all blends with CI additives roughly follow this trend. Blends with 10x of additive CI-A show a wide spread of premixed burn fraction values. The difficulty in determining the end of the pre-mixing burn fraction by the software for additive CI-A at 10x concentration is obvious when looking at Figure 6.13, where the change in slope which is defines the end of the pre-mixing phase and start of diffusion burning phase is not as obvious as with other blends with additives.

As expected, blends with additive CI-A, a diesel ignition improver, have a shorter ignition delay (4.9 CAD after TDC) than base diesel fuel (5.3 CAD after TDC). This behaviour is as expected, as the addition of 1x CI-A (i.e. 250 ppm) should enhance the base fuel by 2-3 CN (Cooney, 2012). The extra addition of additive CI-A to base fuel at ten times the normal concentration (10x) reduces the delay further (to 4.7 CAD after TDC), although not proportionally.

The addition of additive CI-I, a gasoline anti-knock additive, and, therefore, a diesel fuel ignition inhibitor lengthened the ignition delay by 0.2-0.4 CAD, as would be expected, when added at 10x concentration (10000 ppm). However, adding 1x CI-I to base fuel had the reverse effect or no effect compared to base fuel, as seen on Figure 6.14. It is known that 5x (5000 ppm) of additive CI-I should reduce the CN by 1-2 (Cooney, 2012). At 1x concentration of CI-I (1000 ppm), the additive does not provide enough of a change in the CN to affect the ignition delay. The slight reduction may be interpreted as experimental error and test-to-test variation. At 10x concentration (10000 ppm), the blend with additive CI-I shows a clear increase in ignition delay of 0.2-0.4 CAD, as expected.

The metallic gasoline anti-knock additive CI-Add also increases the ignition delay of the diesel fuel at 1x concentration. This increase is small, as it is only meant to reduce the fuel's CN by 1.5-2.5 (Cooney, 2012).

Contrary to the combustion vessel experiments, laboratory engine tests were successful in producing experimental data on ignition delay which correlate with the known effect of the additives used.

6.3.2. **Mass and size distribution of particulates with additives**

In addition to cylinder data, the exhaust gases for each test were passed through a differential mobility spectrometer (Cambustion DMS 500) to determine the mass and size distribution of the particulates.

Airborne particulate matter (PM) that is smaller than 2500 nm in diameter can be damaging to the human respiratory and cardiovascular systems (World Health Organisation, 2005). Furthermore, the World Health organisation has identified PM as a carcinogenic agent (World Health Organisation, 2014). Environmental laws over the past 20 years in almost all countries in the world, including the EU, have restricted the emission of PM from various combustion sources including motor vehicles (Seinfeld & Pandis, 2012).

In the case of the EU, the legislated limits of PM emissions from a small or medium duty vehicle have decreased in the past 20 years: from 0.2 g/km to 0.005 g/km in 2014. As the engine bed tests were not conducted in a vehicle, it is difficult to convert the PM emissions to particulate mass per km. However, a comparison can be made of the PM emitted with the fuel blends containing different additives.

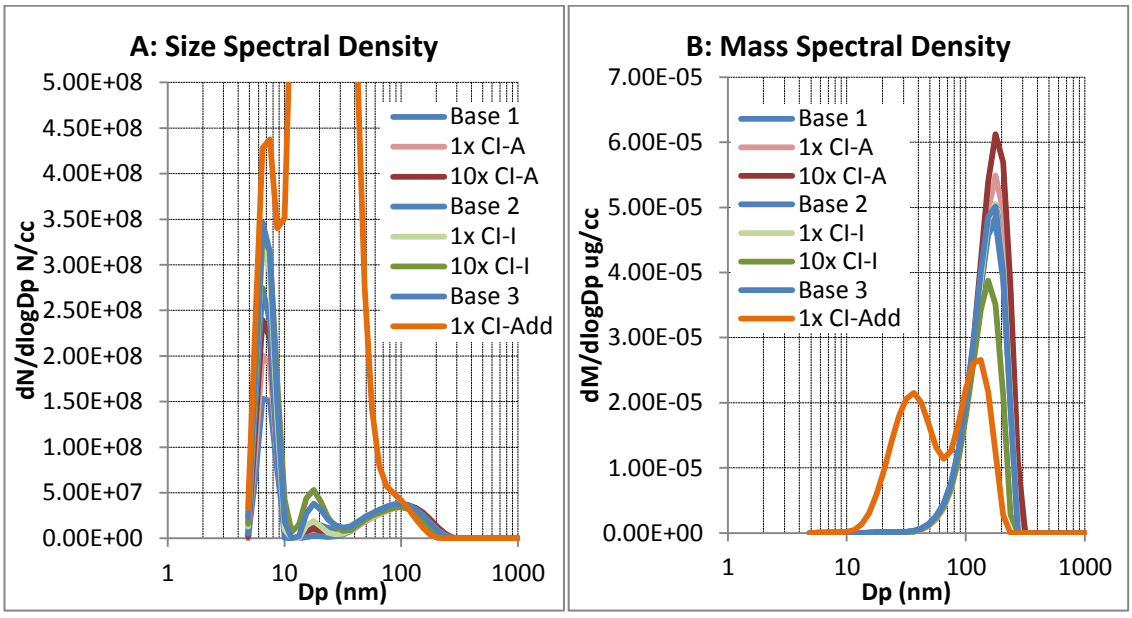

Figure 6.15: Size distribution (number density) (A) and mass density (B) of particulates with various fuel additives

The particulate size distribution on a number basis shows three peak sizes of interest for all blends of additives. These are around 8 nm, 20 nm and 150 Nm, as can be seen on Figure 6.15. Below ~50 nm, the particulate is predominantly consisted of individual particles (nucleation mode), whereas above ~50 nm, the particulate consists of particle agglomerates (accumulation mode) (Hellier, et al., 2013). Premixed combustion tends to produce individual particles, while diffusion controlled combustion encourages aggregation of particles in agglomerates.

It can be observed from Figure 6.15 that:

- Particles of ~8 nm in size are present for all types of additives and the number and mass densities vary greatly between each additive sample. However, as these are very small particles, there is greater uncertainty in their measurements especially with regards to number of particles. Furthermore, these particles, although numerous, contribute very little towards the mass spectral density, due to their small size (see Figure 6.15(B)).
- Particles of ~20 nm in size occur for all blends of additives at about 10 to 50 million particles per cubic centimetre. For the blend with additive CI-Add, the amount of particles rises to above 2 billion particles per cubic centimetre (off scale on Figure 6.15(A)), with an average diameter of ~20 nm. It is suggested that the metallic component of the organo-metallic molecule in additive CI-Add could be acting as a nucleation site for early soot material to condense onto, leading to more numerous smaller particles (~20 nm). Without these metallic nucleation sites, the early soot material would more likely have been condensing onto the already formed soot primary spherules, increasing their size, as would appear to be the case with the non-metallic additive blends (see Figure 6.15(B)) which have tended to have more particles of larger diameter than CI-Add.
- The larger particles (~120 nm) are agglomerates present for all blends of additives. Their number is minor compared to the smaller sized particles, but they account for the largest mass, as pictured in Figure 6.15. Their large size (~120 nm) suggests that they are likely to be soot agglomerations.

The large number of smaller particles generated with additive CI-Add would increase the health risks of this additive, as smaller particles (<50 nm) can penetrate deep into the lungs, past the respiratory system defences which are most effective for particles greater than 50 nm. On the other hand, the reduction of particle size due to additive CI-Add could lead to easier Diesel particulate filter (DPF) regeneration, as the small particles, having a larger surface area per unit mass, would be oxidised more easily to CO_2 by the filter. Nevertheless, there remains a question of what will happen to the metallic component of the particulate and whether it will be retained by the filter and thus risk damaging it by wearing its active surface.

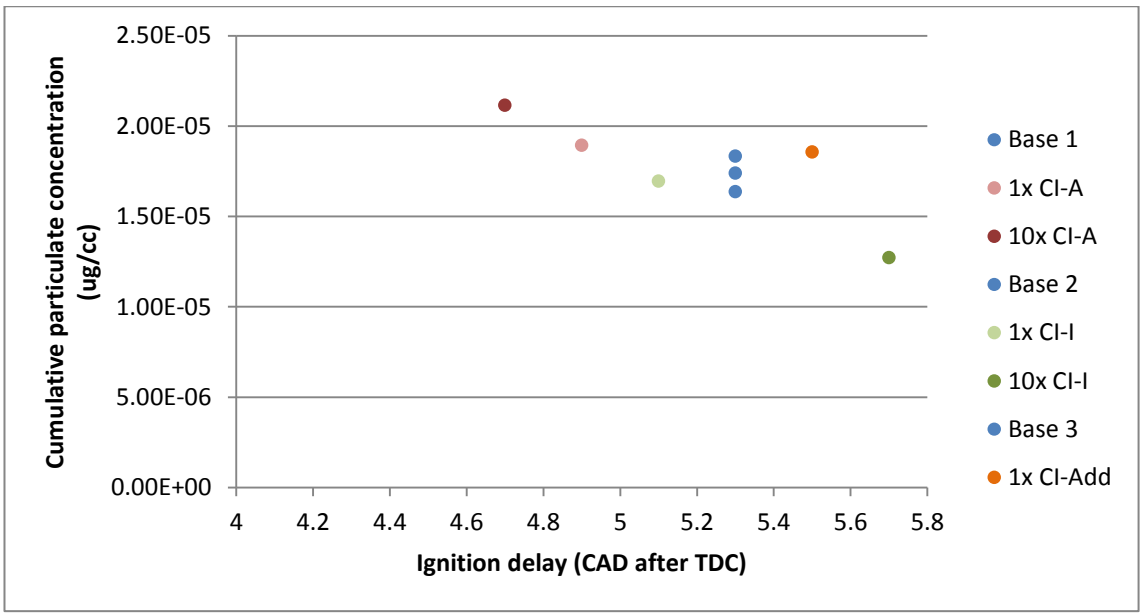

Figure 6.16: Cumulative mass concentration of particles of particulate matter (using 1g/ m^3 as density, and volume data) vs. ignition delay

Figure 6.16 shows that there is a linear inverse relationship between ignition delay and cumulative mass concentration of particles. That is, a smaller mass of particulates is associated with longer ignition delays. This is as to be expected, because a long ignition delay increases the time available for pre-mixing and therefore the proportion of premixed combustion. This results in the production of fewer soot particles as the particles that manage to form during premixed combustion are better oxidised. The blend with additive CI-Add also follows the trend, despite the large quantity of particulates around 20 nm in size.

6.3.3. **Exhaust pollutant emissions with combustion modifier additives**

The combustion generated emissions for each blend of diesel fuel with combustion modifier additives were passed through a Horiba exhaust gas analyser to determine the concentrations of O_2, CO_2, CO, NO_x and unburnt hydrocarbon (THC) emissions. All these gases, except THC were measured on a dry molar basis.

6.3.3.1. Carbon monoxide (CO)

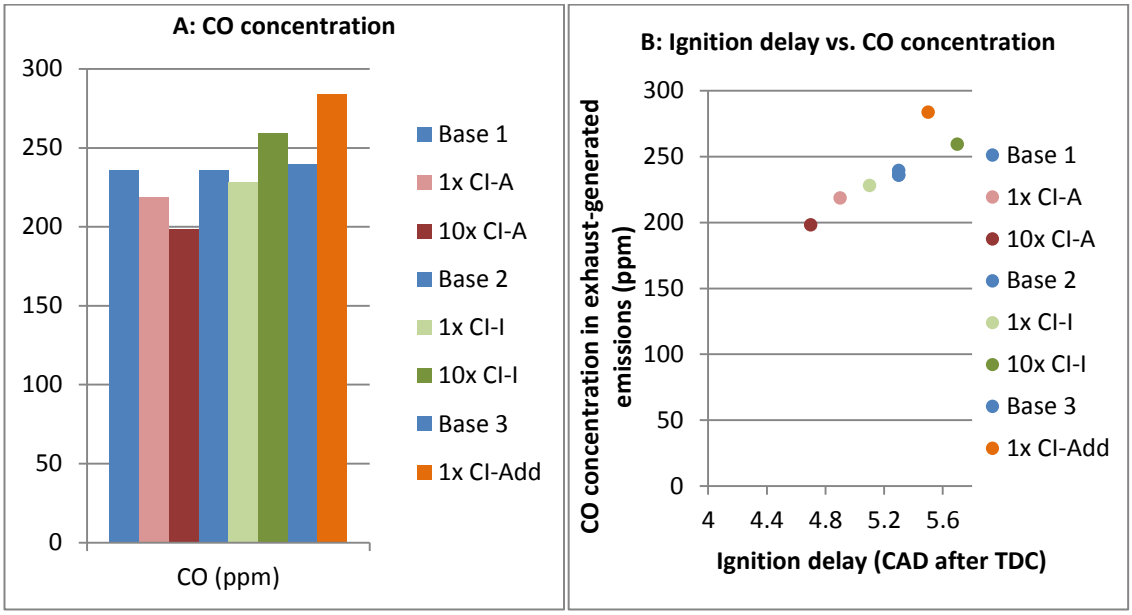

Figure 6.17: Average carbon monoxide (CO) content in exhaust emissions with combustion modifier additives (A) and vs. average ignition delay (B)

The concentration of carbon monoxide (CO) in exhaust with combustion modifier additives can be seen in Figure 6.17. When ignition delay was shortened (CI-A), there were less CO emissions. In contrast, blends with additive CI-I or CI-Add (which increased ignition delay) created more CO emissions when they were burnt.

CO emissions are usually associated with either fuel rich combustion or quenching. The former is more likely to occur with a short ignition delay, leading to less premixed fuel, while the latter (quenching) is likely to occur with long ignition delays, causing late combustion in the expansion stroke, when the lower temperatures due to expansion discourage full oxidation of CO to CO_2. In this instance, the results follow the opposite trend in the case of rich combustion and thus cannot be easily explained with the limited information available. It is suggested that because the long ignition delays are cause by anti-knock additives, their principal function of absorbing combustion radicals may also inhibit full CO oxidation to CO_2.

6.3.3.2. Carbon Dioxide (CO_2) and Oxygen (O_2)

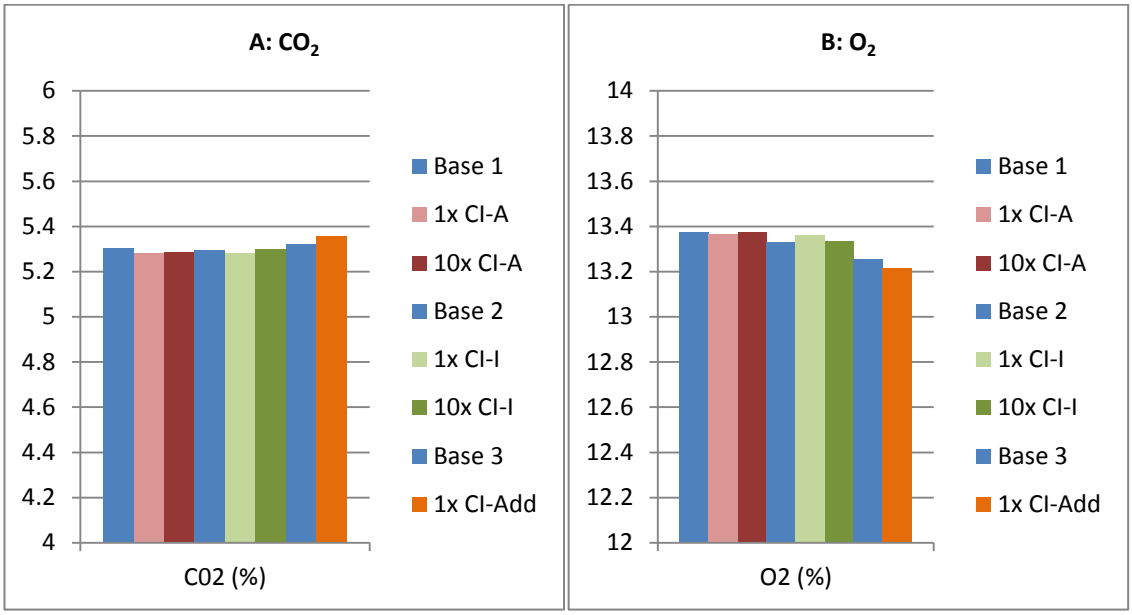

Figure 6.18: Average carbon dioxide (CO_2) (A) and oxygen (O_2) (B) concentrations in exhaust emissions with combustion modifier additives

The oxygen and carbon dioxide concentrations in the exhaust with combustion modifiers can be seen in Figure 6.18. All results fall within 0.2% or less of each other; the CO_2 and O_2 concentrations follow opposite trends, with an additive that causes a decrease in O_2 also causing an increase in CO_2, which is as expected.

6.3.3.3. Unburnt hydrocarbons (THC) and Nitrous oxides (NO_x)

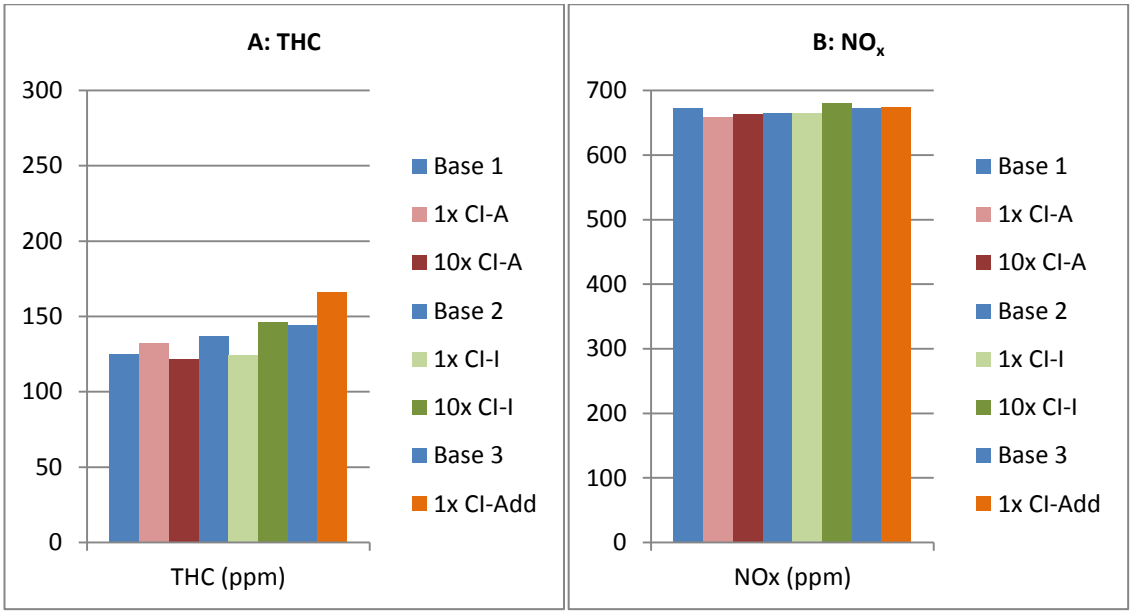

Figure 6.19: Average unburnt hydrocarbon (THC) (A) and nitrous oxides (NO_x) (B) content in exhaust emissions with combustion modifier additives

The unburnt hydrocarbon emissions as well as the nitrous oxide emissions resulting from combustion with CI additives can be seen in Figure 6.19. On the whole, the THC concentration

seems to increase with the addition of the combustion inhibitor CI-Add. This could, most likely, be a result of the inhibitor lengthening the ignition delay and causing some over-dilation of the air-fuel mixture at the fringes of the fuel spray.

NO_x emissions are mostly affected by combustion temperature. The temperature changes somewhat with ignition delay, when the ignition timing is fixed, due to the variations in combustion relative to TDC and the magnitude of the volume in which energy is released. NO_x variations due to temperature are altered when the combustion equivalence ratio changes, or when EGR is used to reduce the temperature in the combustion chamber. Figure 6.19 shows that the CI additives did not have any effect on the NO_x content probably due to their concentration being too small, resulting in, overall, a neutral effect on temperature of the various factors outlined above.

6.4. Conclusions from combustion experiments

The addition of combustion modifier additives (CI) to diesel fuel has affected the combustion characteristics in the engine, as expected. Adding diesel ignition improvers to base fuel resulted in a decrease in ignition delay, while anti-knock additives increased the ignition delay compared to base fuel with no additives. The analysis of the engine exhaust gases has shown that additives have only a small effect on the exhaust gases, except for the organo-metallic additive CI-Add, whose particulate emissions suggested an effect from the metallic component of the additive.

In contrast to the effects of additives on diesel engine combustion, no evidence of additive effects was seen in the heat release or ignition delay from combustion experiments carried out in a constant volume combustion vessel. Combustion vessel experiments are well suited to the observation of fuel spray and flames, as well as the analysis of premixed combustions. However, the results presented in this chapter have shown that a constant volume combustion vessel is not as useful to carry out the analysis of the combustion of diesel fuels with additives. The ignition delay varied but this was partly due to event-to-event variations in pre-combustion of hydrogen with air. The large size of the vessel made it impossible for the fuel sprays to utilise a substantial proportion of the oxidising gases left in the vessel after the hydrogen/air pre-combustion, without wetting severely the vessel walls with fuel. A smaller vessel, better matched to the fuel spray, may be more suitable for diesel fuel combustion in a constant volume vessel.

Chapter 7

Conclusion

The thesis presented a wide ranging set of experiments aimed at assessing the effects of diesel fuel additives on diesel engine injection system performance and combustion with fuel additives, in particular:

- A diesel fuel pump and common rail rig which allowed individual control of pump speed, fuel temperature and fuel delivery pressure was designed by the author. This rig was used to investigate whether a wide range of diesel fuel additives had an effect on the torque required to drive the pump over a wide range of pump speeds and delivery pressures. Various fuel temperatures, including sub-zero waxing conditions of fuel were also investigated in the pump rig.
- The droplet size distribution of a diesel fuel spray at sub-zero temperatures was assessed, in conditions when fuel wax was formed. The effect of anti-wax additives on the spray droplet size distribution was also investigated.
- The effects of various additives on ignition delay of diesel combustion in a constant volume combustion vessel and in a diesel engine were investigated. The exhaust emissions of the diesel engine were also investigated with various additives added the fuel.

The above tests were carried out to determine whether individual additives had the potential to affect parts of the injection as well as combustion and emissions. Some of the additives were designed to modify combustion, while others (e.g. detergents) could have affected combustion and emissions as a side effect. Nevertheless, such side-effects are important and need to be known, if present. As a result of the research in this thesis, a stronger understanding of the effects and limitations of diesel fuel additives on certain aspects of the combustion process and diesel injection system was acquired.

It has been found that in a fuel delivery system resembling that of an engine, the torque required to operate a fuel pump was mostly governed by the required fuel pressure, and that the relationship between the two is linear. Furthermore, higher pump speeds and lower fuel temperatures increased torque required to operate the fuel pump; it was also found that this increase was linearly related to pump speed and fuel temperature.

It has been found that for all additives, the frictional torque and, therefore, the torque required to drive the pump was not affected significantly by the additives. Friction modifiers (FM), which were expected to reduce the torque required to drive the fuel pump, did not show any change in the drive torque. The lack of effect on torque is believed to be due to the way this type of additive works. All tests in the fuel pump rig were carried out with 50 ppm of FM additive which is the usual level used to avoid damage to the internal, highly stressed by contact, surfaces of the pump. The 50 ppm of additive FM-N was sufficient to coat all the pump internal surfaces which were subject to boundary lubrication in the pump. It is believed that the 50 ppm FM-N added to each fuel blend provided maximum boundary lubrication to the pump.

The behaviour of waxing fuel was investigated by exposing the flowing fuel to sub-zero temperatures by means of a heat exchanger. Behaviour not typical of a vehicle engine was seen because the wax formation was proven to undergo a coating cycling pattern in the heat exchanger where wax wormed, melted and reformed in a cyclic pattern. It was possible to explain this behaviour in detail in Chapter 4.

During the cold (sub-zero temperature) spray experiments it was found that wax crystals, which are too large to go through a standard diesel fuel filter, had no effect on the spray atomisation process. Instead, it is believed that the increase that was observed in the droplet size distribution was not due to waxing but rather due to the increase in viscosity of the fuel, as a result of its decrease in temperature. This explained why fuel blends with anti-wax additive did not show any effect on the spray droplet size distribution. This lead to the conclusion that large wax crystals, which are problematic in blocking fuel filters in vehicles, have no significant effect on the spray characteristics. In vehicles, wax is therefore only likely to be problematic in blocking the fuel filter. One likely explanation for the lack of an effect from wax on the spray droplet size distribution is that the very large shear rates experienced by the fuel in the small injection passages breaks down the wax crystals.

A constant volume combustion vessel was found to be unsuitable for carrying out observations of combustion characteristics of fuels with additives. A large test-to-test variability was found in ignition delay, partly due to variability in various parameters of the pre-combustion event of hydrogen with air. On the other hand, the use of combustion modifier additives (CI) showed consistent effects in a diesel engine: adding diesel ignition improvers to the base fuel resulted in a decrease in ignition delay, while gasoline anti-knock additives increased the ignition delay. It

was therefore concluded that combustion vessels, although indispensable for optical and spray work, were not suited for experiments with fuel additives, as the changes in the combustion characteristics were too small to be experimentally discernable. Engine bed tests have had a much greater success in that regard.

The analysis of the engine exhaust gases showed that additives did not affect the exhaust gas composition significantly, except for additive CI-Add, an organo-metallic additive, which showed a large increase in particulate emissions. It is possible that the metallic component of the molecule is freed during combustion and may act as a condensation side (nucleus) for particulate precursors, causing the large rise is observed particulates.

The work presented in this thesis has shown that additives generally only affect the fuel properties for which they are designed, and often do not affect the macroscopic behaviour of the fuel.

It is recommended that future work could focus on testing additives in engines, rather than constant volume vessels, when the effect of an additive on combustion intended effect or side effect is being evaluated.

It was observed that additives in relatively small quantities (hundreds of ppm) can affect significantly the ignitability or suppression of ignition in a diesel engine. It may be possible to use such additives to control Homogeneous-Charge-Compression-Ignition (HCCI) as this may be a fruitful area of future research.

The anti-wax additives used in this research did not always show adequate suppression of the formation of wax crystals, in the particular setup used for this research. This is an area which could benefit from future research to clarify the role of the anti-wax additive.

Bibliography

ACEA, AAM, EMA & JAMA, 2006. *Worldwide Fuel Charter.* 4th ed. s.l.:s.n.

Al-Khodair, M. et al., 2009. Effects of drag reducing agents (DRAs) on engine deposits. *Saudi Aramco journal of technology,* Issue WINTER, pp. 1-5.

Armas, O., Martinez-Martinez, S. & Mata, C., 2011. Effect of an ethanol-biodiesel-diesel blend on a common rail injection system. *Fuel processing technology 92,* pp. 2145-2153.

ASTM, 2010. *D4539-10 - Standard test method for filterability of diesel fuels by low-temperature flow test (LTFT),* West Conshohocken, USA: ASTM International.

ASTM, 2012. *D4308-12 - Standard test method for electrical conductivity of liquid hydrocarbons by precision meter,* West Conshohocken: ASTM International.

ASTM, 2013. *D975 - Standard Specification for diesel fuel oils,* West Conshohocken: Astm International.

ATC, 2004. *Fuel additives and the environment,* s.l.: Technical Committee of Petroleum Additive Manufacturers in Europe.

ATC, 2007. *Lubricant additives and the environment,* s.l.: Technical Committee of Petroleum Additive Manufacturers in Europe.

Baert, R. S. et al., 2009. Design and operation of a high pressure, high temperature cell for HD diesel spray diagnostics: guidelines and results. *SAE Technical Paper 2009-01-0649.*

Belz, K. & Koch, P., 1991. *Filter element which conducts static electricity.* USA, Patent No. US 4999108 A.

Berman, N., 1978. Drag reduction by polymers. *Annual review of fluid methanics,* Volume 10, pp. 47-64.

Birgel, A., Ladommatos, N. & Aleiferis, P., 2008. Deposit formation in the holes of diesel injector nozzles: A critical review. *SAE technical paper.*

Blaisot, J. B. & Yon, J., 2005. Droplet size and morphology characterization for dense sprays by image processing: application to the Diesel spray. *Experiments in Fluids 39,* pp. 977-994.

Caprotti, R., Breakspear, A. & Graupner, O., 2007. *Beyond 2008: The challenges for diesel detergency*. Esslingen, Infineum UK, VDO Automotive Germany.

Carney, P. S., Duncan, A. D. & Wilkes, F. M., 2004. *Anti-Static lubricity additive for ultra low sulfur diesel fuels.* USA, Patent No. EP 1328609 B1.

Cestoil Chemical Inc., 2012. *Wax anti-settling Additives (WASA).* [Online] Available at: www.cestoil.com/wasa.html [Accessed 5 June 2013].

Cooney, A., 2012. *e-mail conversation.* London: s.n.

Dumouchel, C., Yongyingsakthavorn, P. & Cousin, J., 2009. Light multiple scattering correction of laser-diffraction spray drop-size distribution measurements. *International Journal of multiphase flow,* Volume 35, pp. 277-287.

Ejim, C., Fleck, B. & Amirfazli, A., 2007. Analytical study for atomization of biodiesels and their blends in a typical injector: Surface tension and viscosity effects. *Fuel 86,* pp. 1534-1544.

Elkotb, M. M., 1982. Fuel atomization for spray modelling. *Prog. Energy Combust Sci, Vol 8,* pp. 61-91.

European Standard, 1997. *EN 116: Diesel and domestic heating fuels - Determination of cold filter plugging point,* Brussels: European committee for standardization.

Fdida, N., Blaisot, J.-B., Floch, A. & Dechaume, D., 2010. Drop-size measurement techniques applied to gasoline sprays. *Atomization and sprays 20 (2),* pp. 141-162.

Ferguson, C. R., 1986. *Internal combustion engines: Applied thermosciences.* New York: John Wiley & sons.

Han, S. et al., 2010. Impact of alkyl methacrylate-maleic anhydride-alkyl methacrylate terpolymers as cold flow improver on crystallization behavior of diesel fuel. *Process safety and environmental protection 88,* pp. 41-46.

Hellier, P., Ladommatos, N., Allan, R. & Rogerson, J., 2012. The Influence of Fatty Acid Ester Alcohol Moiety Molecular Structure. *Energy & fuels,* 26(3), pp. 1912-1927.

Hellier, P., Ladommatos, N., Allan, R. & Rogerson, J., 2013. Combustion and emissions characteristics of toluene/n-heptane and 1-octene/n-octane binary mixtures in a direct injection compression ignition engine. *Combustion and Flame,* Volume 160, pp. 2141-2158.

Heywood, J. B., 1988. *Internal combustion engines fundamentals.* New York: Mc Graw Hill.

Higgins, B., Siebers, D., Mueller, C. & Aradi, A., 1998. *Effects of an ignition-enhancing, diesel-fuel additive on diesel-spray evaporation, mixing, ignition and combustion.* s.l., The combustion institute, pp. 1873-1880.

Hiroyasu, H., 1985. Diesel engine combustion and its modeling. *Diagnostics and modeling of combustion in reciprocating engines, COMODIA 85,* pp. 53-75.

Hiroyasu, H. & Kadota, T., 1974. Fuel droplet size distribution in diesel combustion chamber. *SAE paper 740715.*

Ickes, A. M., Bohac, S. V. & Assanis, D. N., 2009. Effect of 2-ethylhexyl nitrate cetane improver on NOx emissions from premixed low-temperature diesel combustion. *Energy Fuels, 23,* pp. 4943-4948.

Jones, A. R., 1977. A review of drop size measurement - the application of techniques to dense fuel sprays. *Prog. Energy Combust. Sci. Vol 3,* pp. 225-234.

Kadarohman, A. et al., 2012. Combustion characteristics of diesel fuel on one cylinder diesel engine using clove oil, eugenol, and eugenyl acetate as fuel bio-additives. *Fuel 90,* pp. 73-79.

Kajdas, C. & Majzner, M., 2001. Boudary lubrication of low-sulphur diesel fuel in the presence of fatty acids. *Lubrication science 14-1,* pp. 83-108.

Kasza, T. & Hancsok, J., 2011. Investigation of fuel components produced by the isomerization of bio-paraffin mixtures. *Hungarian journal of industrial chemistry,* 39(1), pp. 121-126.

Keskin, A., Guru, M. & Altiparmak, D., 2011. Influence of metallic based fuel additives on performance and exhaust emissions of diesel engine. *Energy conversion and management 52,* pp. 60-65.

Khonsari, M. M. & Booser, E. R., 2001. *Applied tribology - Bearing design and lubrication.* New York: John Wiley & sons, Inc.

Labeckas, G. & Slavinskas, S., 2005. Influence of fuel additives on performance of direct-injection Diesel engine and exhast emissions when operating on shale oil. *Energy conversion and management 46,* pp. 1731-1744.

Leonard, J., 1981. Static electricity in hydrocarbon liquids and fuels. *Journal of Electrostatics,* Volume 10, pp. 17-30.

Leonard, J. T., 1981. *Generation of electrostatic charge on fuel handling systems: A literature survey. Report 8484,* Washington, D.C.: Naval research laboratory.

Lovell, W. G., Campbell, J. M. & Boyd, T., 1948. Knocking characteristics of hydrocarbons. *Industrial and engineering chemistry,* Volume 40, pp. 2388-2438.

Lu, X.-c., Qiao, X.-q., Cheng, J. & Huang, Z., 2007. Experimental investigation of the influence of fuel viscosity on the spray characteristics of diesel nozzle. *Journal of Shanghai Jiaotong University (Science), Vol E-12, No.1,* pp. 61-65.

Malvern Instruments Ltd., 1997. *RT Sizer 97 instructions manual,* s.l.: Malvern instruments Limited.

Malvern Instruments LTD, n.d. *Technical paper: Basic principles of particle size analysis,* Worcestershire: Malvern Instruments Limited.

McCreath, C. G., 1971. The effect of fuel additives on the exhaust emissions from diesel engines. *Combustion and flame 17,* pp. 359-366.

Mitusova, T. N. et al., 2002. Improvement of the lubricating properties of diesel fuels. *Chemistry and technology of fuels and oils, Vol 38, No. 3,* pp. 167-170.

Park, S. H., Cha, J. & Lee, C. S., 2011. Spray and engine performance characteristics of biodiesel and its blends with diesel and ethanol fuels. *Combustion science and technology 183:8,* pp. 802-822.

Patel, P., 2009. *Transfer report,* London: UCL.

Patel, P., 2013. *PhD Thesis,* London: UCL.

Payri, R., Salvador, F. J., Gimeno, J. & Bracho, G., 2008. Effect of fuel properties on diesel spray development in extreme cold conditions. *Proceedings of the IMechE,* Volume 222 Part D: Journal of Automotive engineering.

Pirro, D. M. & Wessol, A. A., 2001. *Lubrication fundamentals - Second edition, revised and expanded.* New York: Marcel Dekker, Inc..

Priol, L., Baudet, P., Louste, C. & Romat, H., 2006. Theoretical and experimental study (linear stability and Malvern granulometry) on electrified jets of diesel oil in atomization regime. *Journal of electrostatics 64,* pp. 591-596.

Richards, P., 2010. *Email conversation* [Interview] (29 November 2010).

Robert Bosch GmBH, 1999. *Diesel accumulator fuel-injection system common rail.* Stuttgart: Robert Bosch GmBH.

Russell, T., 2013. *Conversation in UCL* [Interview] (17 April 2013).

Russell, T., 2014. *Email conversation* [Interview] (29 October 2014).

Seinfeld, J. & Pandis, S., 2012. *Atmospheric chemistry and physics: from air pollution to climate change.* s.l.:John Wiley & Sons.

Stanislaus, A., Marafi, A. & Rana, M. S., 2010. Recent advances in the science and technology of ultra low sulfur diesel (ULSD) production. *Catalysis Today*, Volume 153, pp. 1-68.

Svrcek, M. N., Miller, S. L. & Edwards, C. F., 2010. Diesel spray behavior at compression ratios up to 100:1. *Atomization and sprays, 20 (5),* pp. 453-465.

Szenasi, F. R., 1990. *Torsional analyses of variable frequency drives.* Reno, Nevada, ASD Applications in utility power plants, EPRI/PEAC Seminar.

Tabata, M., Fujii, H., Arai, M. & Hiroyasu, H., 1990. Mean drop diameter of a diesel spray in a vaporising process (2nd report. Results at an elevated temperature and pressure environment). *日本機械学会論文集 B編 [0387-5016],* 56(521), pp. 214-220.

Takeuchi, K., Murayama, H., Senda, J. & Yamada, K., 1983. Droplet size distribution in diesel fuel sprays. *Bulletin of the JSME, Vol 26, No 215,* pp. 797-804.

Taylor, C. F., 1985. *The internal combustion engine in theory and practice.* 2nd ed. Cambridge: M.I.T. Press.

TSI, 2006. *Phase doppler particle analyser (PDPA)/Laser doppler velocimetry (LDV) - Operations manual,* Shoreview, MN, USA: TSI incorporated.

Wang, X. et al., 2010. Experimental and analytical study on biodiesel and diesel spray characteristics under ultra-high injection pressure. *International Journal of heat and fluid flow 31,* pp. 659-666.

Warholic, M., Massah, H. & Hanratty, T., 1999. Influence of drag-reducing polymers on turbulence: effects of Reynolds number, concentration and mixing. *Experiments in fluids,* Volume 27, pp. 461-472.

Wei, D. & Spikes, H., 1986. The lubricity of diesel fuels. *Wear,* Volume 111, pp. 217-235.

Williams, J. A., 1994. *Engineering tribology.* Oxford: Oxford university press.

World Health Organisation, 2005. *WHO Air quality guidelines for particulate matter, ozone, nitrogen dioxide and sulfur dioxide - Global Update 2005.* [Online] Available at: http://whqlibdoc.who.int/hq/2006/WHO_SDE_PHE_OEH_06.02_eng.pdf [Accessed 2 March 2014].

World Health Organisation, 2014. *Agents Classified by the IARC Monographs, Volumes 1–109.* [Online]

Available at: http://monographs.iarc.fr/ENG/Classification/ClassificationsAlphaOrder.pdf [Accessed 2 March 2014].

Yule, A. et al., 1998. PDA measurements of fuel effects on atomization and spray structure from a diesel engine injector. *SAE paper 982544.*

Zama, Y., Ochiai, W., Furuhata, T. & Arai, M., 2011. Experimental study on spray angle and velocity distribution of diesel spray under high ambient pressure conditions. *Atomization and sprays, 21 (12),* pp. 989-1007.

Zhang, H., Liu, H. & Wang, S., 2009. A new alternating copolymerized derivative as a cold flow improver for diesel fuel. *Pet. Sci. 6,* pp. 82-85.

Appendix A: Design calculations

Sizing the torque sensor

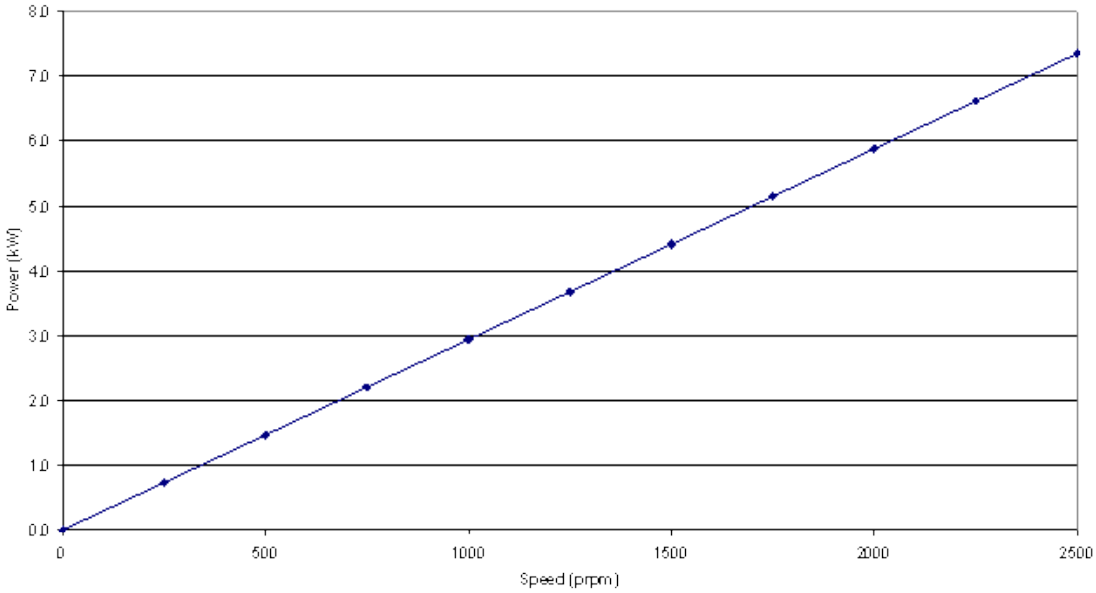

Figure 7.1: Pump power requirements for 0.75 cc/rev and at 2000 bar

When acquiring the diesel fuel pump, a specifications graph (Figure 7.1) was provided of Power vs. pump speed at 2000 bar fuel delivery pressure and 0.75 cc/rev fuel flow.

It is known from the relationship between torque and power that power is equal to torque times rotational speed.

$$P = T\omega \quad (9)$$

Where P is power in watts, T is torque in Nm, and ω is rotational speed in radians per second.

Using Figure 7.1, and solving for torque:

$$T = \frac{P}{\omega} = \frac{7400}{2500 \times {}^{2\pi}/_{60}} = 28.26\ Nm \quad (10)$$

It was assumed that 28.26 Nm would be around the maximum torque experienced by the torque sensor as 2000 bar fuel pressure is beyond the fuel pressure that will be reached with these experiments, and the pump flow rate for the rig used in the thesis was controlled through pump speed. Accounting for errors and the fact that the torque may oscillate a +/- 50 Nm torque sensor was chosen.

Sizing the electric motor

Using Figure 7.1, it has been predicted that regardless of the pump rotational speeds, the torque output required from the electric motor will be constantly high (around 28 Nm). In order to be able to supply a constant high torque even at low speeds, a three phase motor with a high power output and inverter setup was purchased.

The 11 kW Marell motor chosen has a 35.73 Nm full load torque, allowing it to rotate the pump under the most extreme conditions (rated at 28.26 Nm). Furthermore, its inverter allows for this torque to be provided at speeds as low as 16% of maximum speed (480 RPM).

Sizing the ethylene glycol tank and chiller system

For economic reasons, the chiller was chosen to be a "cold hands" type chiller, where a cold coil is dipped into a fluid to cool it down. The chiller has a 265 W cooling capacity Q_{glycol} at -30°C, its minimum design temperature.

The first step was to calculate the heat transfer required to cool down the fuel from room temperature (30°C) to the desired temperature (-25°C). This could be predicted using the heat transfer equation

$$Q_{fuel} = \dot{m} C_p \Delta T \quad (11)$$

$$Q_{fuel} = \dot{v} \rho C_p \Delta T \quad (12)$$

Where $\dot{v}$ is the volumetric flow rate of fuel, ρ is the fuel density, C_p is the fuel's thermal conductivity, ΔT is the difference between starting and desired fuel temperature, and Q_{fuel} is the heat transfer required to cool down the fuel, in W.

Density of diesel fuel (ρ)	840 kg/m^3
Volumetric flow rate ($\dot{v}$)	1.5 L/min
Heat capacity of diesel fuel (Cp)	2000 J/kgK
Temperature difference (ΔT)	55°C

Table 7.1: Values for fuel calculation

The flow rate used is 1.5 L/min, a value which was acquired experimentally using a flow meter on the fuel pump system. The fuel density and heat capacity were set as constants, and the temperature difference is that of going between 30 to -25°C. These values are summarised in Table 7.1. Using the energy equation, it can be found that the heat transfer between the fuel and the ethylene glycol tank, required to cool down the fuel, is Q_{fuel} = 2310 W.

The ethylene glycol tank was chosen to have a volume of 150L. By knowing the ethylene glycol tank capacity, the energy required to cool down the bath using the cold hands chiller can be found using the heat transfer equation

$$E = V\rho C_p \Delta T \quad (13)$$

Where V is the tank volume and E is the finite amount of energy required to cool the ethylene glycol in the tank, in Joules. Looking at a drop in temperature of 5 degrees (say from -30 to -25°C), one gets 3.135 MJ.

Density of ethylene glycol (use water) (ρ)	1000 kg/m^3
Volume of tank	150 L
Heat capacity of ethylene glycol (use water) (Cp)	1000 J/kgK
Temperature difference (ΔT)	5°C

Table 7.2: Values for chiller calculations

Knowing the energy required to heat up or cool down the tank (3.135 MJ), and knowing the cooling capacity of the chiller (265 W), and heat transfer required to cool down the fuel (2310 W), the time to cool down the ethylene glycol by 5°C (using the chiller) can be compared to the time taken to heat up the ethylene glycol (using fuel at 30°C) using $E = Qt$, where t is the time required to provide the amount of energy. When heating up, the equation becomes:

$$t = \frac{E}{Q_{fuel}} = \frac{3135000}{2310} = 22.62\ minutes \quad (14)$$

When the tank is cooled back down, this becomes

$$t = \frac{E}{Q_{glycol}} = \frac{3135000}{265} = 3.29\ hours \quad (15)$$

It has been decided that 20 minutes was a long enough time to do experiments within a 5°C error margin, allowing slow enough heating up of the fuel as a result of the ethylene glycol temperature rising., Additionally, 3 hours was deemed not too long a wait to cool down the tank by 5°C, considering only one or two fuel additive tests would be made in the same 24 hour day.